Collective modes investigated by inelastic scattering and charge-exchange reactions with magnetic spectrometers

Muhsin N. Harakeh

Kernfysisch Versneller Instituut

4th CNS International Summer School (CISS05)

Outline

- **Introduction on Giant Resonances (GRs)**

  What are GRs? Why study GRs?

- **Isoscalar giant resonances; compression modes**

  Inelastic α-scattering $\Rightarrow$ ISGMR, ISGDR

- **Isovector charge-exchange modes**

  (^{3}He,t) & (d,^{2}He) charge-exchange reactions

  $\Rightarrow$ GTR, IVSGMR, IVSGDR; GT$^+$ Strength

- **Outlook**

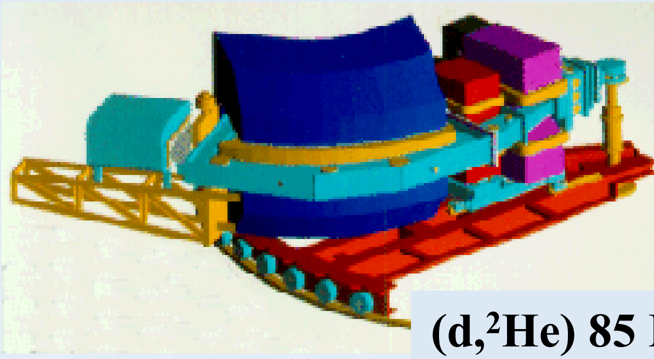

BBS@KVI

(d,^{2}He) 85 MeV/u
(^{3}He,t) 60 MeV/u
(t,^{3}He) 43 MeV/u

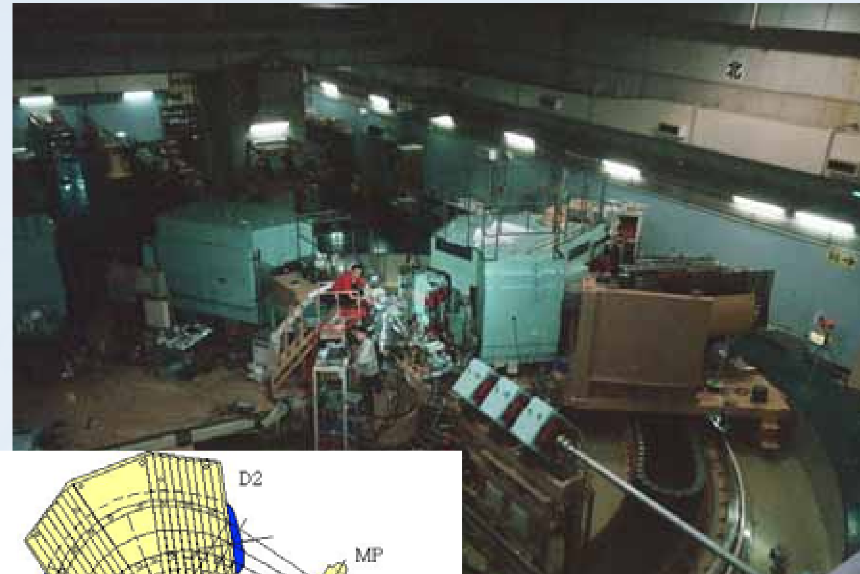

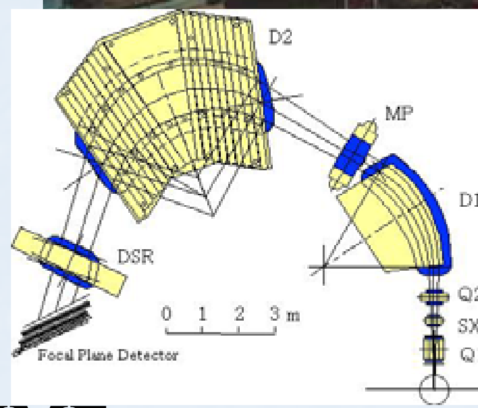

Grand Raiden@ RCNP

(^{3}He,t) 140 MeV/u
Also done
(p,n) (n,p) 300 MeV

S800@NSCL **(t,^{3}He) 115 MeV/u**

TRIUMF **(n,p) (π-CEX)**
IUCF **(p,n) (^{3}He,t)** **K600**
iThemba **(p,p)** **K600**
Texas A&M
…etc

SHARAQ Spectrometer

Spectroscopy of **HA**dron systems with **R**adio**A**ctive **Q**uantum beams

Parameters

- Momentum resolution $\Delta p/p < 1/15000$
  $\delta E_x \sim 300$ keV for $A=8$, $E=300$MeV/u
- Maximum rigidity $B\rho = 6.8$Tm ($\rho = 4.8$m)
- Solid angle $\Delta\,\Omega = 12$ msr
- Momentum acceptance +/- 3%

High-quality RI beam-line

- Dispersion matching

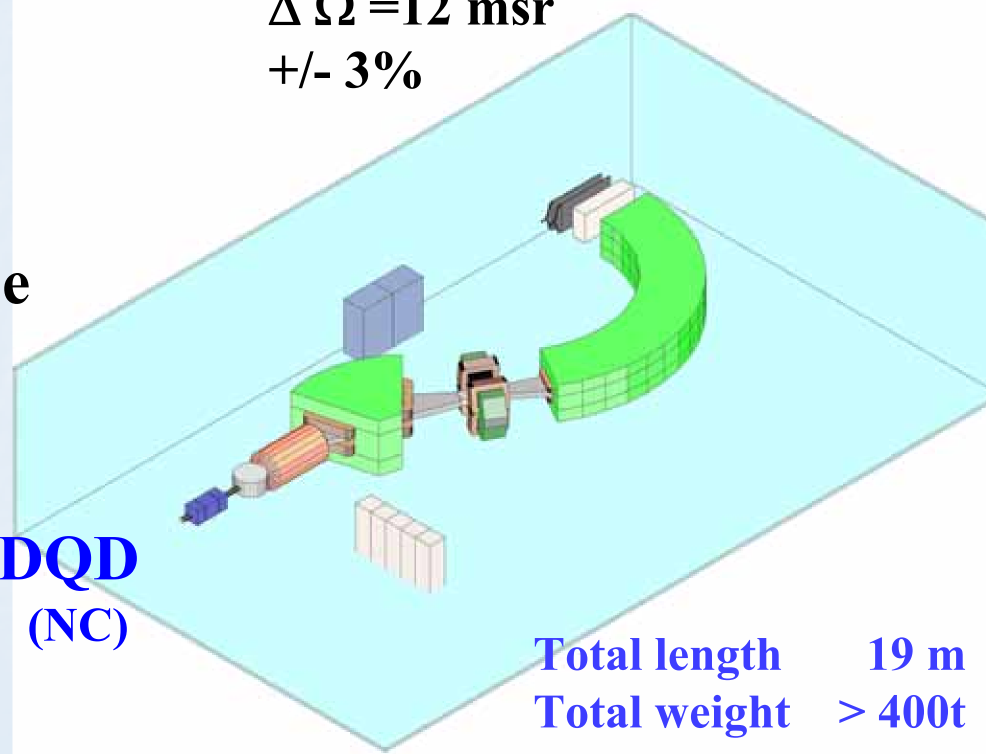

QQDQD
(SC) (NC)

Giant resonances: fundamental high-frequency modes of nuclear excitation

- Interesting to study on own merit: E_x, Γ, %EWSR;

  Microscopic structure $\Rightarrow$ compare to theory:

  HF+RPA; RMFT, RRPA, etc.
- Effective interactions, medium effects (meson-coupling constants); IVSGDR 0^- strength (pion quantum numbers)

Moreover,

- Equation of state (EOS)

  ISGMR, ISGDR $\Rightarrow$ Incompressibility, symmetry energy

  $$K_A = K_{vol} + K_{surf} A^{-1/3} + K_{sym}((N-Z)/A)^2 + K_{Coul} Z^2 A^{-4/3}$$

KVI

- **IVGDR, IVSGDR, IVGMR ⇒ n-skin thickness; isospin mixing**
- **Collective-flow in H.I. collisions**
- **Astrophysics: Input for supernova explosions, neutron stars**

Microscopic picture: GRs are coherent (1p-1h) excitations induced by single-particle operators.

- **Excitation energy depends on i) multipole L ($L\hbar\omega$, except for isoscalar monopole and isoscalar dipole GRs, $2\hbar\omega$ & $3\hbar\omega$, respectively), ii) strength of effective interaction and iii) collectivity.**
- **Exhaust appreciable % of EWSR and/or NEWSR**
- **Acquire a width due to coupling to continuum and to underlying 2p-2h configurations.**

Nucleus → **Many-body system with a finite size**

Vibrations → **Multipole expansion with** r, Y_{lm}, τ, σ

	$\Delta S=0, \Delta T=0$	$\Delta S=0, \Delta T=1$	$\Delta S=0, \Delta T=1$	$\Delta S=1, \Delta T=1$	$\Delta S=1, \Delta T=1$
L=0: Monopole	ISGMR r^2Y_0	IAS τY_0	IVGMR $\tau r^2 Y_0$	GTR $\tau \sigma Y_0$	IVSGMR $\tau \sigma r^2 Y_0$
L=1: Dipole	ISGDR r^3Y_1		IVGDR $\tau r Y_1$		IVSGDR $\tau\sigma r Y_1$
L=2: Quadrupole	ISGQR r^2Y_2		IVGQR $\tau r^2 Y_2$		IVSGQR $\tau\sigma r^2 Y_2$
L=3: Octupole	LEOR, HEOR r^3Y_3				

Isoscalar Excitation Modes of Nuclei

Giant **Resonance**: **Coherent vibration of nucleons in a nucleus.**

Compression modes : ISGMR, ISGDR

$$E_{ISGMR} = \hbar\sqrt{\frac{K_A}{m\langle r^2\rangle}}$$

$$E_{ISGDR} = \hbar\sqrt{\frac{7}{3}\frac{K_A + \frac{27}{25}\varepsilon_F}{m\langle r^2\rangle}}$$

The nucleus incompressibility:

$$K_A = \left[r^2\left(d^2(E/A)/dr^2\right)\right]_{r=R_0}$$

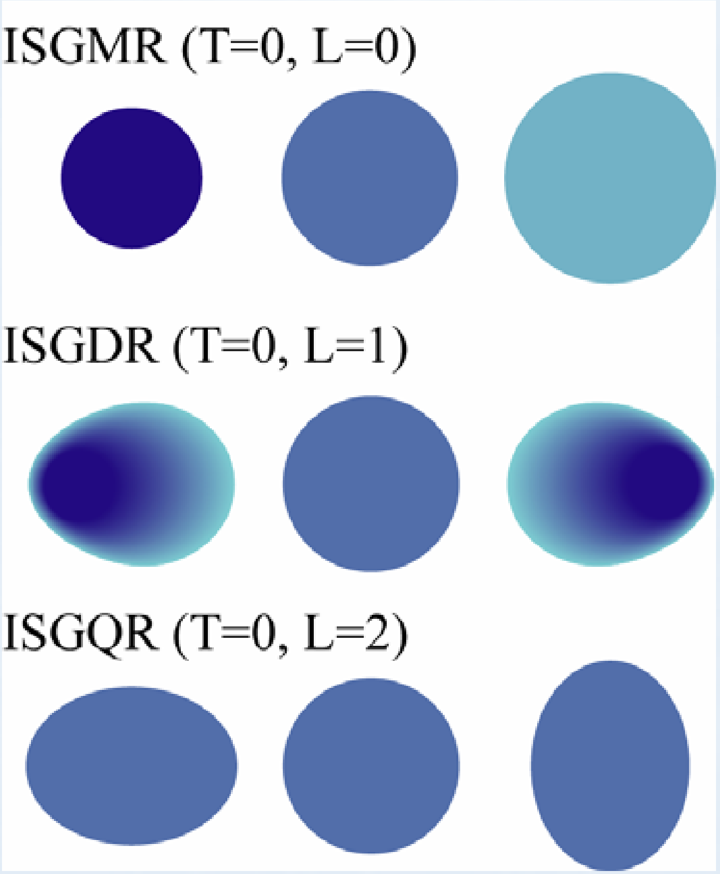

In HF+RPA calculations,

$$K_{nm}=\left[9\rho^2\frac{d^2(E/A)}{d\rho^2}\right]_{\rho=\rho_0}$$

Nuclear matter

E/A: binding energy per nucleon **K_A: incompressibity**

ρ : nuclear density **ε_F: Fermi energy**

ρ_0 : nuclear density at saturation

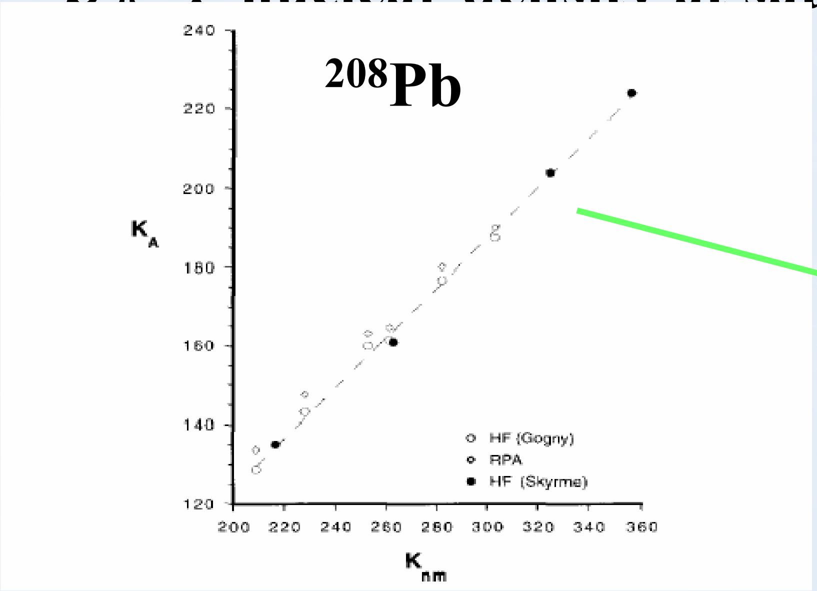

K_A is obtained from excitation energy of ISGMR & ISGDR

K_A =0.64K_{nm}- 3.5

J.P. Blaizot, NPA591 (1995) 435

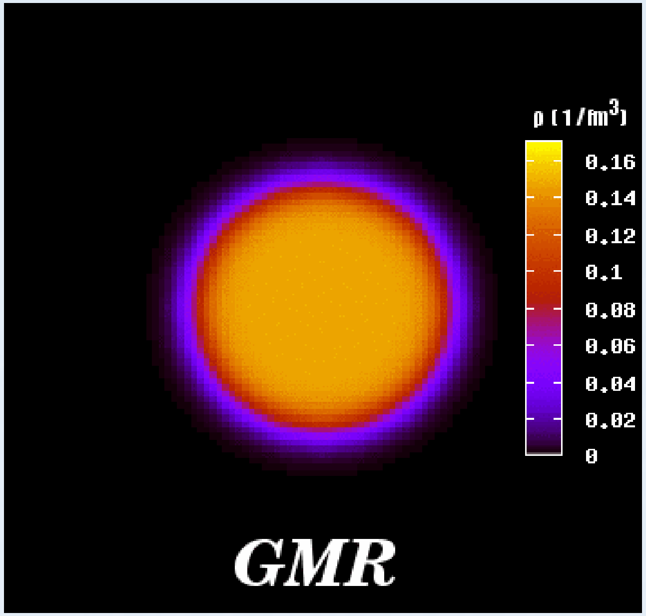
ρ (1/fm3)
0.16
0.14
0.12
0.1
0.08
0.06
0.04
0.02
0
GMR

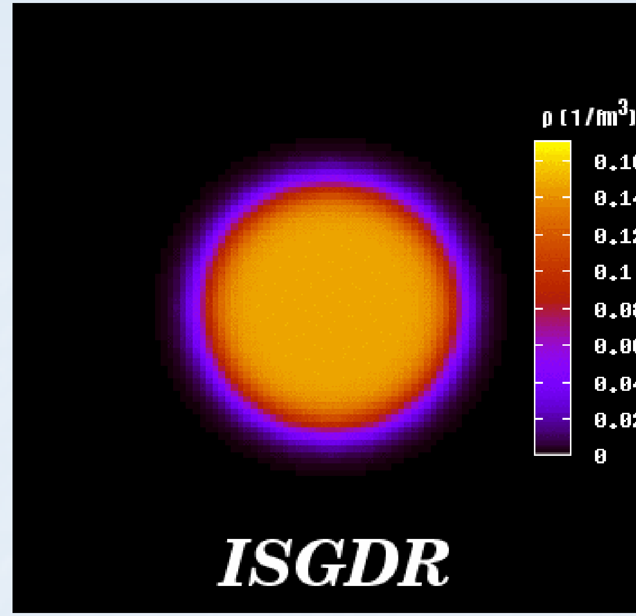
ρ (1/fm3)
0.16
0.14
0.12
0.1
0.08
0.06
0.04
0.02
0
ISGDR

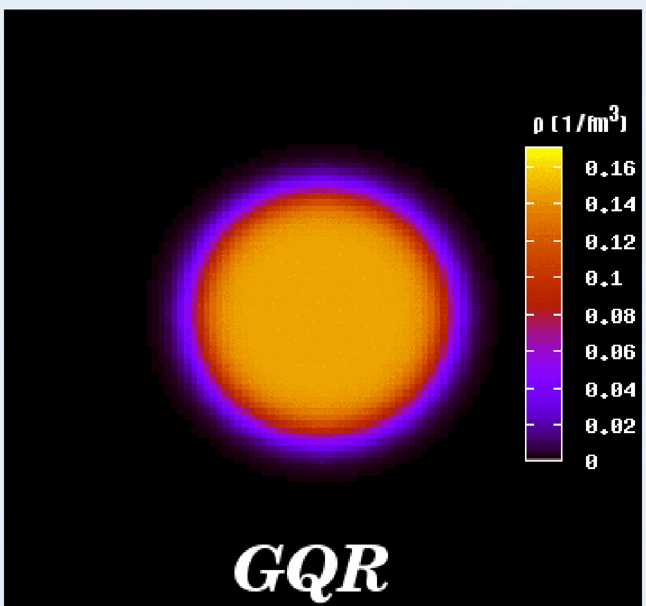
ρ (1/fm3)
0.16
0.14
0.12
0.1
0.08
0.06
0.04
0.02
0
GQR

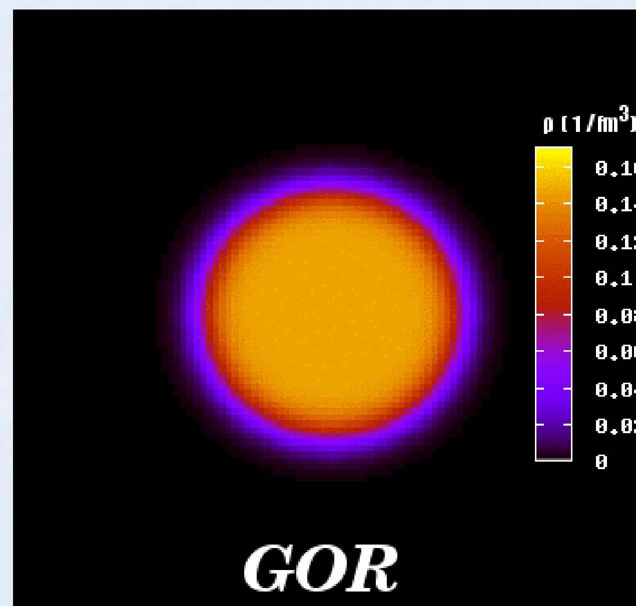
ρ (1/fm3)
0.16
0.14
0.12
0.1
0.08
0.06
0.04
0.02
0
GOR

HF+RPA; ISGDR in ^{208}Pb

I. Hamamoto el al.

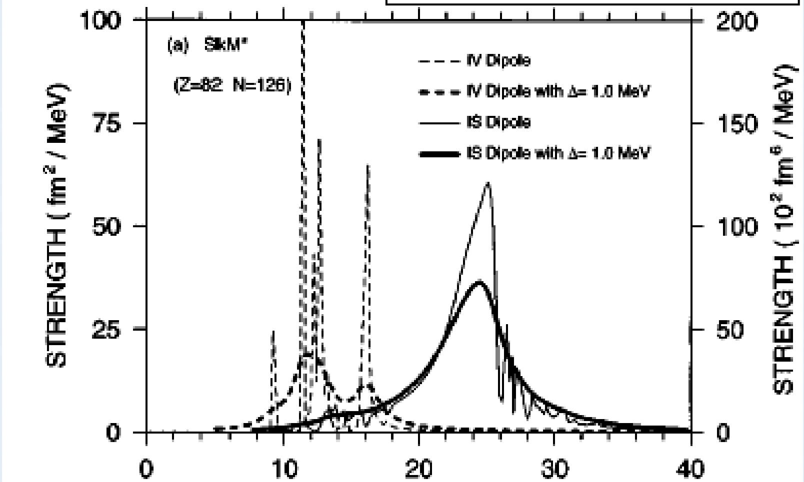

J. Pikarewicz

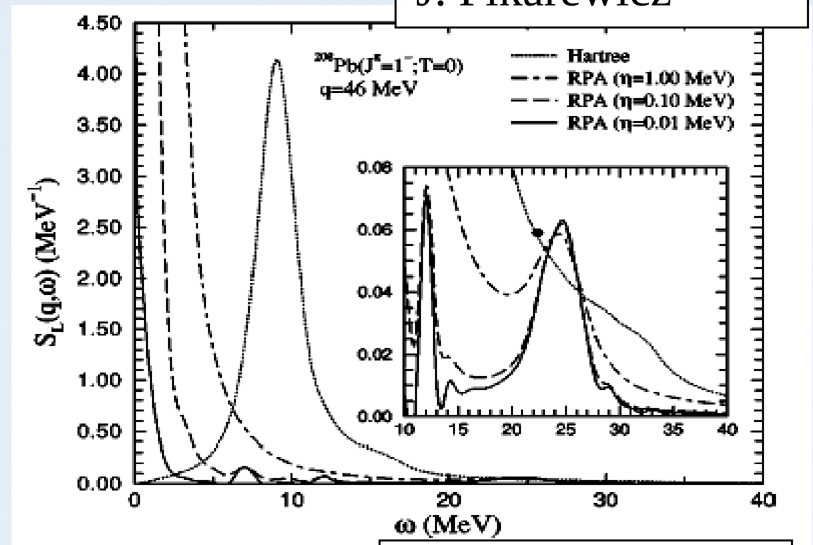

G. Colo et al.

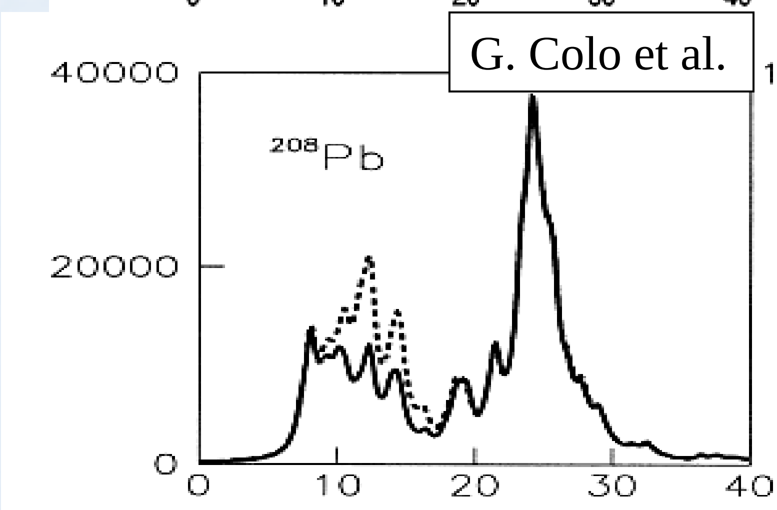

D. Vretenar et al.

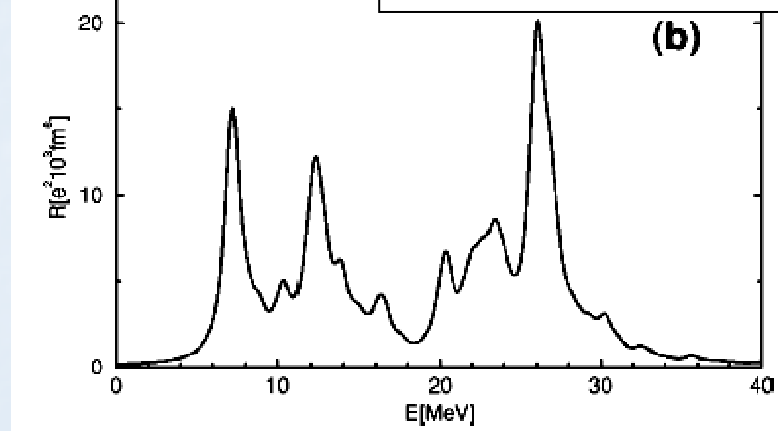

ISGQR, ISGMR, ISGDR

KVI (1977)

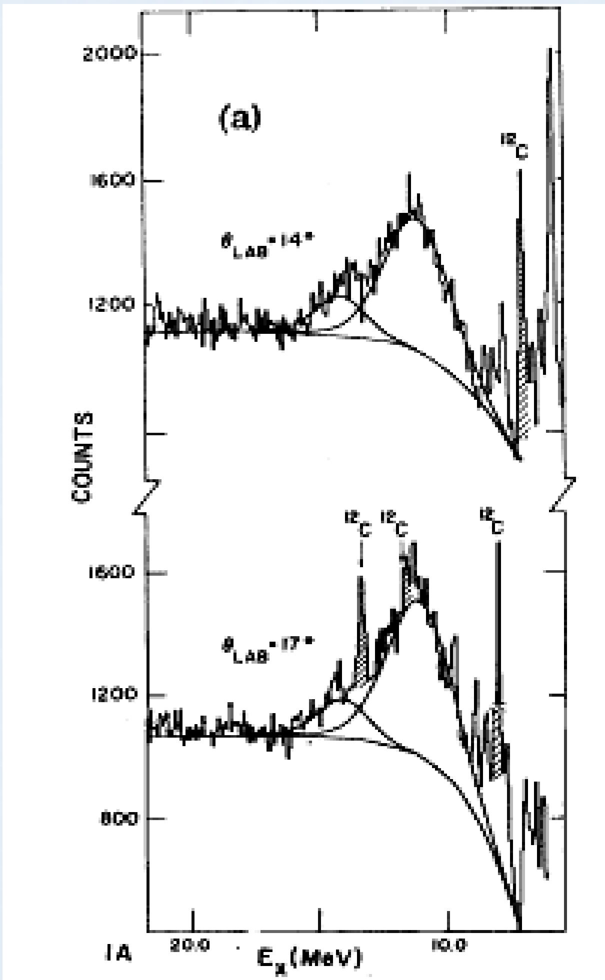

TAMU(2000)

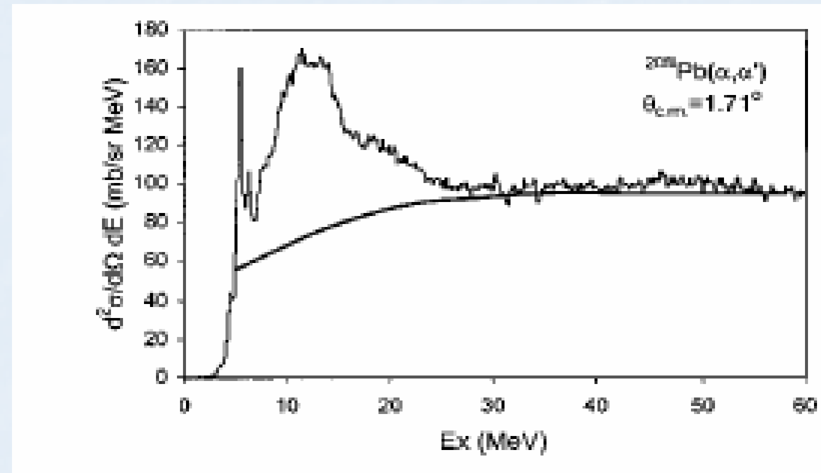

⇑

E_α=240 MeV

Large instrumental background!

⇐ ^{208}Pb(α,α′) at E_α=120 MeV

KVI

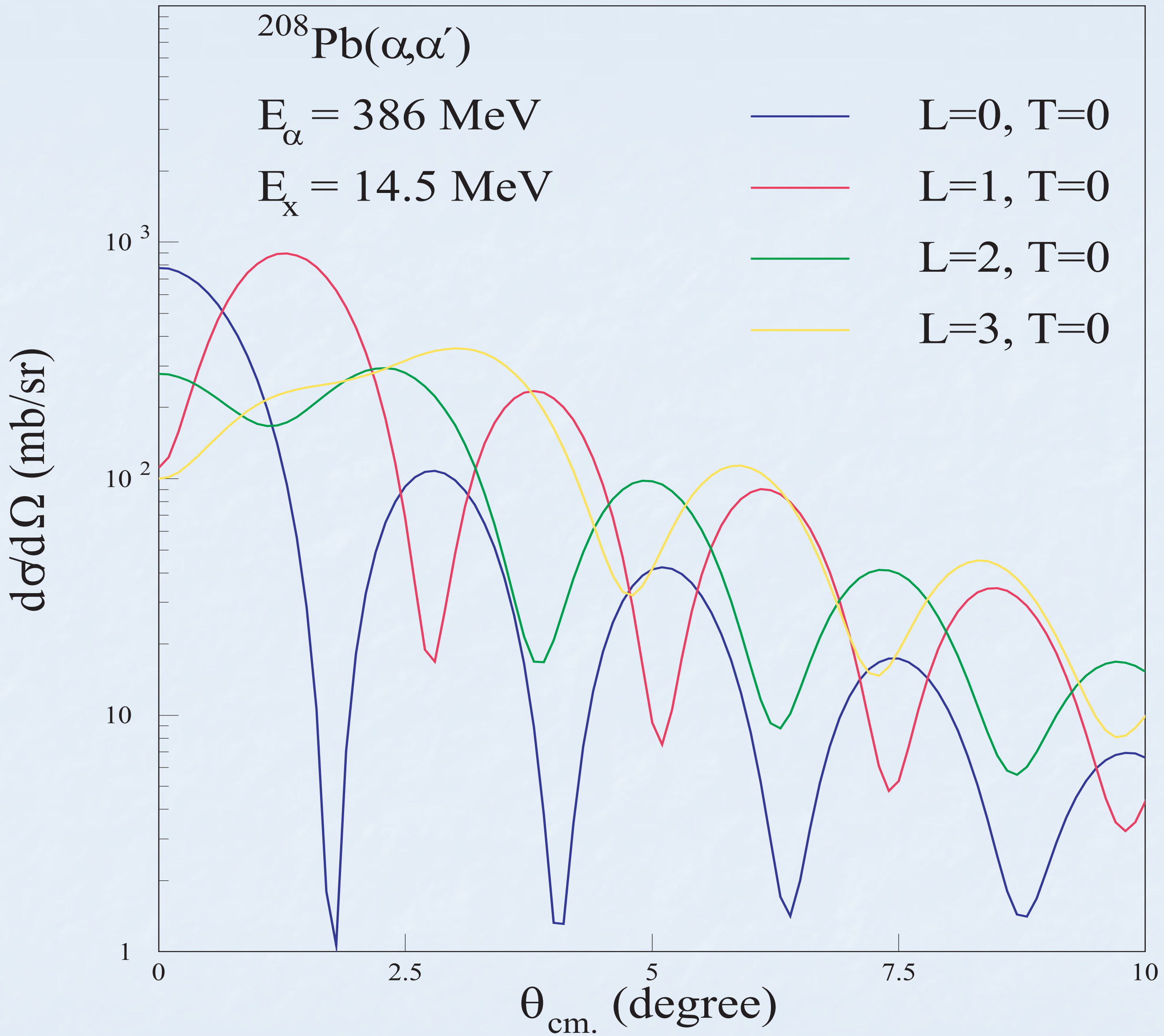

ISGMR, ISGDR

ISGQR, HEOR

100 % EWSR

At E_x= 14.5 MeV

Uchida et al., RCNP

(α,α’) spectra at 386 MeV

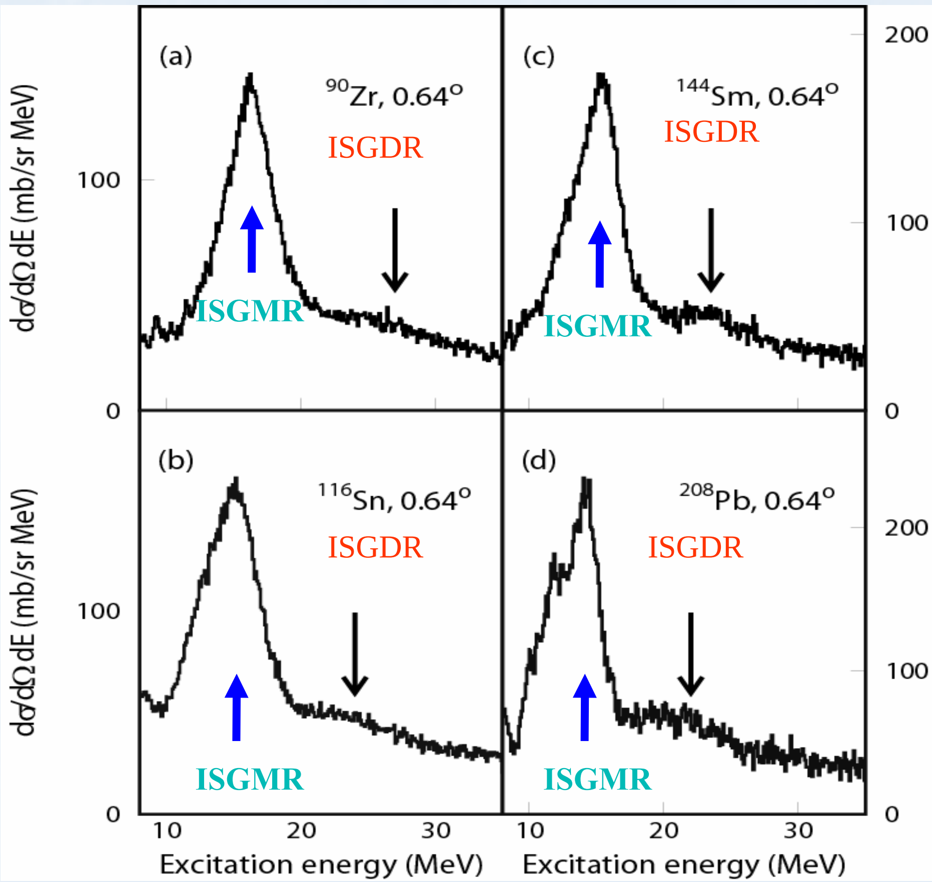

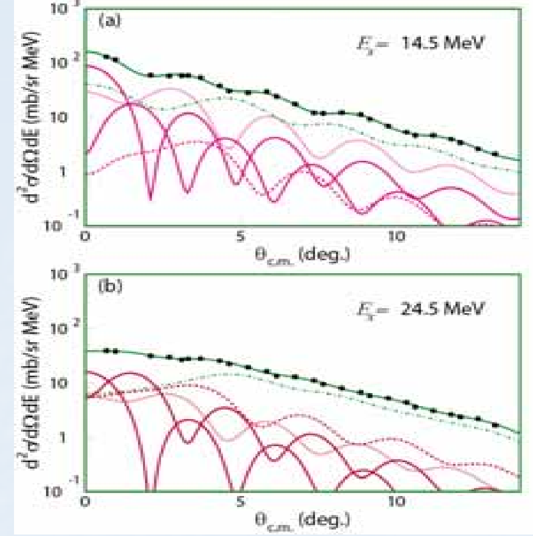

^{116}Sn

MDA results for L=0 and L=1

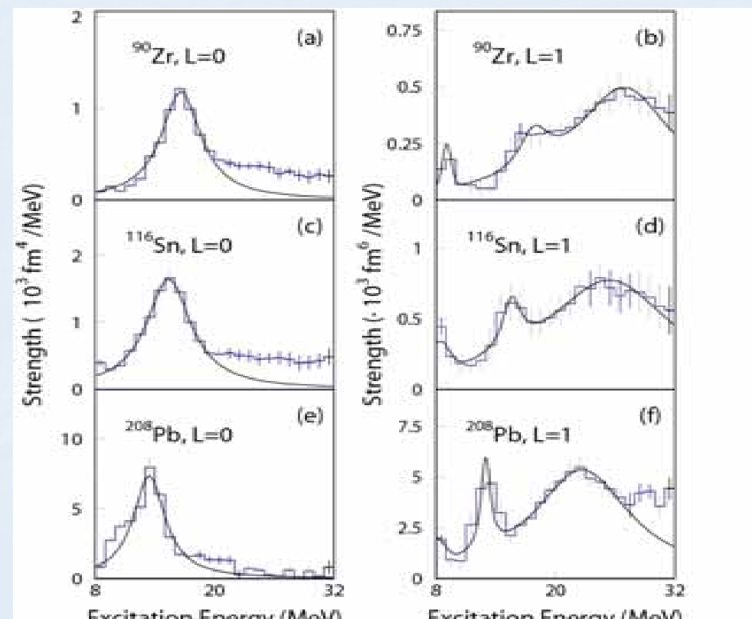

Multipole decomposition analysis (MDA)

$$\left(\frac{d^2\sigma}{d\Omega dE}(\vartheta_{c.m.},E)\right)^{ex.} = \sum_L a_L(E)\left(\frac{d^2\sigma}{d\Omega dE}(\vartheta_{c.m.},E)\right)_L^{calc}$$

$$\left(\frac{d^2\sigma}{d\Omega dE}(\vartheta_{c.m.},E)\right)^{ex.} : \text{Exprimenta l cross section}$$

$$\left(\frac{d^2\sigma}{d\Omega dE}(\vartheta_{c.m.},E)\right)_L^{calc} : \text{DWBA cross section (unit cross section)}$$

$a_L(E)$: EWSR fraction

a. ISGR (L<15)+ IVGDR (through Coulomb excitation)

b. DWBA formalism; single folding $\Rightarrow$ transition potential

$$\delta U(r,E) = \int d\vec{r}'\,\delta\rho_L(\vec{r}',E)[V(|\vec{r}-\vec{r}'|,\rho_0(r')) + \rho_0(r')\frac{\partial V(|\vec{r}-\vec{r}'|,\rho(r'))}{\partial\rho_0(r')}$$

$$U(r) = \int d\vec{r}'\,V(|\vec{r}-\vec{r}'|,\rho_0(r'))\rho_0(r')$$

Transition density

- **ISGMR Satchler, Nucl, Phys, A472 (1987) 215**

$$\delta\rho_0(r,E) = -\alpha_0\left[3 + r\frac{d}{dr}\right]\rho_0(r)$$

$$\alpha_0^2 = \frac{2\pi\hbar^2}{mA<r^2>E}$$

- **ISGDR Harakeh & Dieperink, Phys. Rev. C23 (1981) 2329**

$$\delta\rho_1(r,E) = -\frac{\beta_1}{R\sqrt{3}}\left[3r^2 + \frac{d}{dr} + 10r - \frac{5}{3}<r^2>\frac{d}{dr} + \varepsilon\left(r\frac{d^2}{dr^2} + 4\frac{d}{dr}\right)\right]\rho_0(r)$$

$$\beta_1^2 = \frac{6\pi\hbar^2}{mAE}\frac{R^2}{(11<r^4> - (25/3)<r^2>^2 - 10\varepsilon<r^2>)}$$

- **Other modes Bohr-Mottelson (BM) model**

$$\delta\rho_L(r,E) = -\delta_L\frac{d}{dr}\rho_0(r)$$

$$\delta_L^2 = (\beta_L c)^2 = \frac{l(2l+1)^2}{(l+2)^2}\frac{2\pi\hbar^2}{mAE}\frac{<r^{2l-2}>}{<r^{l-2}>^2}$$

Results of ISGMR/ISGDR

	E_{GMR} (MeV)	Γ (MeV)	EWSR (%)	E_{LEGDR} (MeV)	Γ (MeV)	EWSR (%)	E_{HEGDR} (MeV)	Γ (MeV)	EWSR (%)
^{90}Zr	16.6 (0.1)	4.9 (0.2)	101 (3)	17.8 (0.5)	3.7 (1.2)	7.9 (2.9)	26.9 (0.7)	12.0 (1.5)	67 (8)
^{116}Sn	15.4 (0.1)	5.5 (0.3)	95 (4)	15.6 (0.5)	2.3 (1.)	4.9 (2.2)	25.4 (0.5)	15.7 (2.3)	68 (9)
^{144}Sm	15.3 (0.1)	3.71 (0.12)	84 (4,-25)	14.2 (0.2)	4.8 (0.8)	23 (4,-10)	25.0 (1.7)	19.9 (1.4)	91 (25,-17)
^{208}Pb	13.5 (0.2)	4.0 (0.4)	104 (9)	13.0 (0.1)	1.1 (0.4)	7.0 (0.4)	22.8 (0.3)	11.9 (0.4)	111 (6)

ΔE is about 0.1 MeV

KVI

L=0

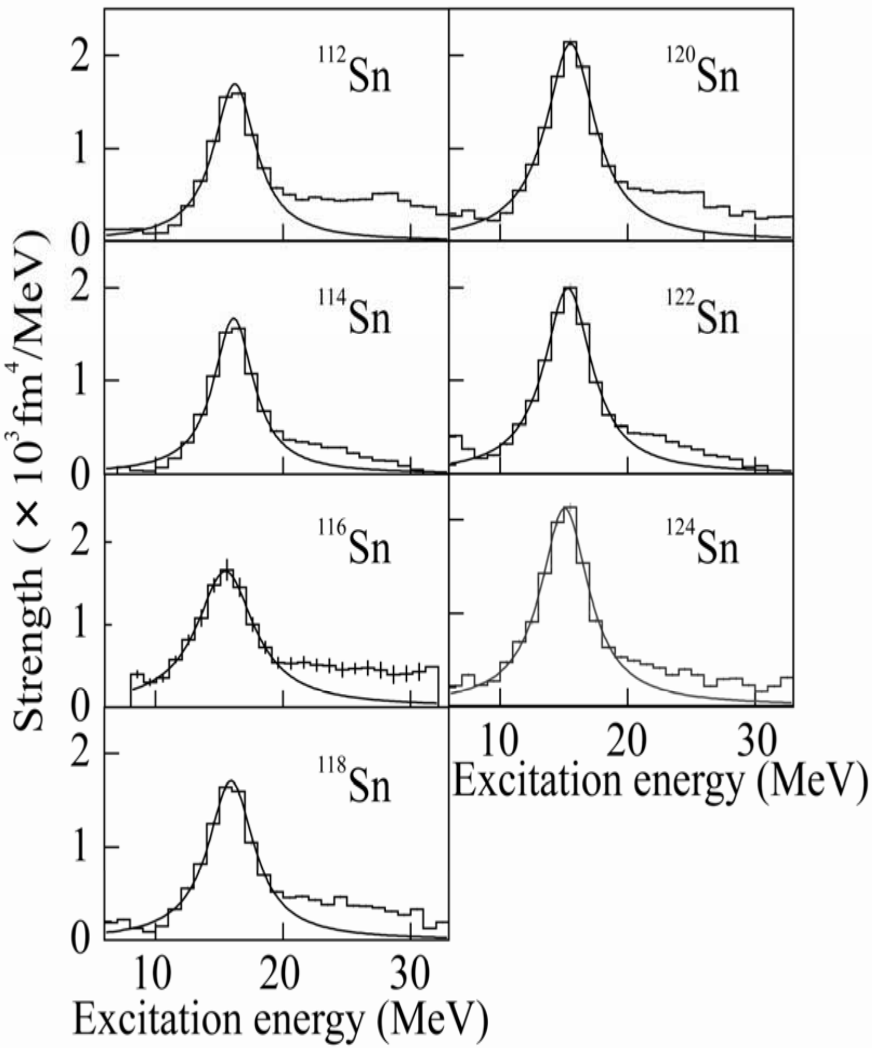

Breit-Wigner shape:

	E_m (MeV)	Γ_m (MeV)
^{112}Sn	16.1 ±0.1	4.4 ±0.2
^{114}Sn	16.0 ±0.1	4.0 ±0.1
^{116}Sn	15.4 ±0.1	5.7 ±0.3
^{118}Sn	15.7 ±0.1	4.6 ±0.2
^{120}Sn	15.3 ±0.1	4.8 ±0.2
^{122}Sn	15.1 ±0.1	4.5 ±0.2
^{124}Sn	14.9 ±0.1	4.5 ±0.3

^{112,114,118,120,122,124}Sn: this work

^{116}Sn: Uchida et al.

ISGMR energy E_{ISGMR}

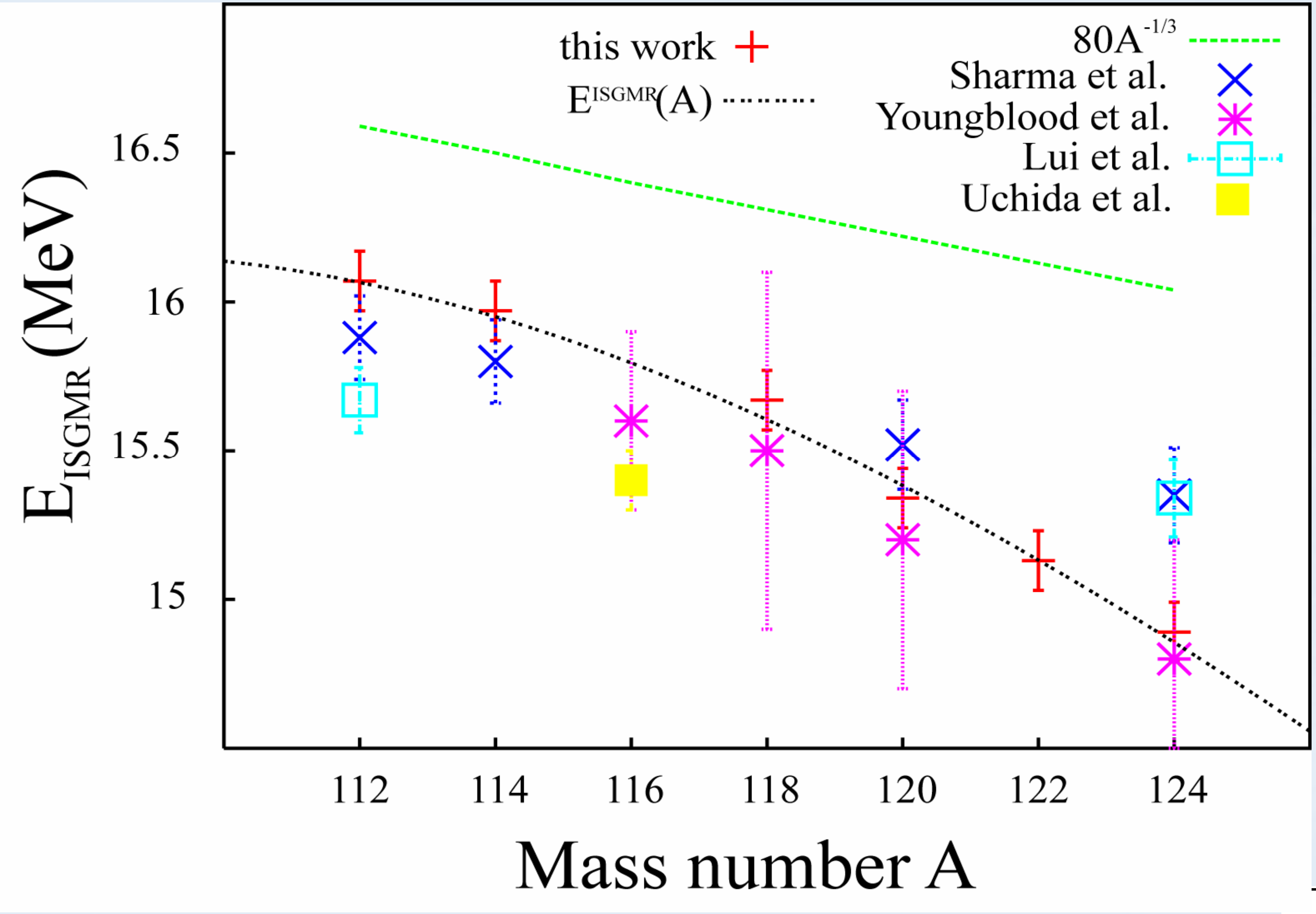

^{208}Pb

	E_{ISGDR} (MeV)		E_{ISGMR} (MeV)	K_{nm} (MeV)
	HE	LE		
Uchida et al. (Breit-Wigner)	22.8 (0.3)	13.0 (0.2)	13.5 (0.2)	
Morsch et al.	21.3 (0.8)		13.8	
Djalali et al.	21.5 (0.2)		13.9	
Adams et al.	22.6 (0.2)			
Davis et al.	22.4(0.5)			
Clark et al.	19.9(0.8)	12.2(0.6)	14.17(0.28)	
Hamamoto et al.	23.4	~14	14.1	217
Colo et al.	23.9(22.9 *)	10.9	14.1	215
Piekarewicz et al.	24.4	~8	13.1	224
Vretenar et al.	26.01	10.4	14.1	271
Shlomo and Sanzhur	~25.0	~15	14.48	230
Gorelik and Urin	22.7	11.1	14.3	

* Including the effect of 2p-2h coupling

Decay of giant resonances

- **Width of resonance**

  Γ, $\Gamma^{\uparrow}$, $\Gamma^{\downarrow}$ ($\Gamma^{\downarrow\uparrow}$, $\Gamma^{\downarrow\downarrow}$)

  - **$\Gamma^{\uparrow}$: direct or escape width**
  - **$\Gamma^{\downarrow}$: spreading width**

    $\Gamma^{\downarrow\uparrow}$: pre-equilibrium, $\Gamma^{\downarrow\downarrow}$: compound
- **Decay measurements**

  $\Rightarrow$ Direct reflection of damping processes

  Allows detailed comparison with theoretical calculations

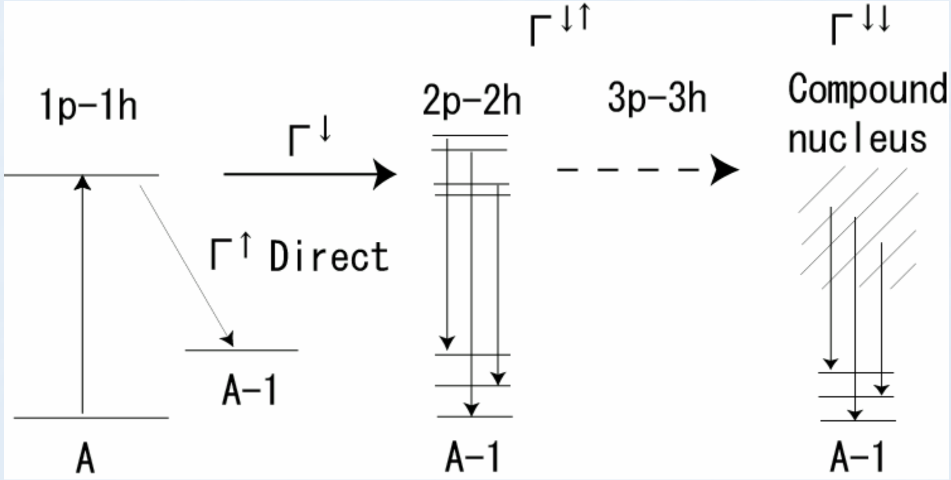

Decay and microscopic structure of ISGDR

Transition operator

$$\mathrm{O}^{L=1} = \cancel{\sum_i r_i Y_0^1} + \sum_i r_i^3 Y_0^1 + ..$$

spurious center of mass motion **overtone**

3 ħω excitation (overtone of c.o.m. motion)

AGOR cyclotron K = 600
light and heavy ions
p < 190 MeV
q/A = ½ ; E/A < 90 MeV

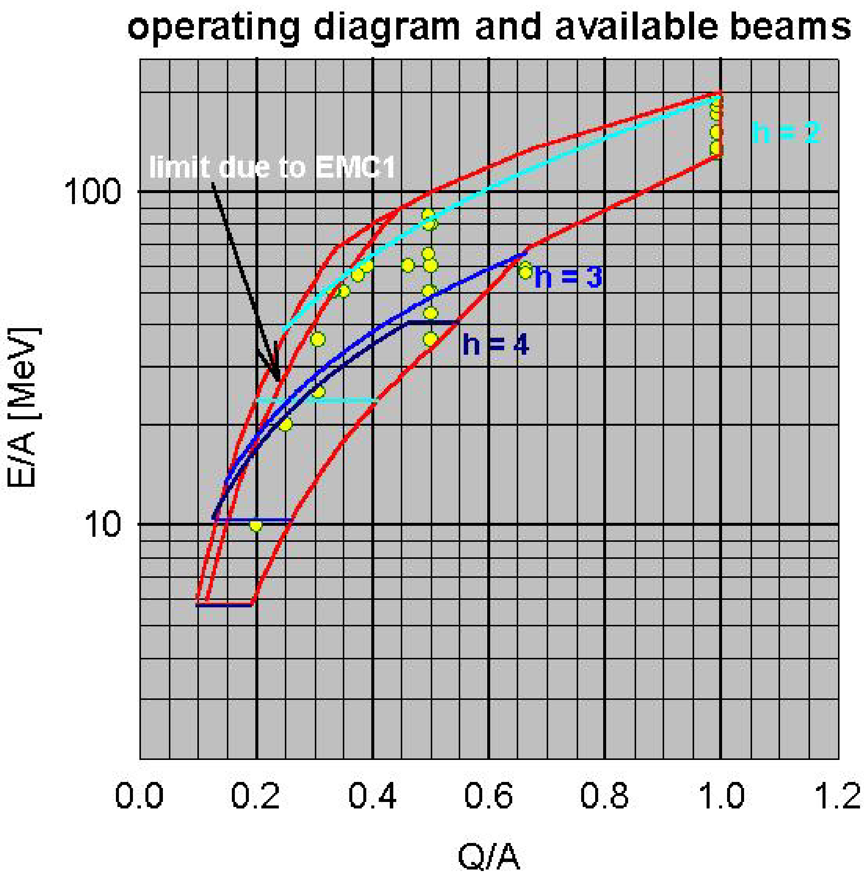

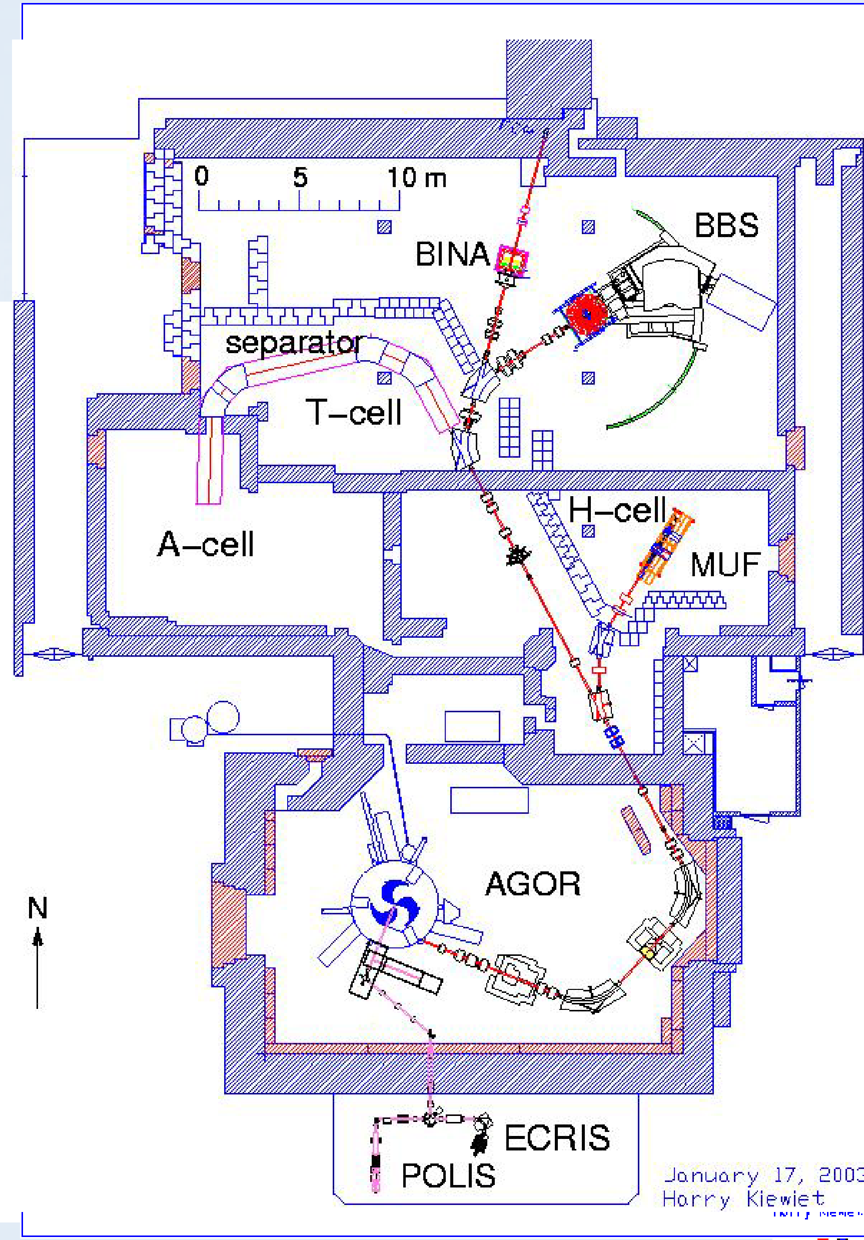

KVI

Equipment

- Big momentum Bite magnetic Spectrometer (BBS)
- its associated Focal-Plane Detectors (ESN)
- various coincidence detectors

  neutrons (EDEN), protons (SiLi-ball), γ's (GeLi, Clover), phoswich detectors
- readout electronics

  DSP, VME, FERA

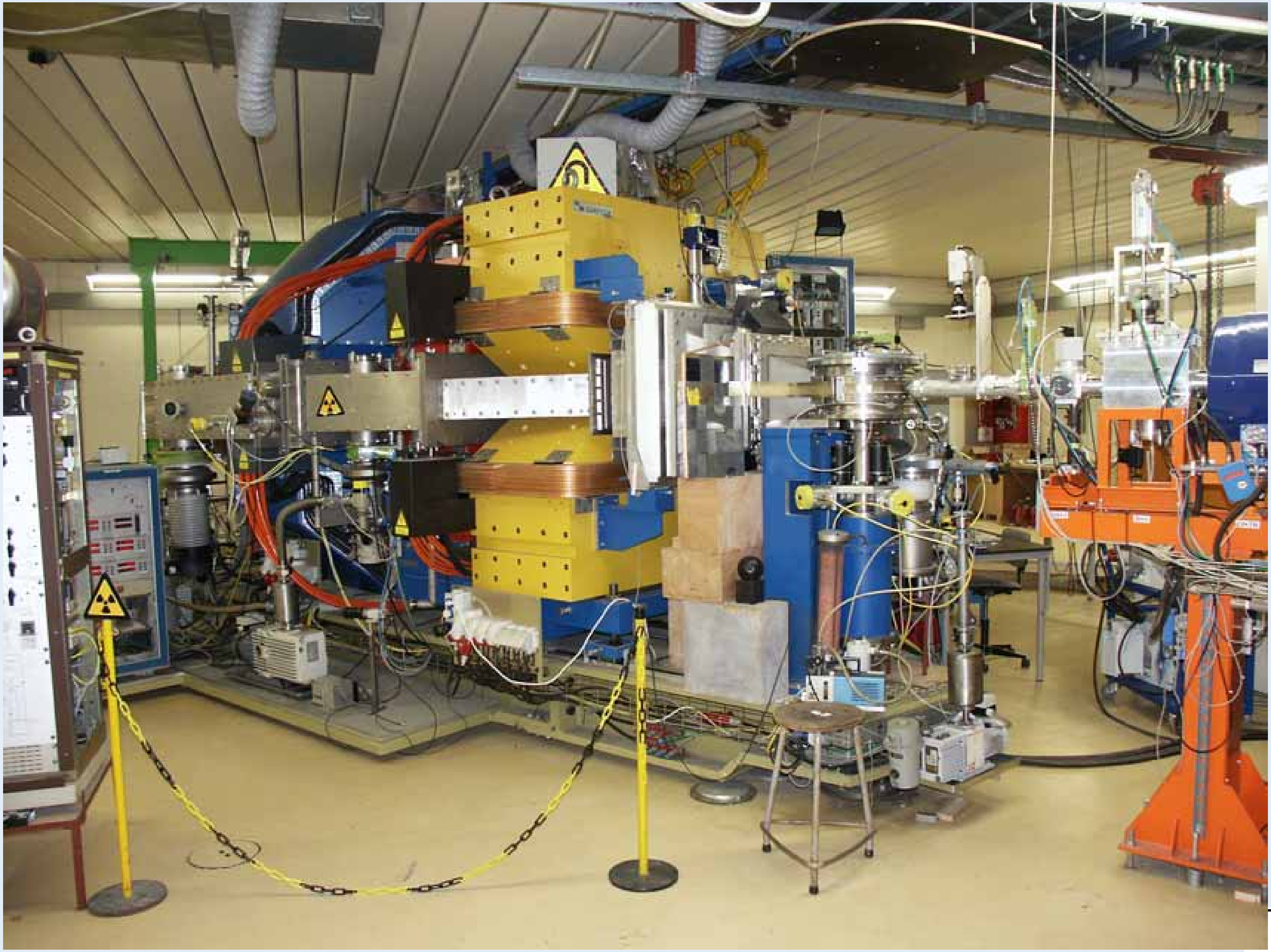

Si-ball
16 Si-detectors at
10 cm from the target
total solid angle: 1 sr

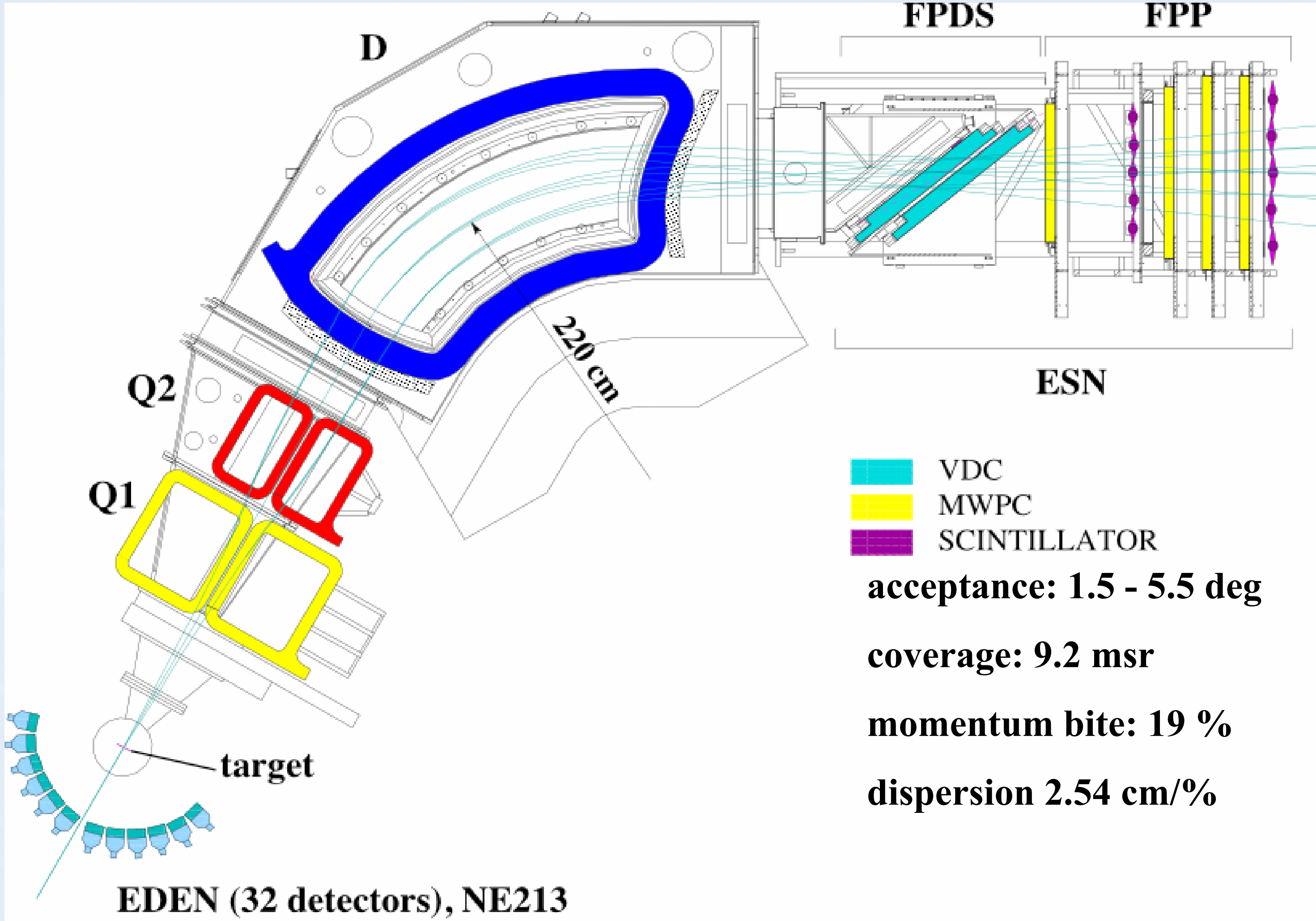

acceptance: 1.5 - 5.5 deg

coverage: 9.2 msr

momentum bite: 19 %

dispersion 2.54 cm/%

total solid angle: 0.37 sr

KVI Big-Bite Spectrometer (BBS)

Setup: ESN detector

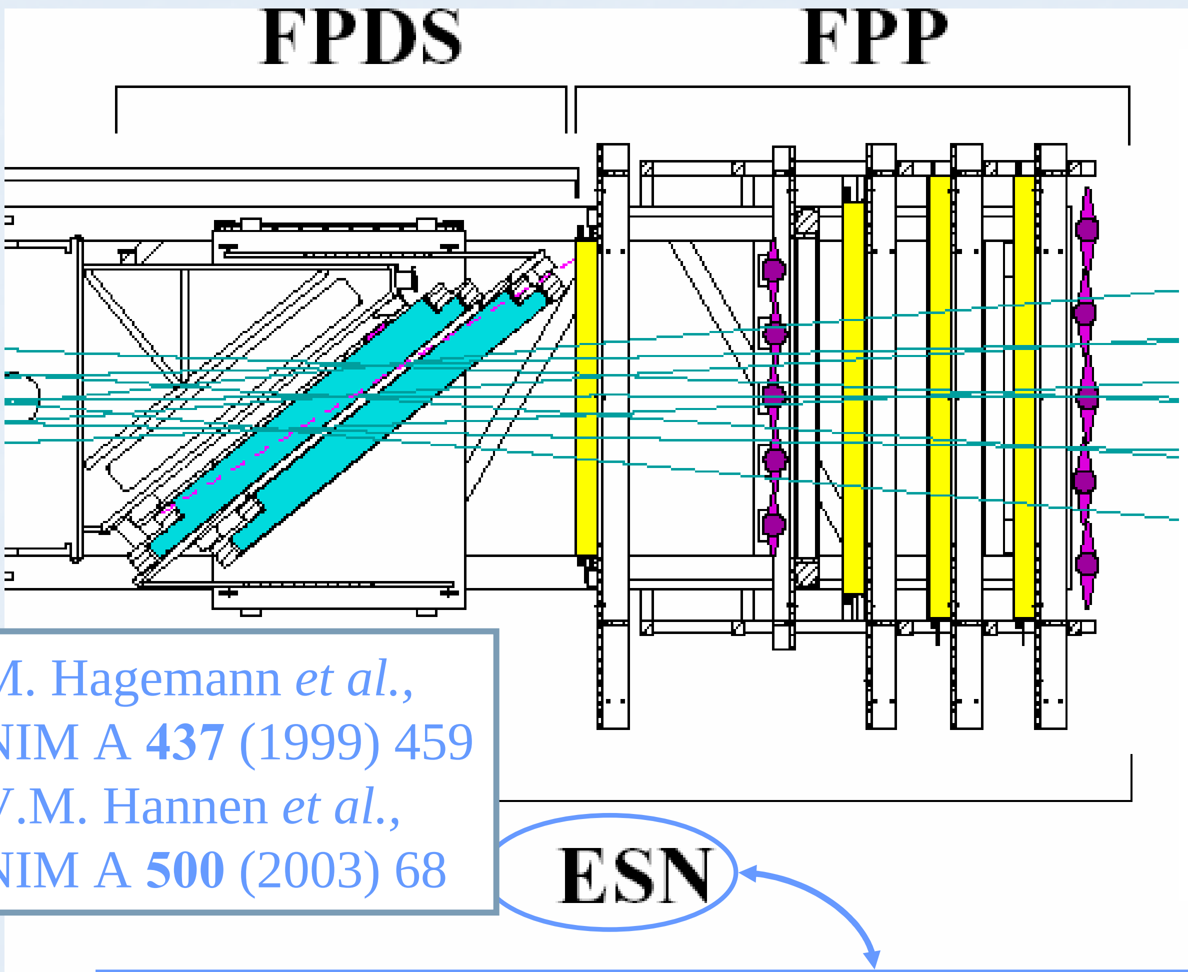

Focal-Plane Detector:
(FPDS): 2 VDCs

Focal-Plane Polarimeter:
(FPP): 4 MWPCs &
graphite analyzer

features a.o.:
fast readout
VDC readout **pipeline TDCs**
VDC decoding using
imaging techniques
DSP based online analysis

M. Hagemann *et al.*,
NIM A **437** (1999) 459
V.M. Hannen *et al.*,
NIM A **500** (2003) 68

Bari, Darmstadt, Gent, Iserlohn, KVI, Milano, Münster, TRIUMF

KVI

Excitation of ISGDR in ^{208}Pb

- In ^{208}Pb located around 22 MeV and width of 4 MeV
- *L=1* angular distribution peaks close to a scattering angle of 0^{o}
- Difficult to identify in nuclear continuum and rides on instrumental background

Singles ^{208}Pb(α,α') 200 MeV ⇒

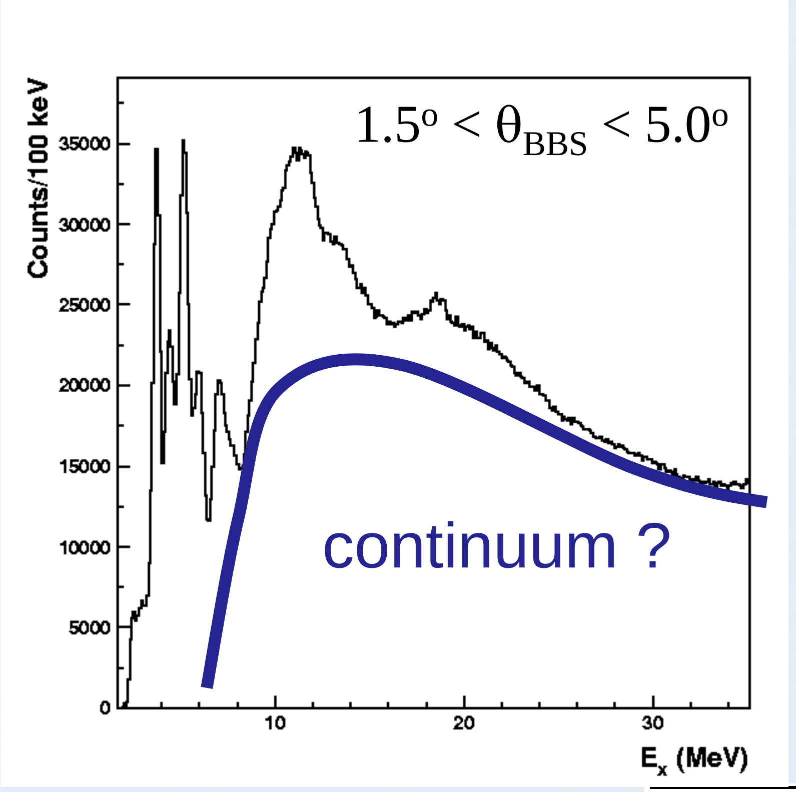

ISGDR L = 1

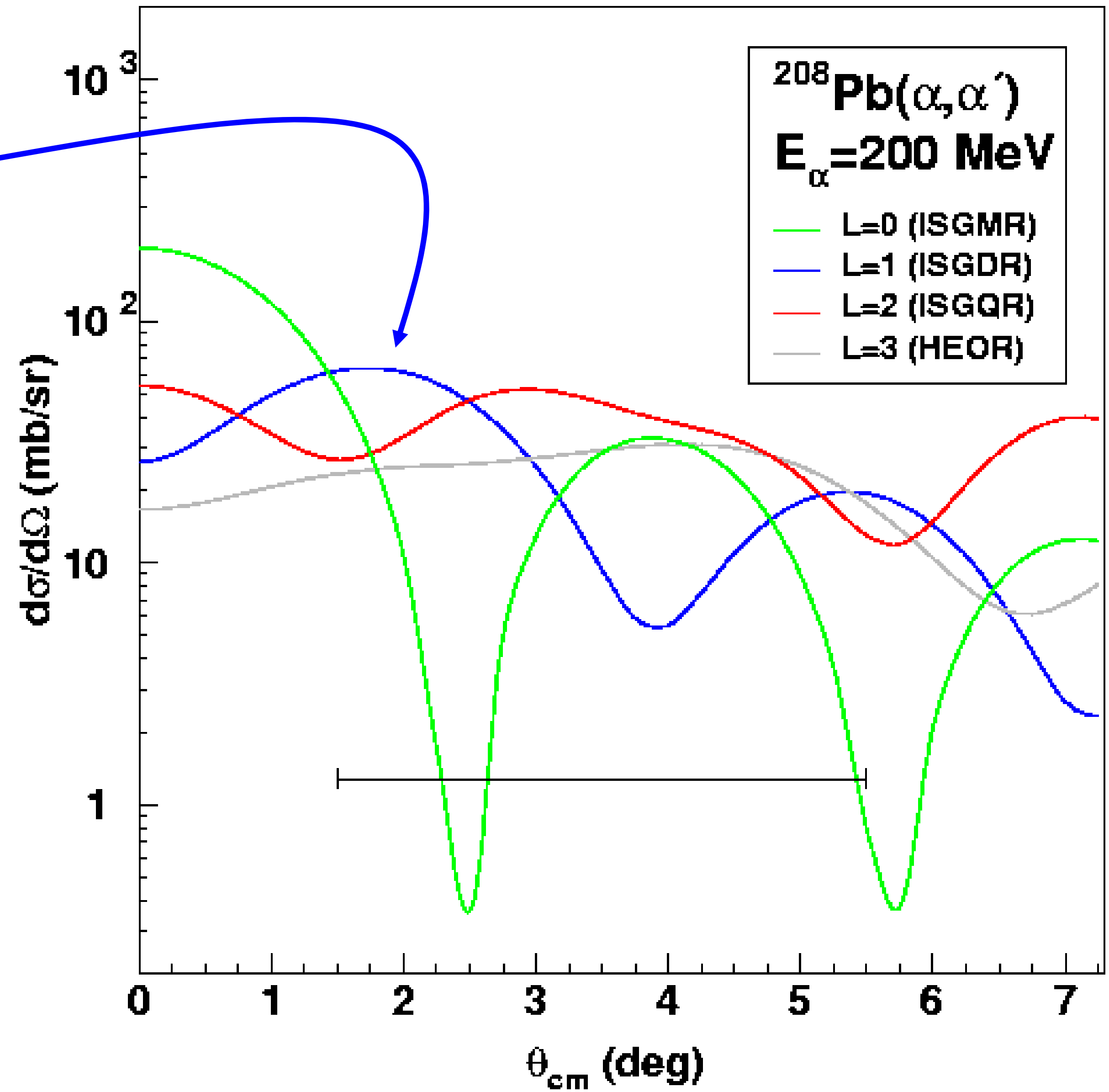

$^{208}Pb(\alpha,\alpha')$
E_α=200 MeV
L=0 (ISGMR)
L=1 (ISGDR)
L=2 (ISGQR)
L=3 (HEOR)
$d\sigma/d\Omega$ (mb/sr)
θ_{cm} (deg)
10^3
10^2
10
1
0
1
2
3
4
5
6
7

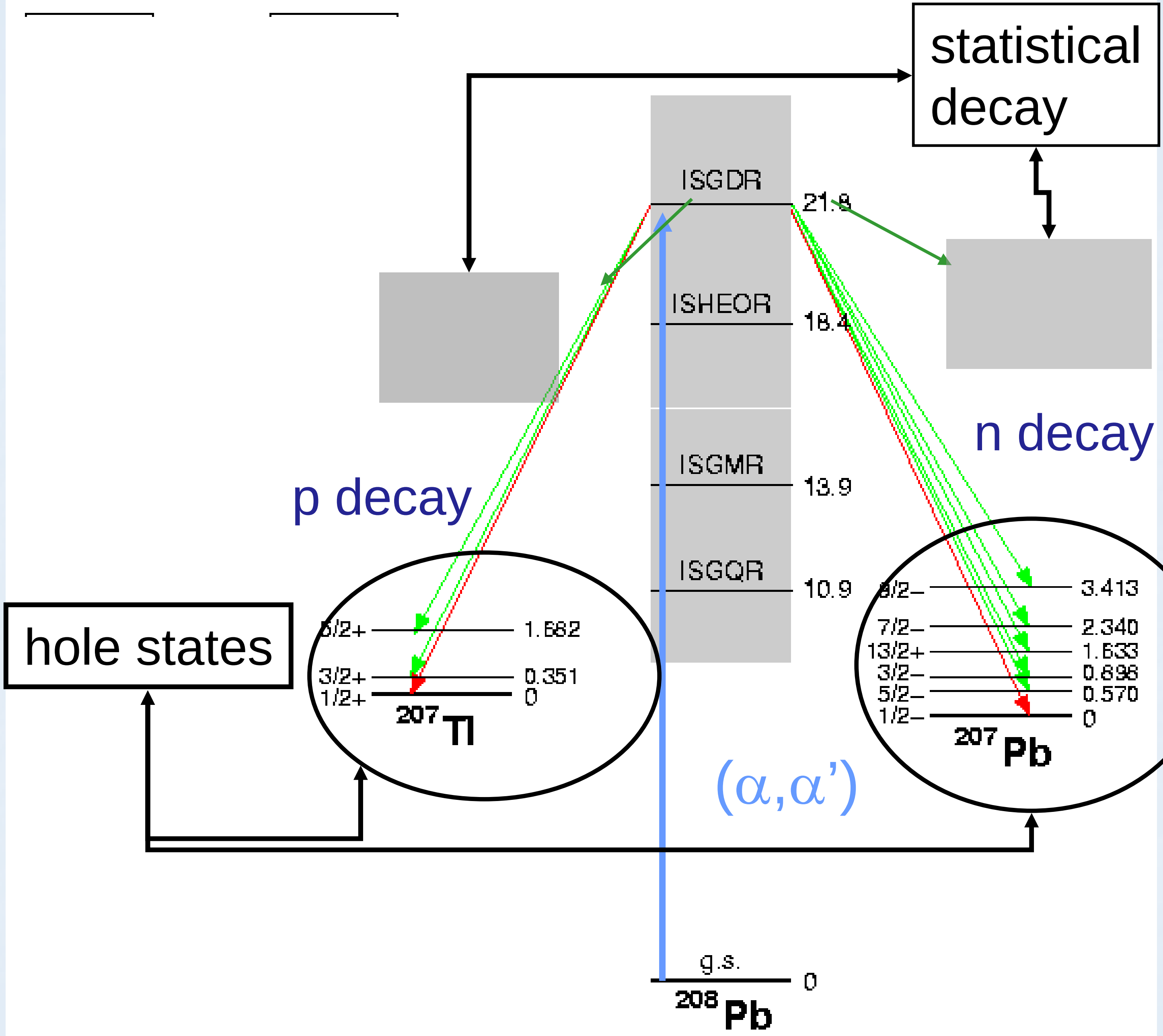
statistical decay
ISGDR
21.9
ISHEOR
18.4
ISGMR
13.9
ISGQR
10.9
n decay
p decay
hole states
5/2+
1.682
3/2+
0.351
1/2+
0
207Tl
9/2–
3.413
7/2–
2.340
13/2+
1.633
3/2–
0.898
5/2–
0.570
1/2–
0
207Pb
(α,α')
g.s.
0
208Pb

Proton-decay detection

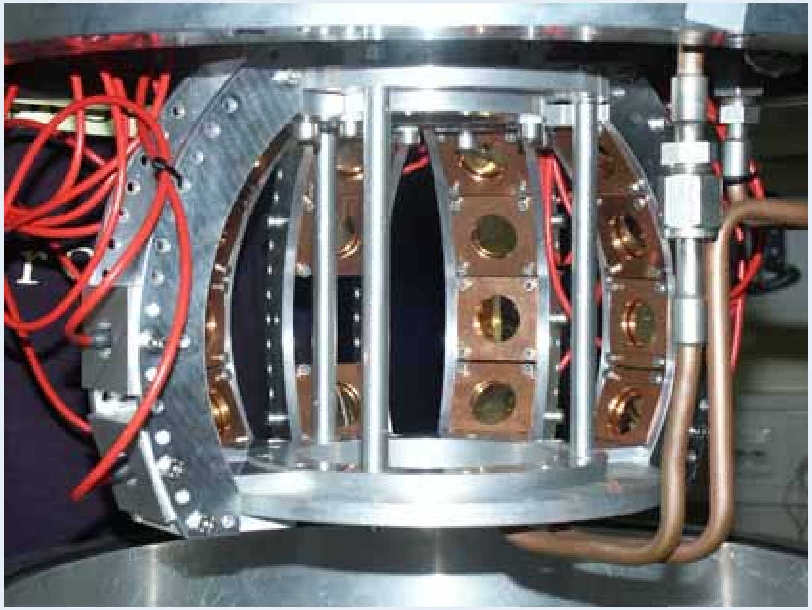

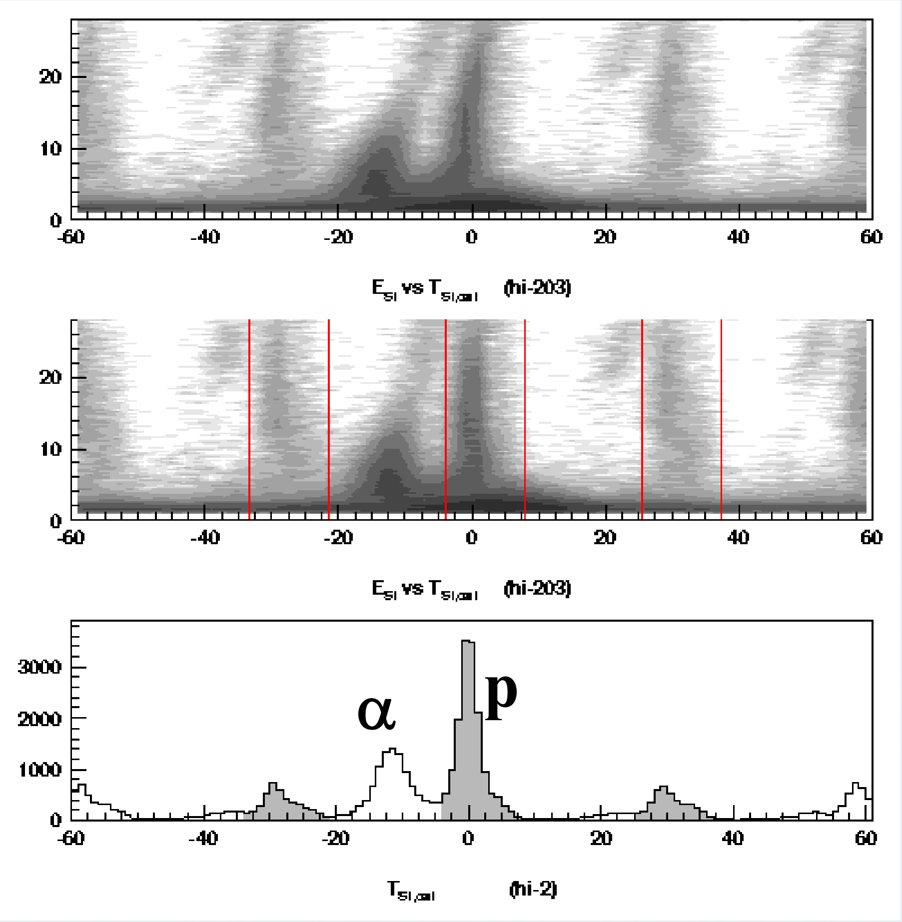

α-p separation using rise time of signal SiLi

Neutron-decay detection

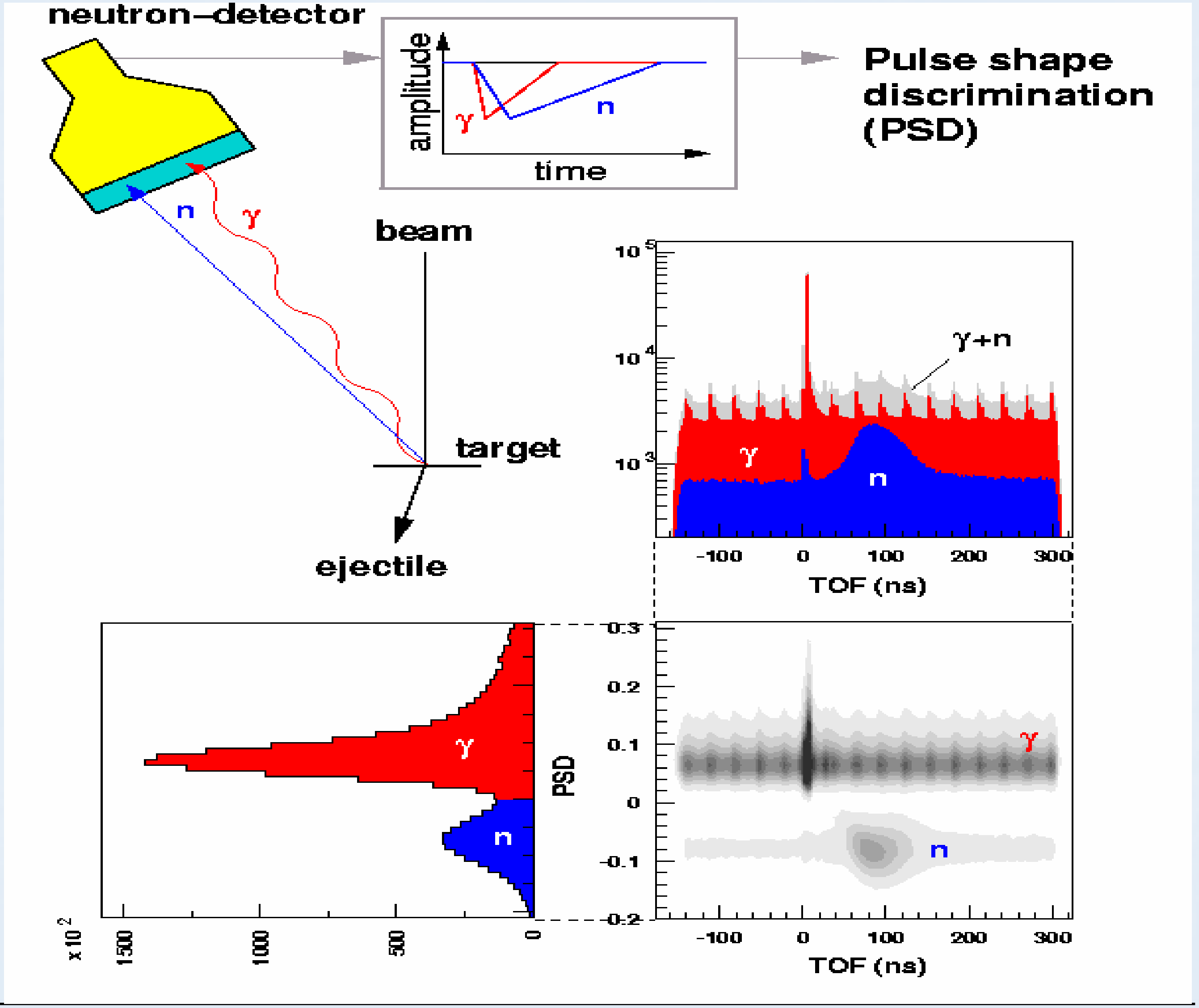

^{208}Pb(α,α' p or n)

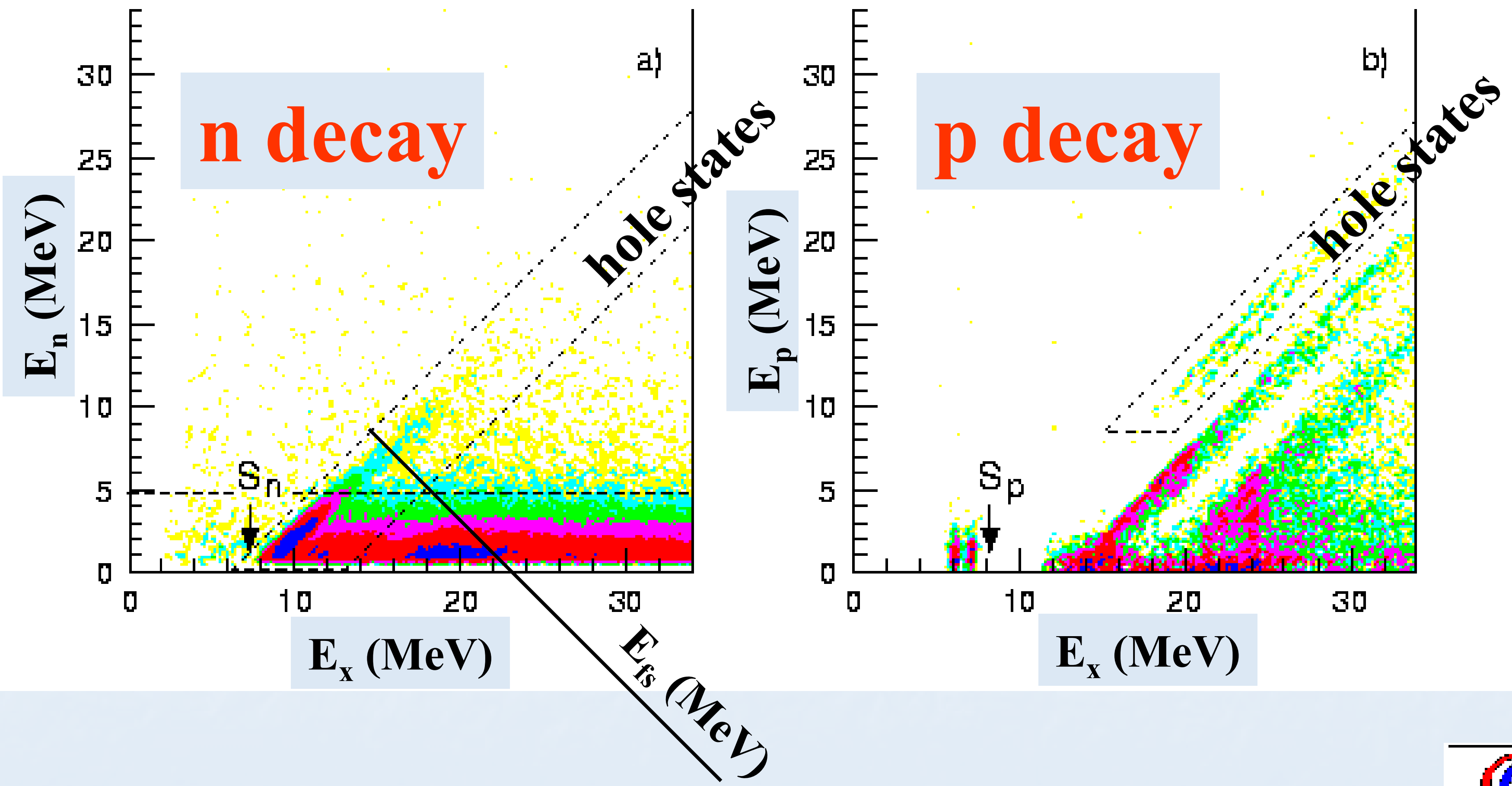

^{208}Pb(α,α') followed by n decay

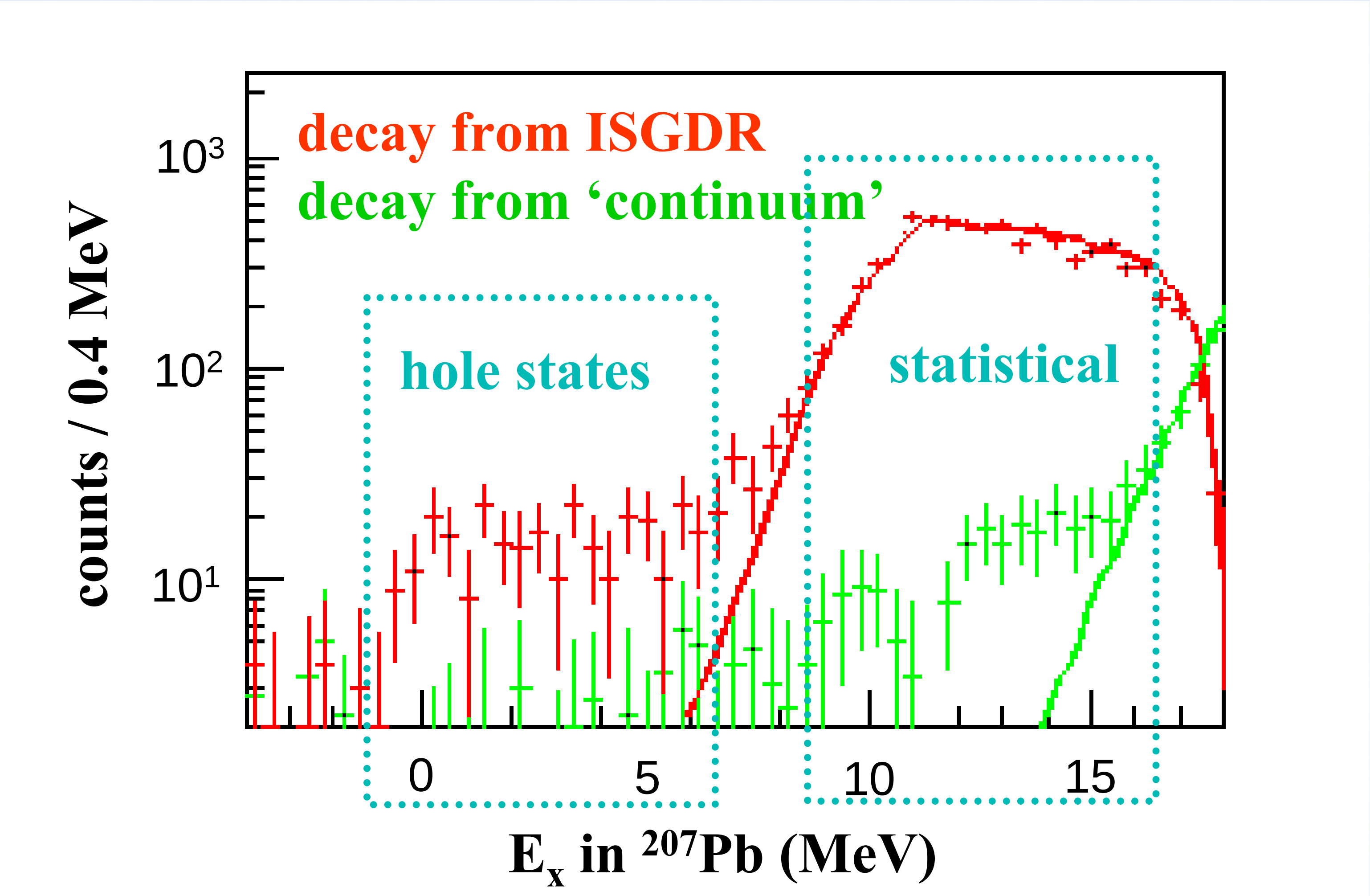

Statistical decay Direct decay

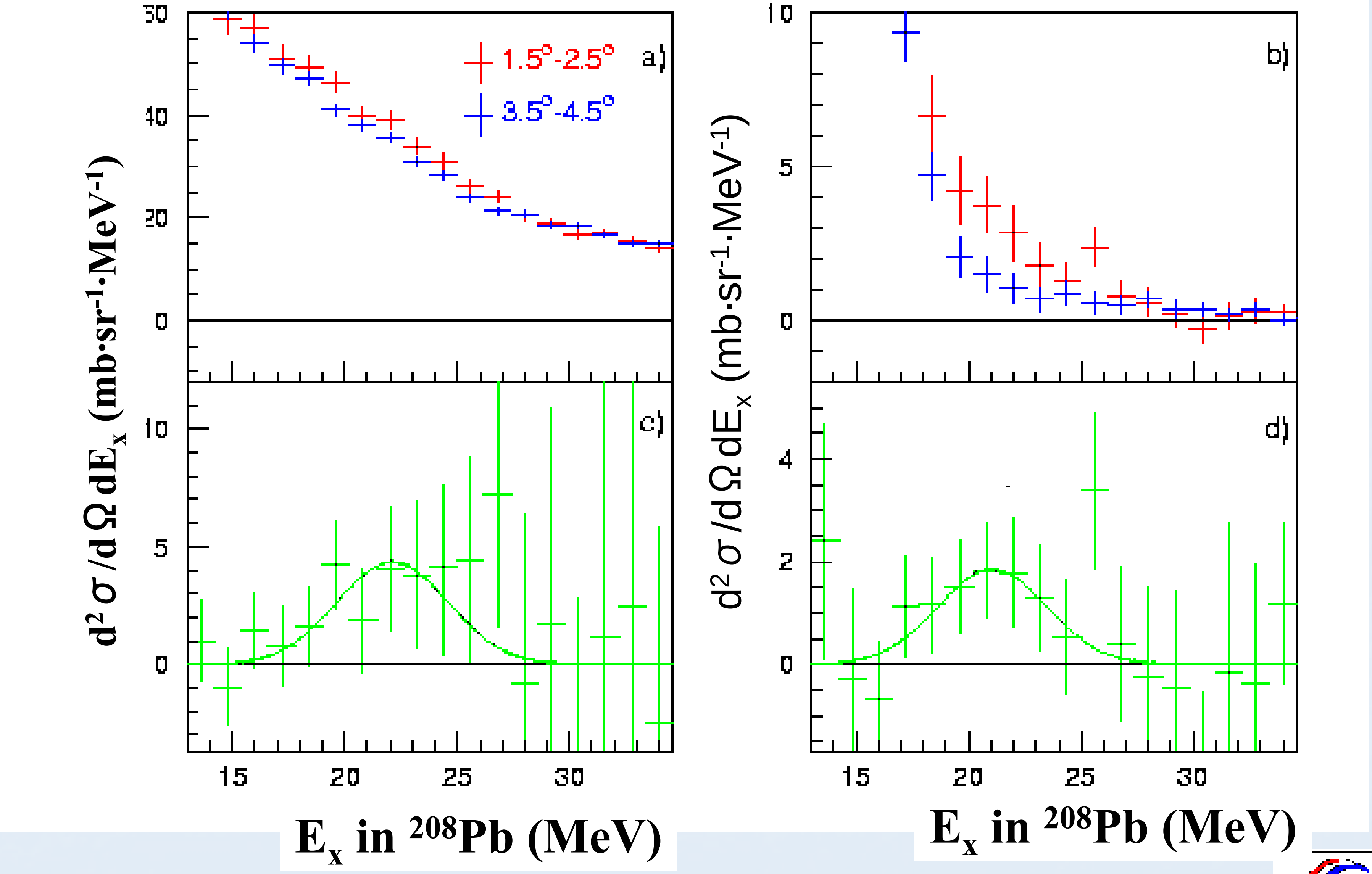

^{208}Pb(α,α') followed by p decay

Decay to hole states in ^{207}Tl; branching ratios predicted by Gorelik *et al.*

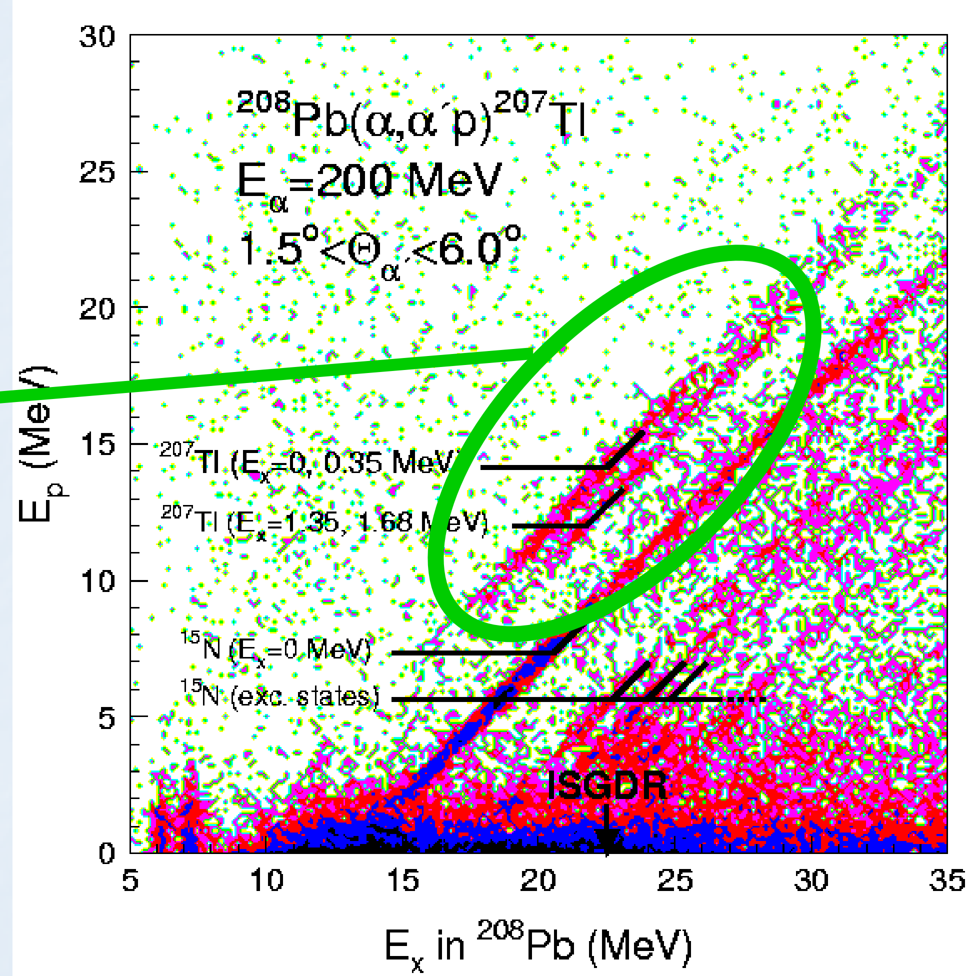

Branching ratios for decay

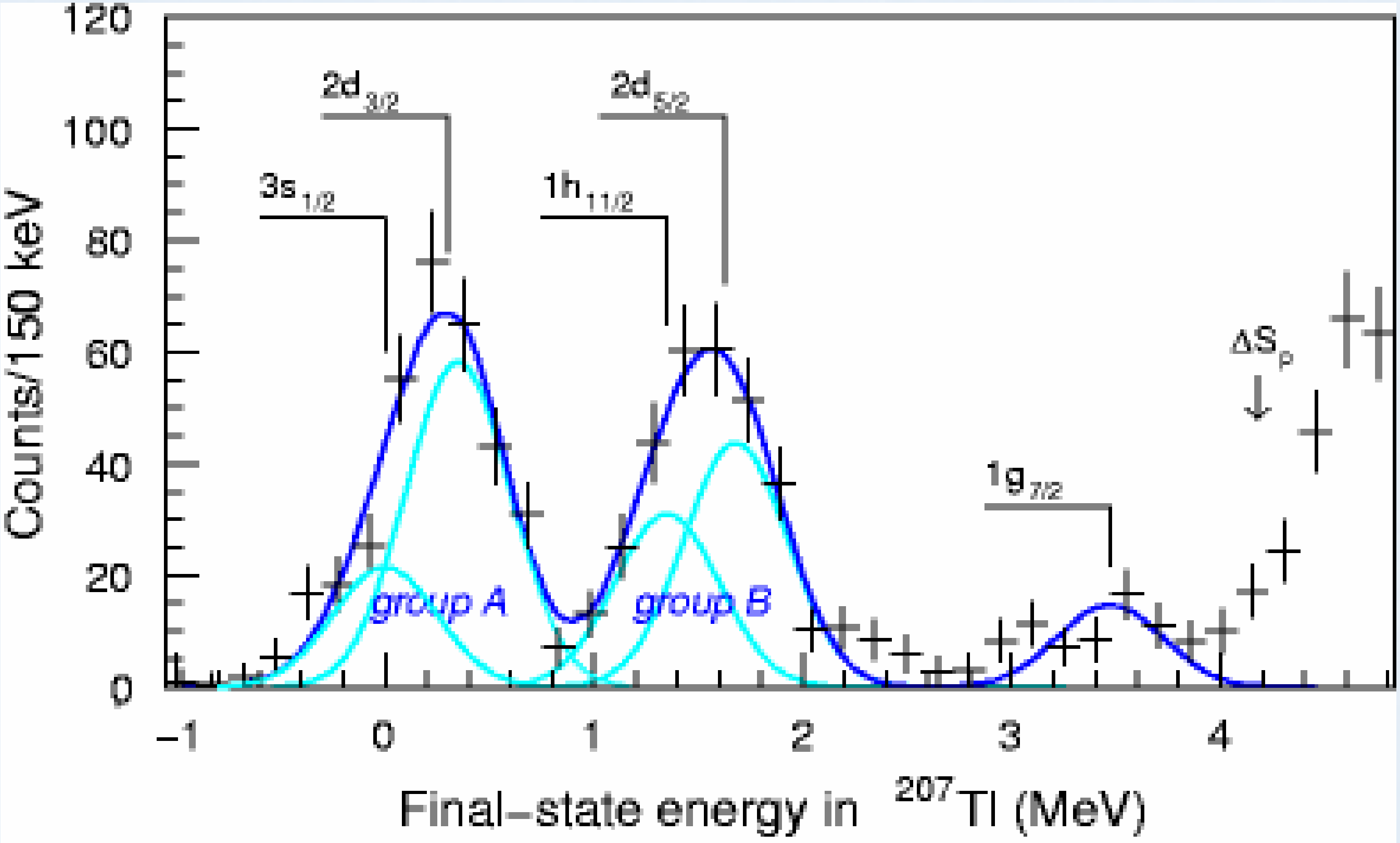

ISGDR in ^{208}Pb in p decay

E_x = 22.1 ± 0.3 MeV
***L = 1* transition**

gated on hole states

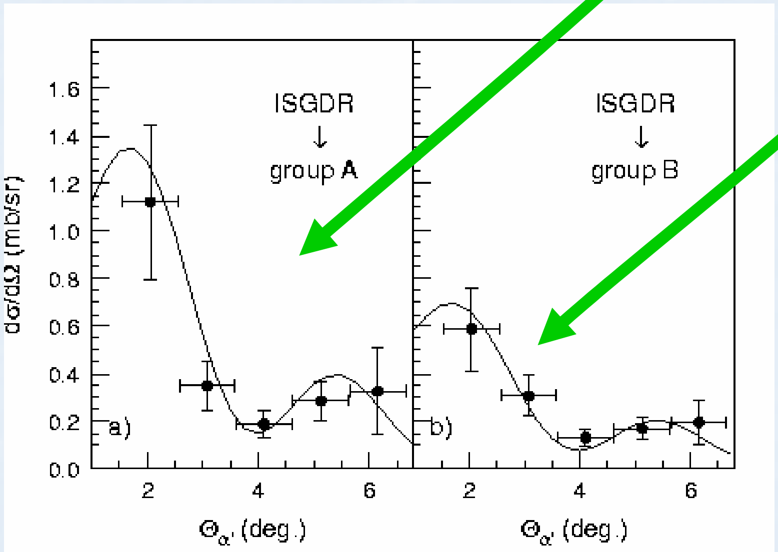

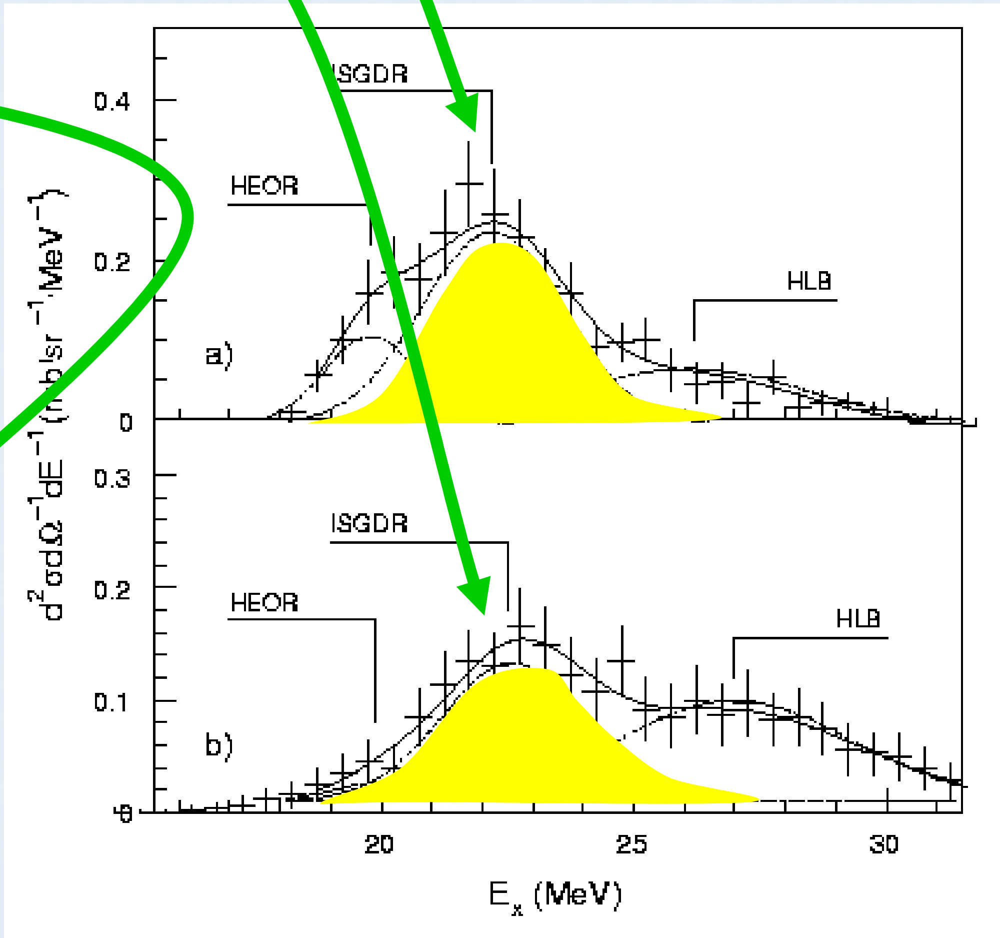

Branching ratios for decay

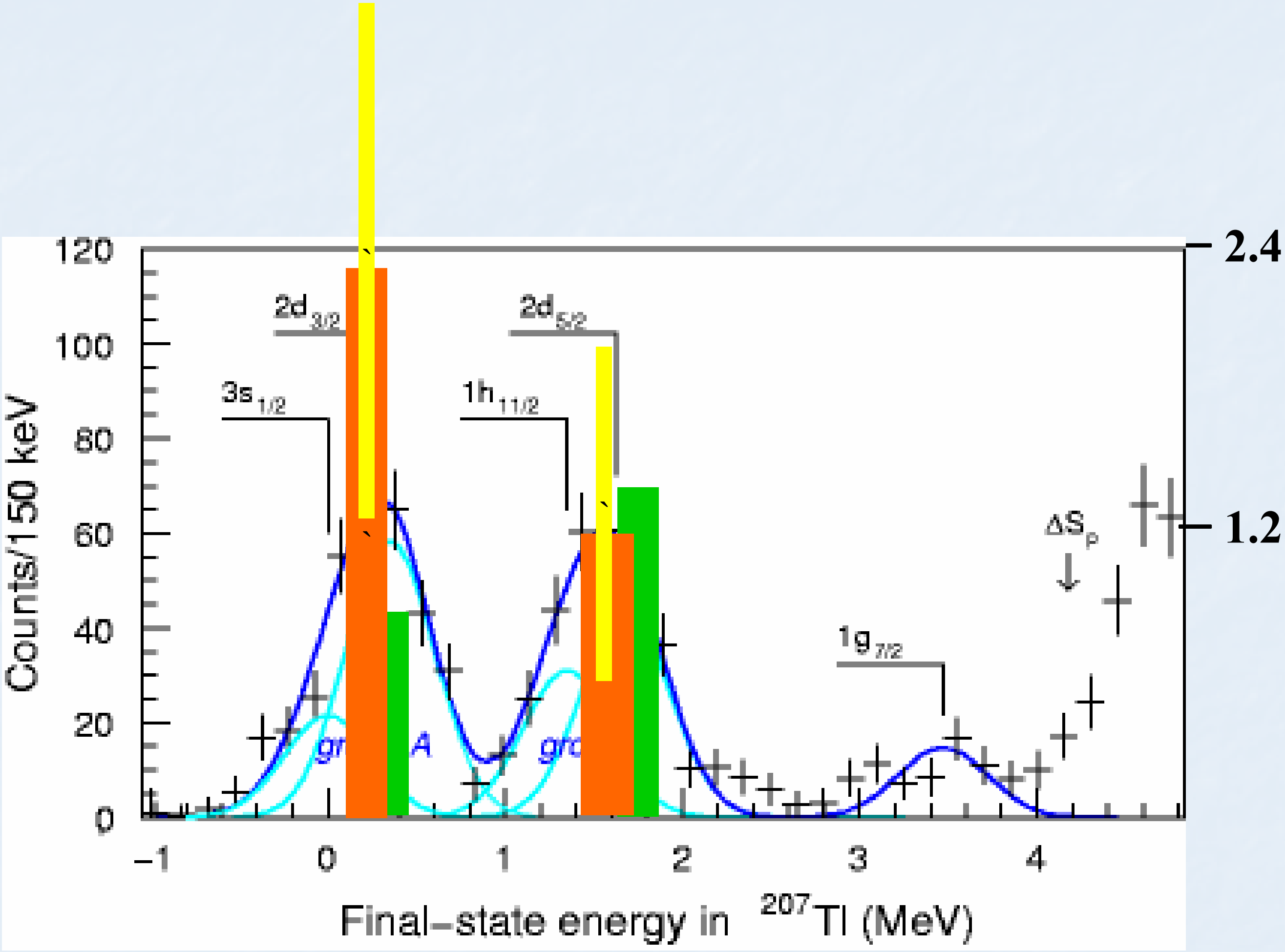

This work

Gorelik et al PRC 62 (2000) 047301

Present Status

1 Djalali et al., 1982
2 Morsch et al., 1983
3 Adams et al., 1986
4 Davis et al., 1997
5 Clark et al., 2001
6 Uchida et al., 2003
7 Uchida et al., 2003
8 this work *p*
9 this work *n*

$E_x = 22.2 \pm 0.2$ MeV

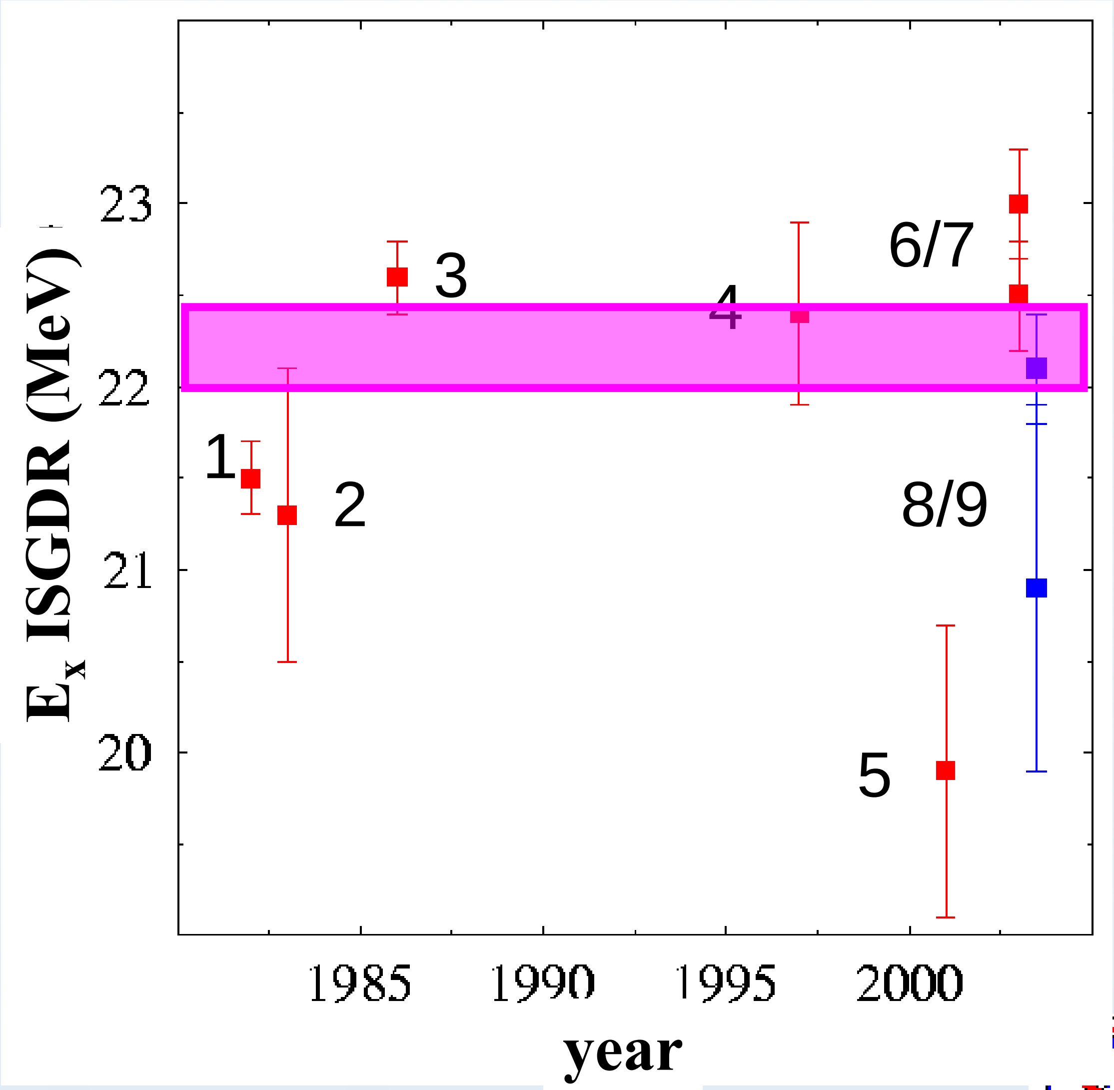

Overtone of the ISGQR? [$r^4 Y_2$]

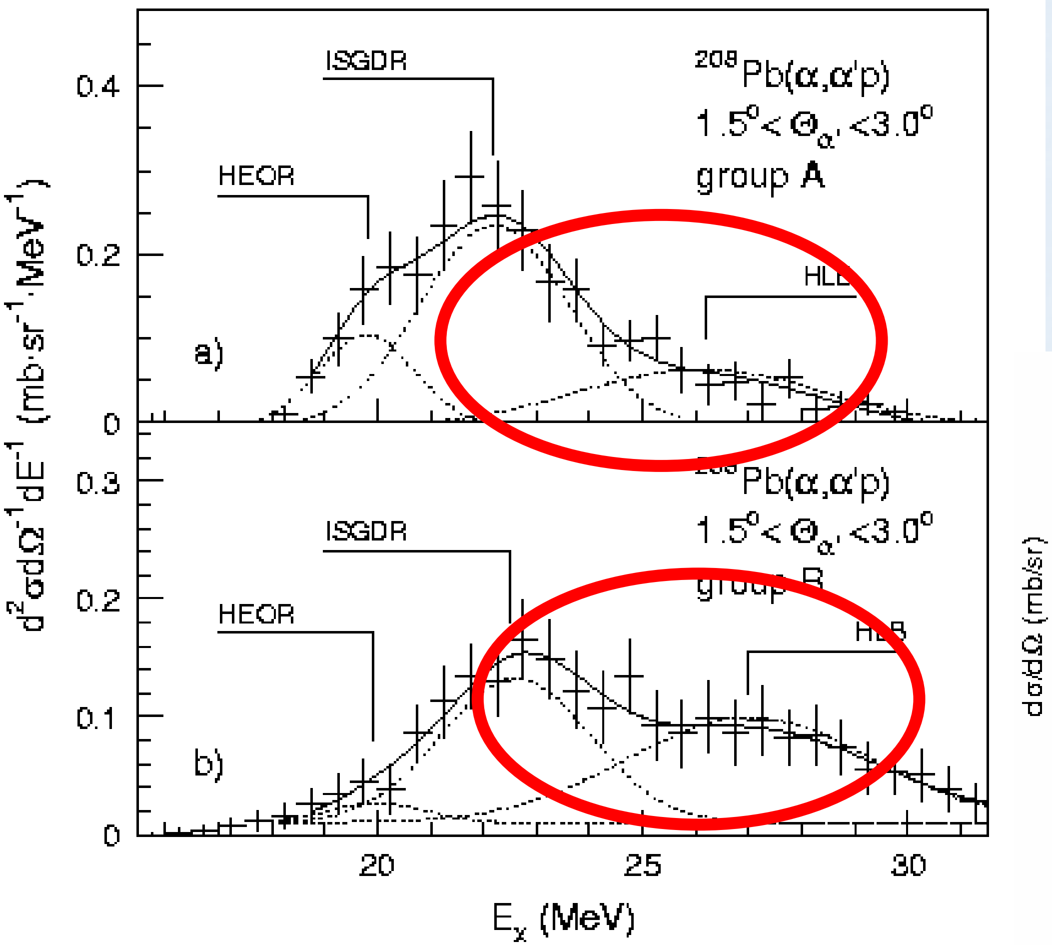

E_x = 26.9 ± 0.7 MeV

Muraviev and Urin
Bull. Acad. Sci. USSR
Phys. Ser. 52 (1988) 123
E_x = 28.3 MeV

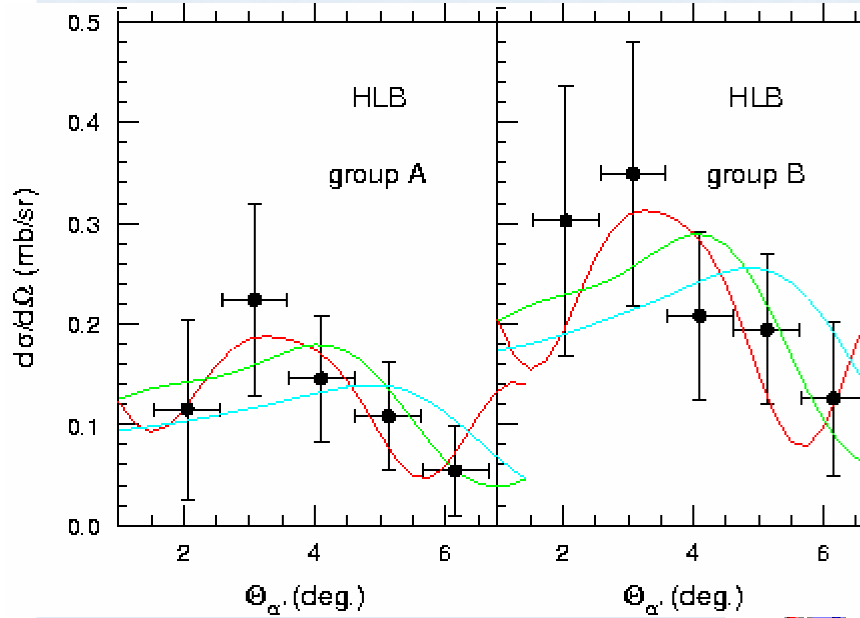

Conclusions!

- **There has been much progress in understanding ISGMR & ISGDR**

  Systematics: E_x, Γ, %EWSR

  $\Rightarrow K_{nm} \approx 220$ MeV

  Microscopic Structure for a few nuclei

- **Observation of a new excitation that could be the quadrupole compressional mode,**

  i.e. overtone of ISGQR

Spin-isospin excitations

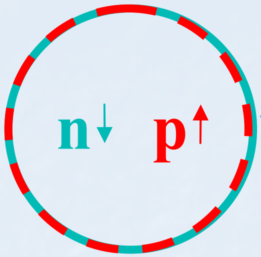

$\Delta L=0$ $\Delta S=1$ $\Delta T=1$

GTR

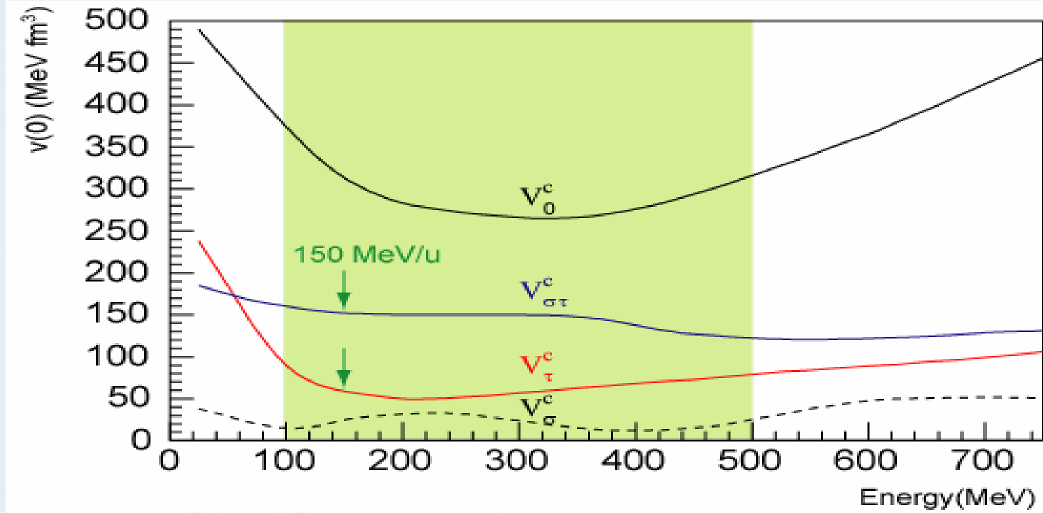

- Gamow-Teller transitions;
  Isospin ($\Delta T=1$)
  Spin ($\Delta S=1$)

Advantages

- Cross section peak at $\theta=0$ deg. ($\Delta L=0$)
- Strong excitation of GT states at E/A=100-500 MeV/u

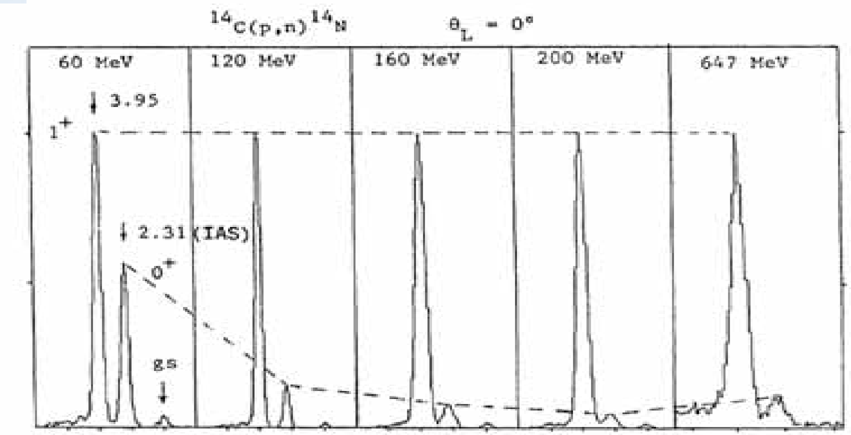

FIG. 4. Zero-degree cross-section spectra for the $^{14}C(p,n)^{14}N$ reactions at the indicated bombarding energies. The spectra have been arbitrarily normalized. From Gaarde (1985) and Rapaport (1989).

KVI

(^{3}He,*t*) Reaction above 150 MeV/u

- **Energy dependence of effective interactions.**
- **150 MeV/A**
  - **V_0 part: Minimum.**
  - **$V_{\sigma t}$ part: Relatively large.**
  - **V_t part: Minimum.**

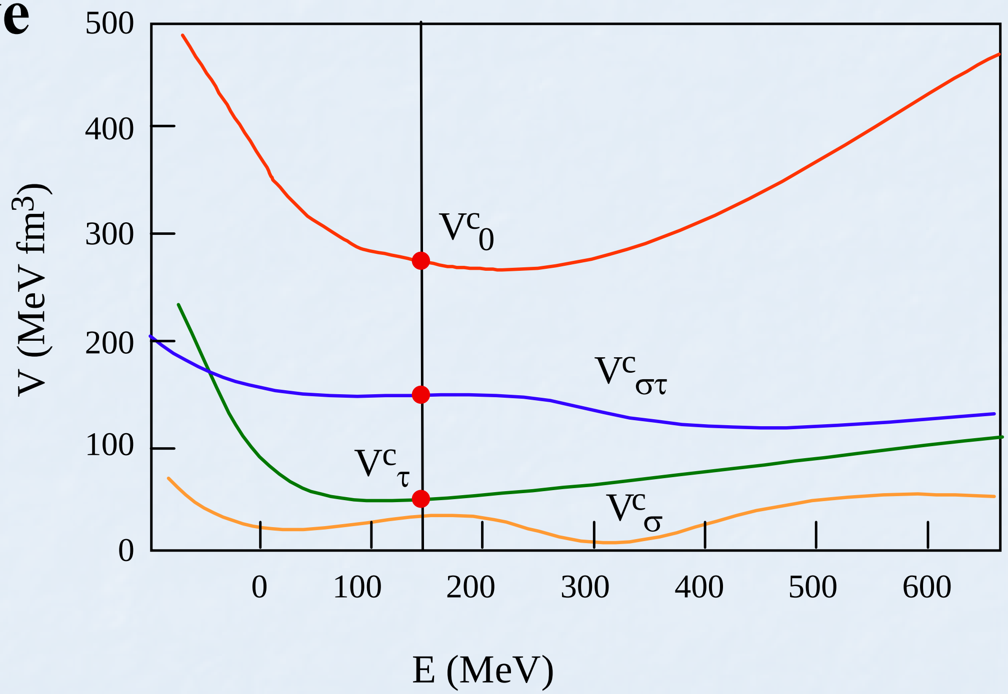

Charge-exchange probes

(p,n)-type ($\Delta T_z = -1$)

- β^--decay
- (p,n)
- (^{3}He,t)
- heavy ion
- (π^+,π^0)

(n,p)-type ($\Delta T_z = +1$)

- β^+-decay
- (n,p)
- (d,^{2}He)
- (t,^{3}He)
- heavy ion (^{7}Li,^{7}Be)
- (π^-,π^0)

•Energy per nucleon (>100 MeV/n)
•Spin-flip vs non-spin-flip
•Complexity of reaction mechanism
•Experimental considerations

Nuclear Classics: spin-flip & GT transitions

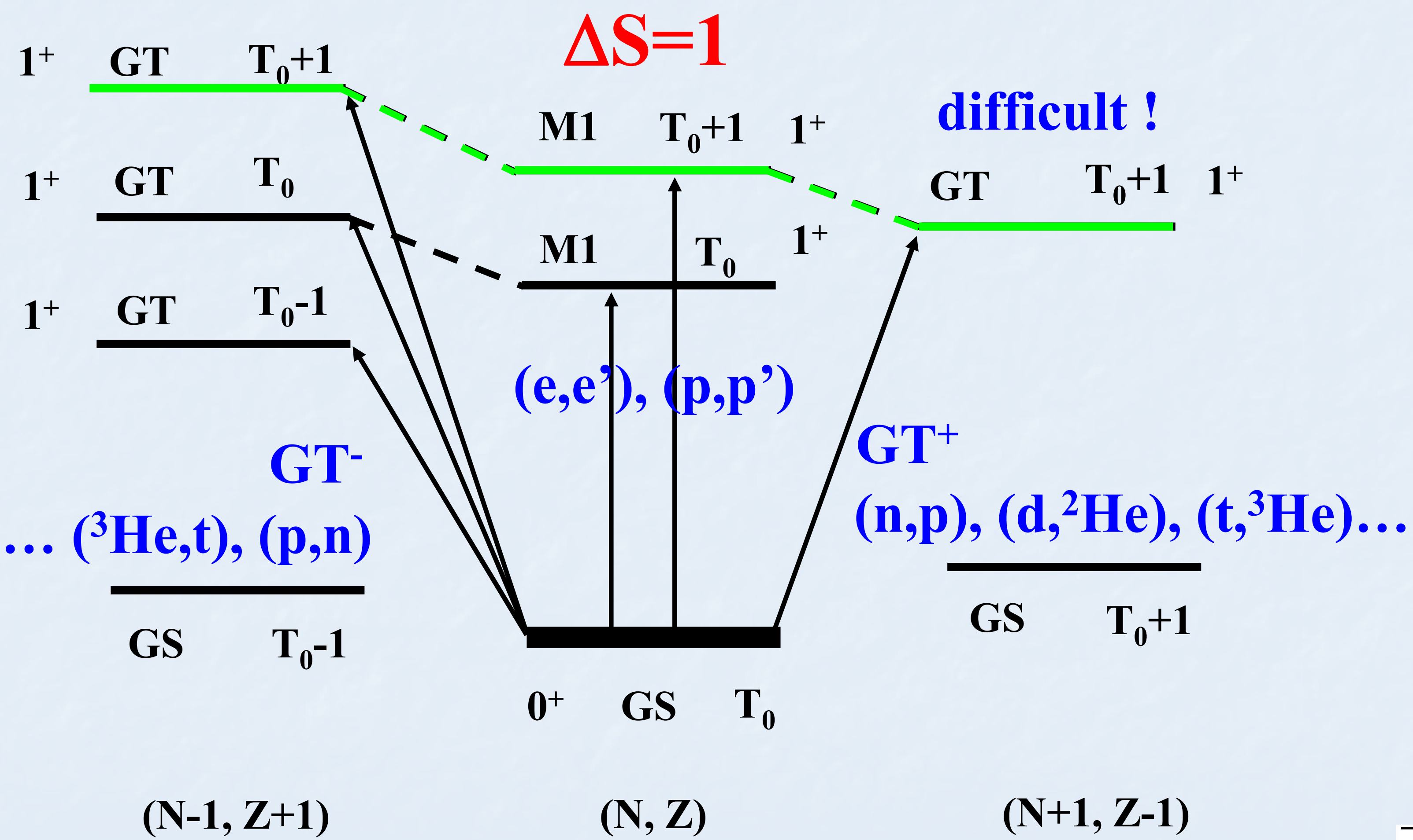

Isovector giant monopole resonances

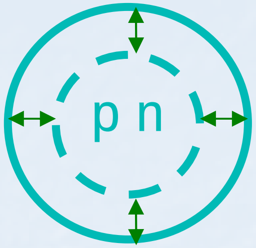

$\Delta L=0\ \Delta S=0\ \Delta T=0$
ISGMR

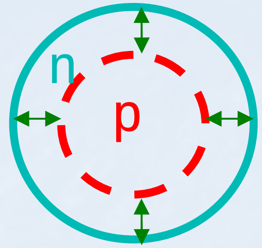

$\Delta L=0\ \Delta S=0\ \Delta T=1$
IVGMR

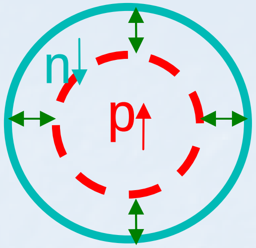

$\Delta L=0\ \Delta S=1\ \Delta T=1$
IVSGMR

$O=r^{\lambda}[\sigma\otimes Y_L]_J\tau_-$

IAS: $\lambda=0$ S=0 L=0 J=0

GTR: $\lambda=0$ S=1 L=0 J=1

IVGMR: $\lambda=2$ S=0 L=0 J=0

IVSGMR: $\lambda=2$ S=1 L=0 J=1

IVSGDR: $\lambda=1$ S=1 L=1 J=0,1,2

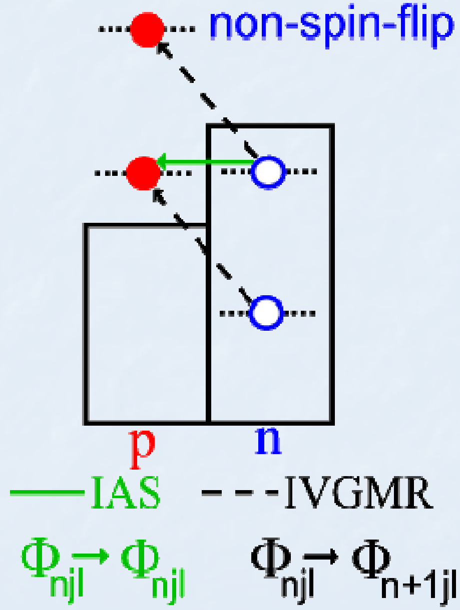

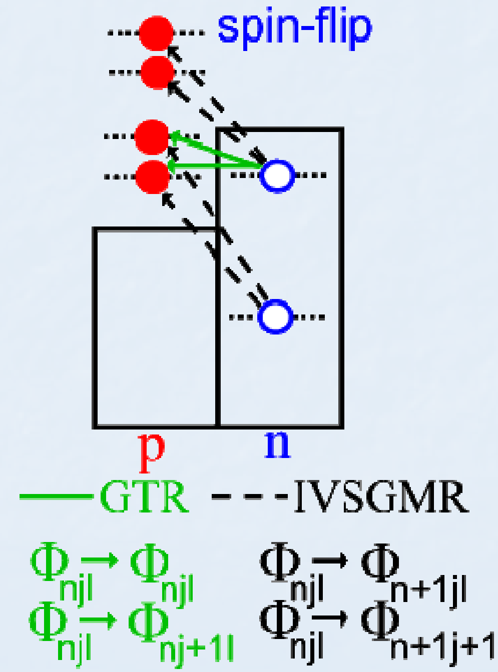

Decay studies

- **Successful:**
  - **GTR, IVSGDR in ^{208}Pb(^{3}He,t+p) at 450 MeV (Akimune et al.)**
  - **IVGMR/IVSGMR in Pb(^{3}He,t+p) at 177 MeV at KVI**

    & 410 MeV at RCNP (Zegers et al.)

- **Unsuccessful:**
  - **IVGMR/IVSGMR ^{124}Sn(^{3}He,t+n) at 200 MeV at IUCF**

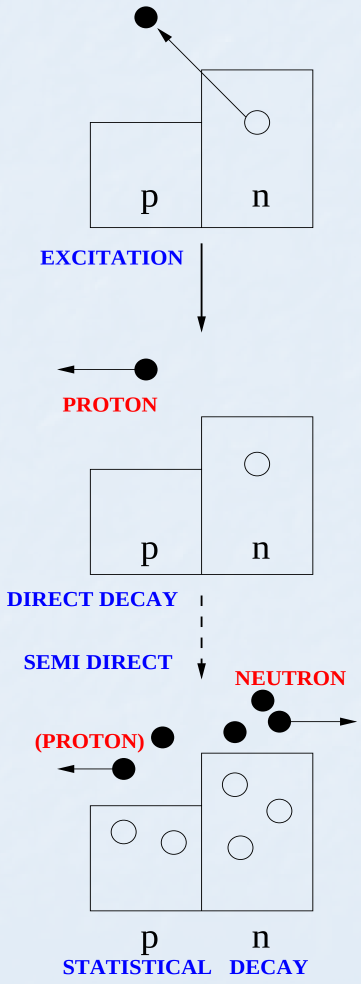

Microscopic Structure of GTR and IVSGDR in ^{208}Bi

- Proton decay of ^{208}Bi:
  - Direct decay dominant
    - $E_x > E_{th}(n) > E_{th}(p)$
    - High Coulomb Barrier (Z=83)
  - Statistical proton decay negligible.
- Angular correlations
  - For IAS and GTR decay isotropic $\Delta L=0$
  - For IVSGDR anisotropic but not strongly
- Direct decay is influenced by:
  - Low n-decay threshold
  - High Coulomb barrier.

- $\Gamma_{GTR}^{\uparrow}/\Gamma \ll \Gamma_{IAS}^{\uparrow}/\Gamma \approx 0.5$
  - **IAS n-decay: isospin forbidden.**
  - **Centroid energy shift: cut off by Coulomb barrier**
- $\Gamma_{IVSGDR}^{\uparrow}/\Gamma > \Gamma_{GTR}^{\uparrow}/\Gamma$
  - **Higher proton energy**

- **Width Γ:**

$$\Gamma = \Gamma^{\uparrow} + \Gamma^{\downarrow}$$

Escape: Direct decay
Spreading: Statistical Decay

$$\Gamma^{\uparrow} = \Gamma^{\uparrow}_{p} = \sum_{i} \Gamma^{\uparrow}_{pi}$$

Partial Escape Width

$$\frac{\Gamma^{\uparrow}_{pi}}{\Gamma} = \frac{\int d^2\sigma_{pi}/(d\Omega_t d\Omega_p)\,d\Omega_p}{d\sigma/d\Omega_t}$$

Branching ratio

Measurement of IVSGMR via $^{208}Pb(^{3}He,t+p)$

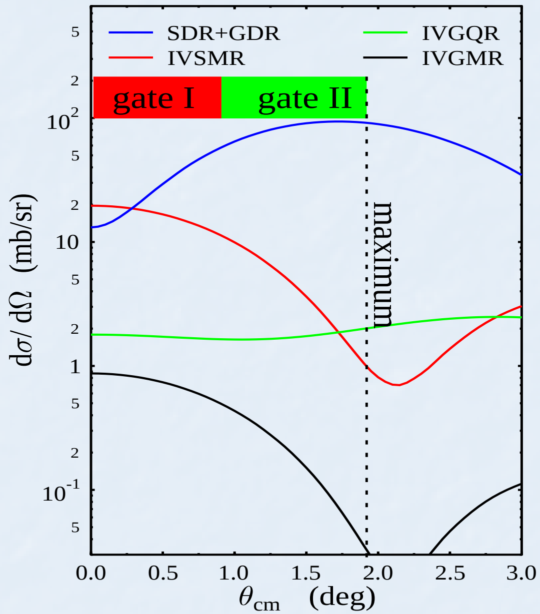

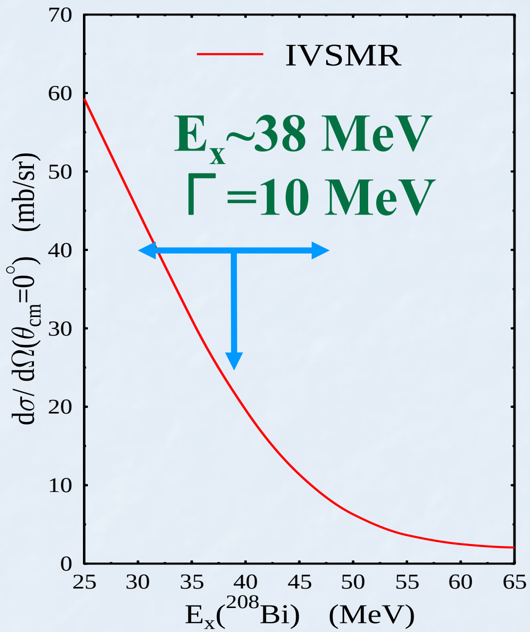

- **DW81 (Raynal)**
- **Effective ^{3}He-N potential**
  - **V_{τ}=0.73±0.01 MeV (IAS)**
  - **$V_{\sigma\tau}$=-2.1 ±0.2 MeV (known ratio to V_{τ})**
  - **$V_{T\tau}$=-2.0 MeV/fm^{2}**
- **most coherent 1p-1h wave-function (normal modes).**

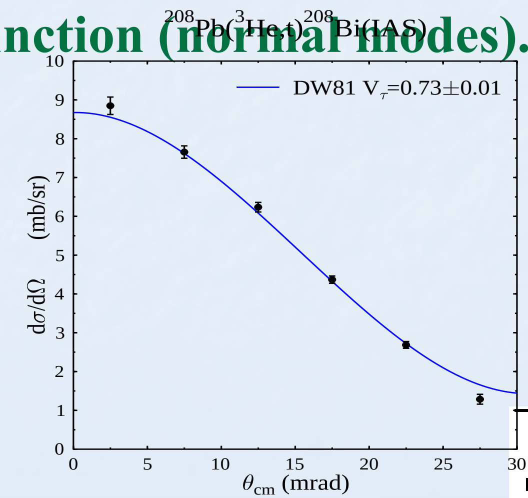

Use *difference-of-angle* to identify the monopole excitations

Continuum suppression

Physical background (continuum) due to:

- breakup-pickup reactions
- quasifree knock-on reactions

IVSGMR is wide (~10 MeV) and lying on top of the continuum.

Continuum has a very flat angular distribution at forward angles

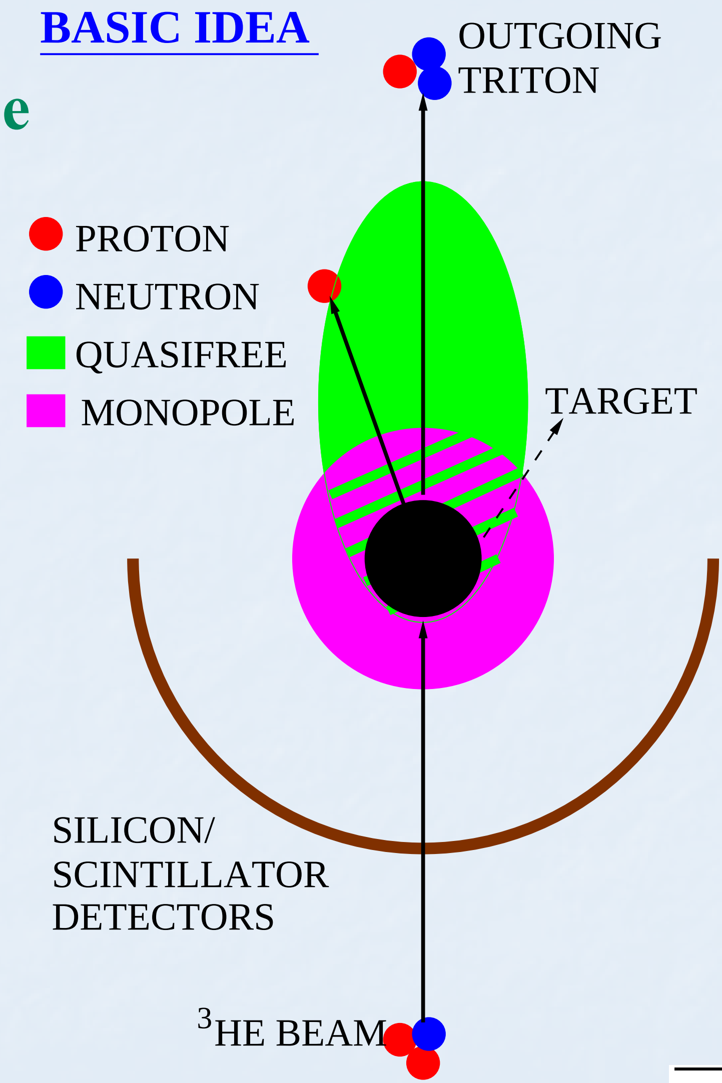

Experiment

- RCNP facility
  K=400 MeV ring cyclotron
  Grand Raiden spectrometer
- Beam: $^{3}He^{++}$, 450 MeV
- Target: ^{208}Pb foil

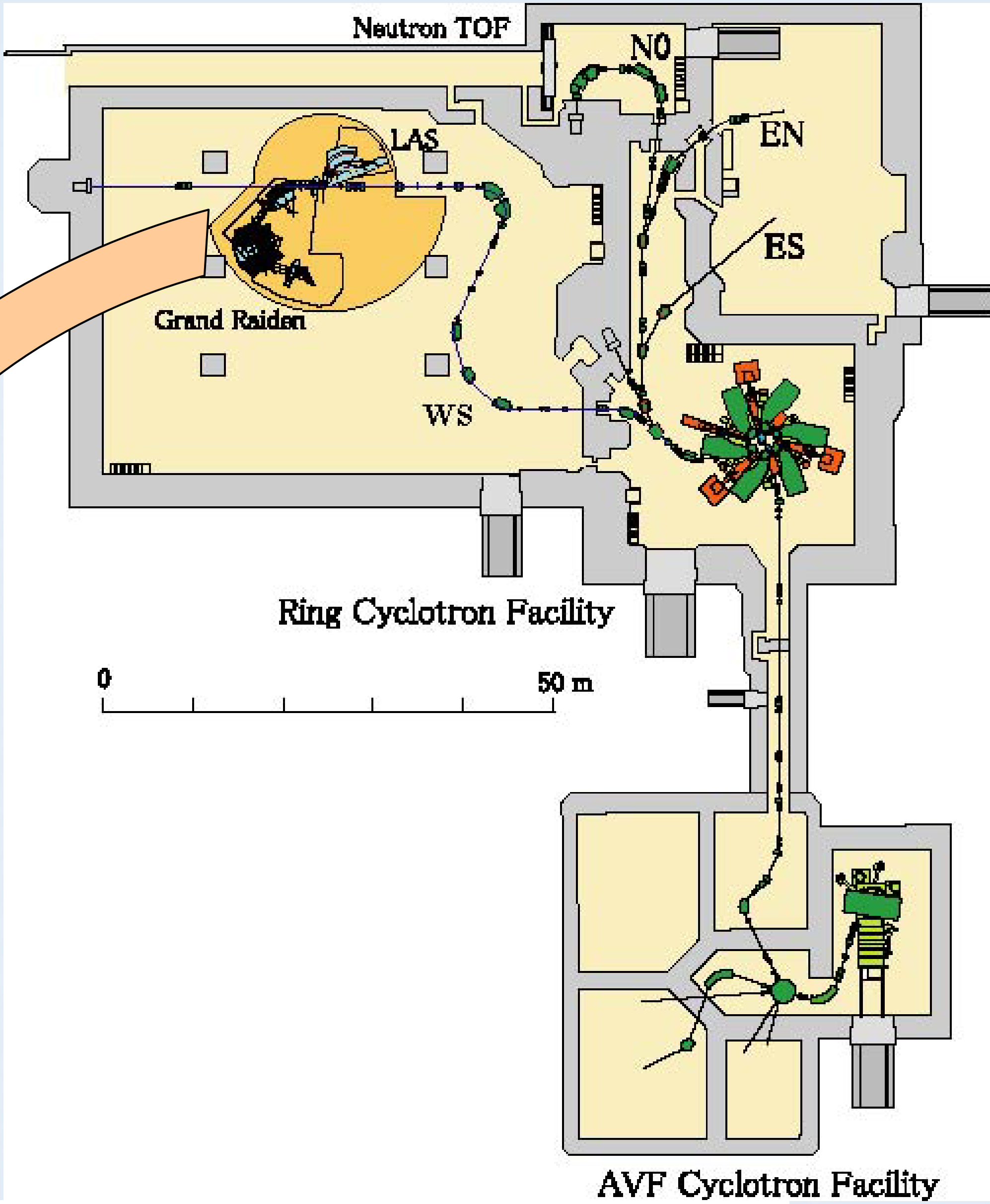

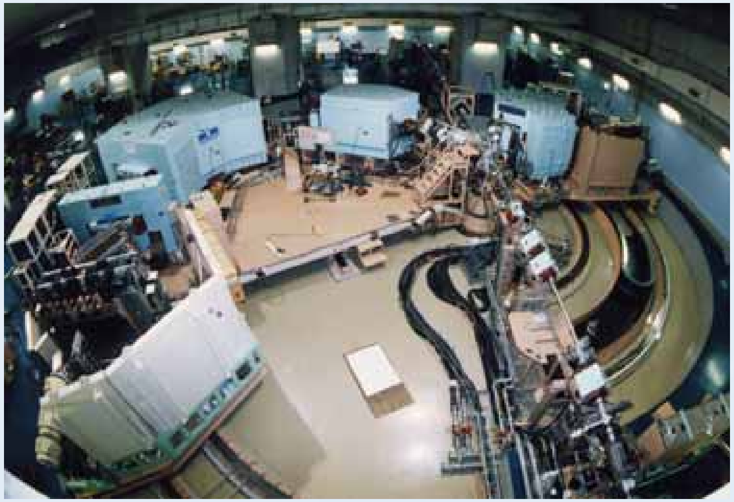

M. Fujiwara et al., NIM A 422 (1999) 484

Experimental Considerations

- **Over-focus mode for Grand-Raiden (H. Fujita et al. NIM A469, 55) refined to get:**

  - **Vertical angle resolution: 0.4° FWHM**
  - **Horizontal angle resolution: 0.2° FWHM**
  - **Negligible systematic errors**
  - **Sieve-slit is used for calibrations**

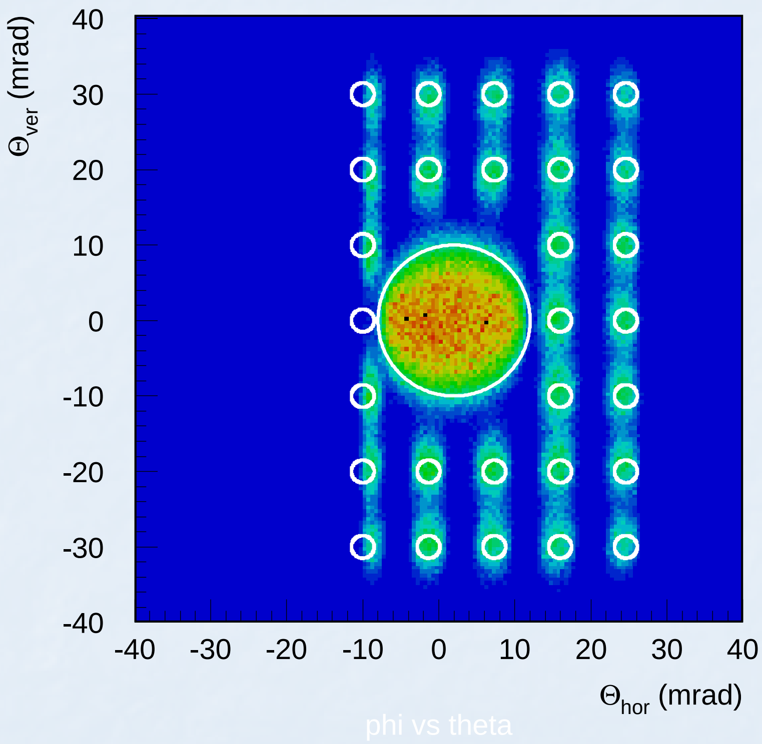

Experiment: 410 MeV ^{3}He-beam @ RCNP

Grand Raiden @ RCNP

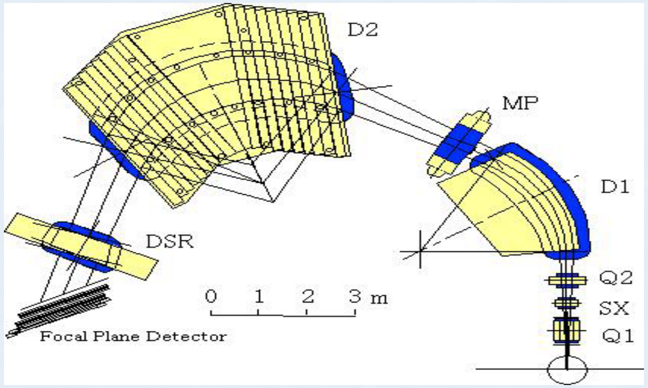

- Measure both t-singles and t-p coincidences.

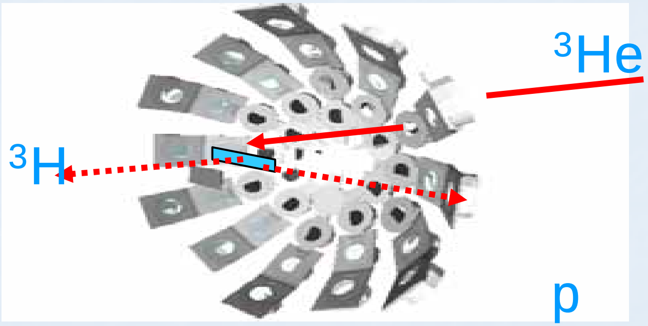

- 8 ΔE-E telescopes
  - 4@113^{o}
  - 4@136^{o}

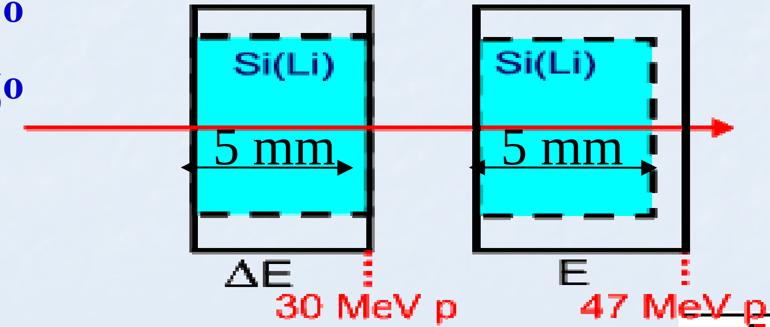

Set-up of the Proton Counter

- Si(Li) detectors with a thickness of 5 mm, covering a solid angle of 5.7% in total.
- 35 keV (^{241}Am test)

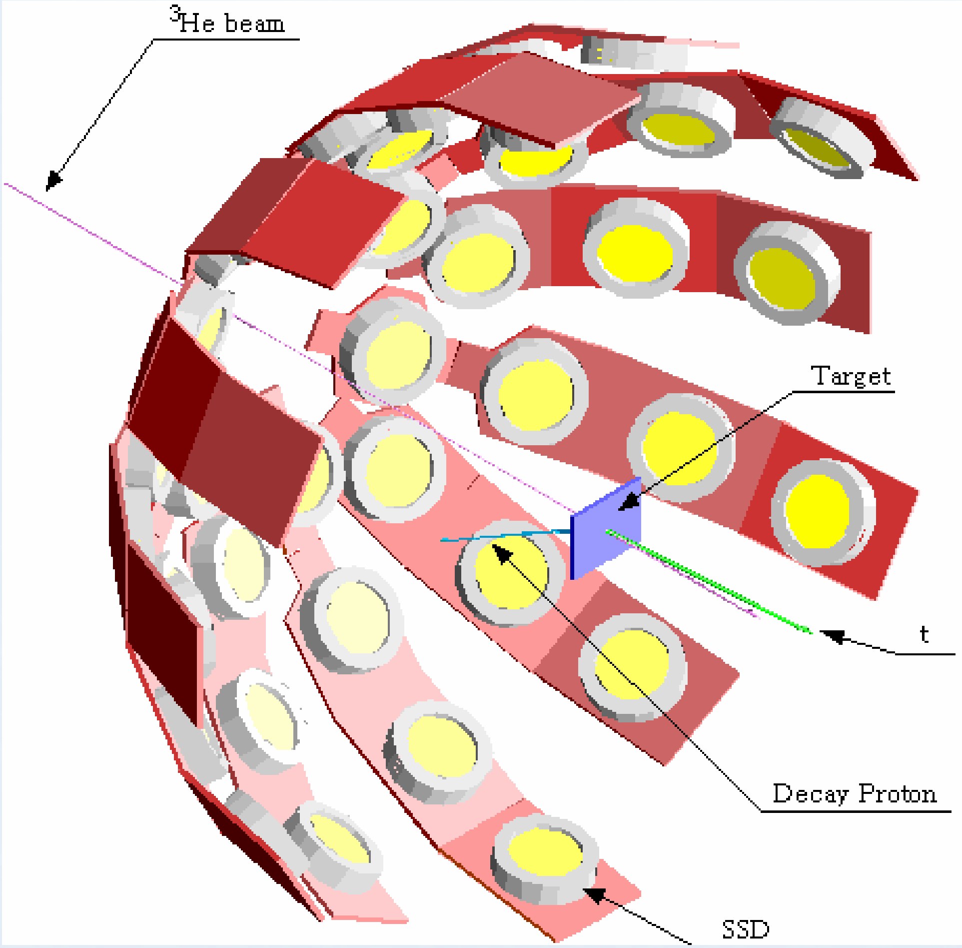

Spin-isospin-flip transitions in charge-exchange reactions and proton decay

A. Krasznahorkay et al., PRC 64 (2001) 067302.
A. Krasznahorkay et al., PRL 82 (1999) 3216.
H. Akimune et al., PRC 52 (1995) 604.
H. Akimune et al., Phys. Lett. B 233 (1994) 107

(^{3}He,t) reactions E(^{3}He)=450 MeV

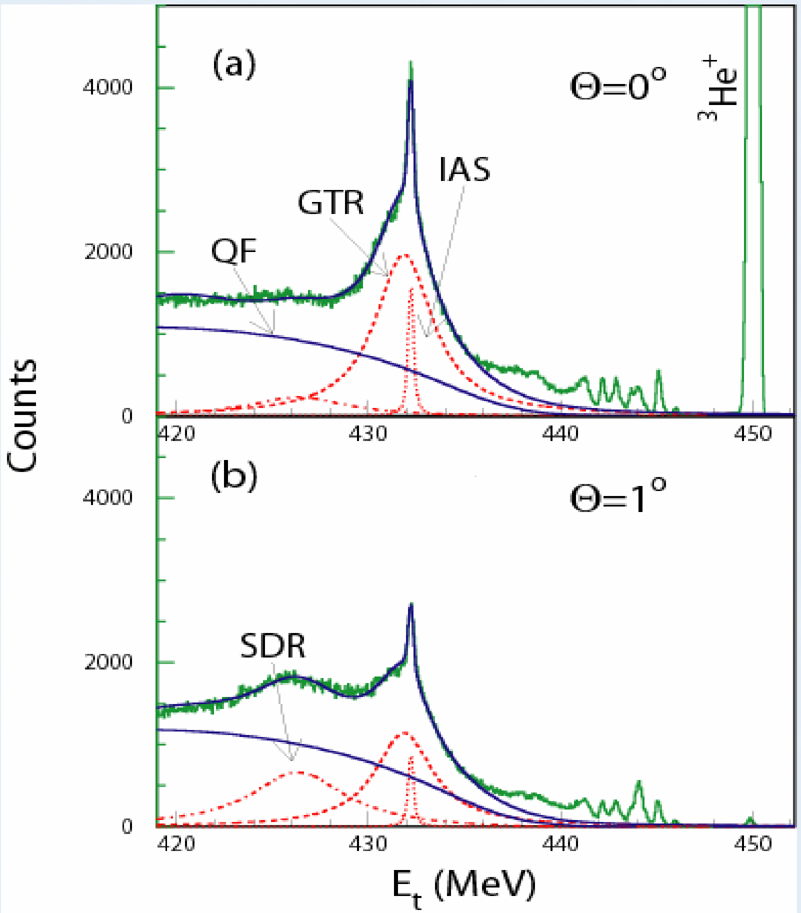

(^{3}He,tp) Coincidence data

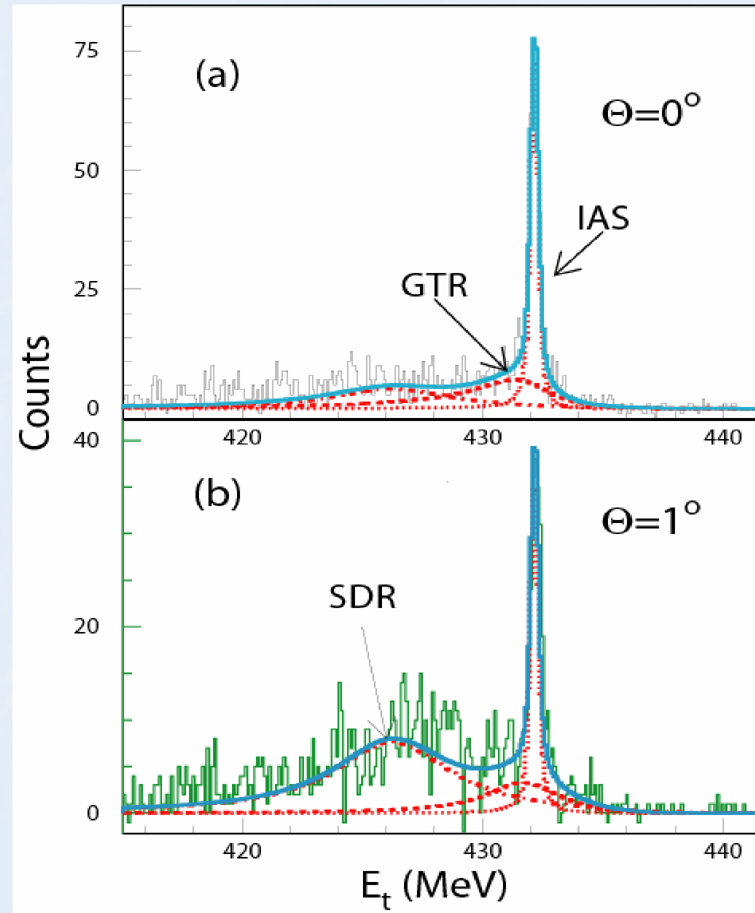

Experimental Results and Theoretical Calculations

- **Partial escape width for GTR**

		Theory		This work	
channel	E_x(keV)	$\Gamma_i^{\uparrow}$(keV)	branch (%)	$\Gamma_i^{\uparrow}$(keV)	branch (%)
$3p_{1/2}$	0	48.7	1.23	58.4±19.8	1.8±0.5
$2f_{5/2}$	570	46.2	2.12	inc. in $p_{3/2}$	
$3p_{3/2}$	898	44.7	2.5	101.5±31.3	2.7±0.6
$1i_{13/2}$	1633	0.87	3.57	8.3±9.4	0.2±0.2
$2f_{7/2}$	2340	5.89	2.97	15.6±7.6	0.4±0.2
$1h_{9/2}$	3413	0.24	0.63	–	–
Total		146.6	13.02	184±49	4.9±1.3

Theory:
E. Moukhai,
V.A. Rodin,
M.H. Urin
Continuum RPA

- **Partial escape width for IVSGDR**

		Theory		This work	
channel	E_x(keV)	$\Gamma_i^{\uparrow}$(keV)	branch (%)	$\Gamma_i^{\uparrow}$(keV)	branch (%)
$3p_{1/2}$	0	103.4	1.23	83.4±24.3	0.99±0.29
$2f_{5/2}$	570	178.1	2.12	170.8±49.3	2.12±0.61
$3p_{3/2}$	898	210.1	2.5	240±69.6	2.86±0.83
$1i_{13/2}$	1633	299.8	3.57	330.4±95.7	3.74±1.08
$2f7_{/2}$	2340	249.3	2.97	282.2±86.8	3.36±0.97
$1h_{9/2}$	3413	52.6	0.63	86.7±25.1	1.03±0.29
Total		1209.6	14.4	1180±340	14.1±4.2

Summary: ^{208}Pb(^{3}He,tp)

- **GTR: $\Gamma^{\uparrow}/\Gamma$~4.9% , $\Gamma^{\uparrow}$=184±49 keV**
  - **Small branching ratio:**
    - **Spreading effect is very important.**
    - **Coupling to underlying 2p-2h states.**
    - **Centroid energy shift caused by**
      High Coulomb barrier.
- **IVSGDR: $\Gamma^{\uparrow}/\Gamma$~14.1% , $\Gamma^{\uparrow}$= 1180±340 keV**
  - **Larger p-decay $\Gamma^{\uparrow}/\Gamma$ compared to GTR.**
    - **E_p: enough higher than**
      Coulomb barrier, centrifugal barrier.
  - **Enhancement of decay to high-spin 1n-hole states**

Results

R.G.T. Zegers et al., PRL 90 (2003) 202501

t singles

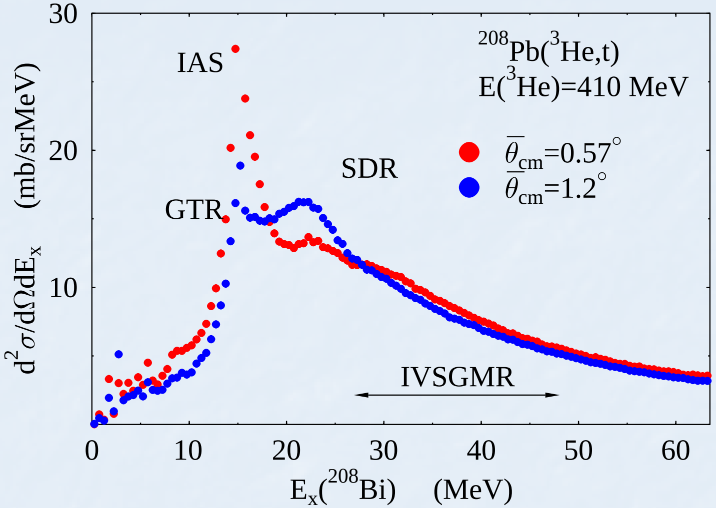

t-p coincidences

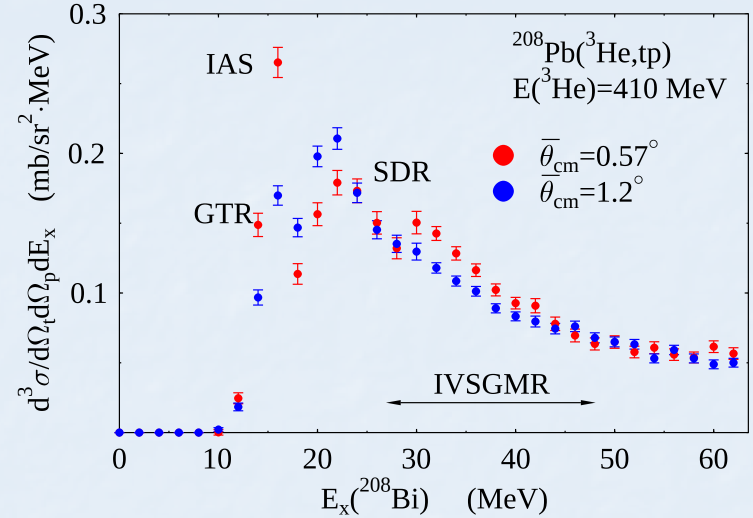

Difference of angles

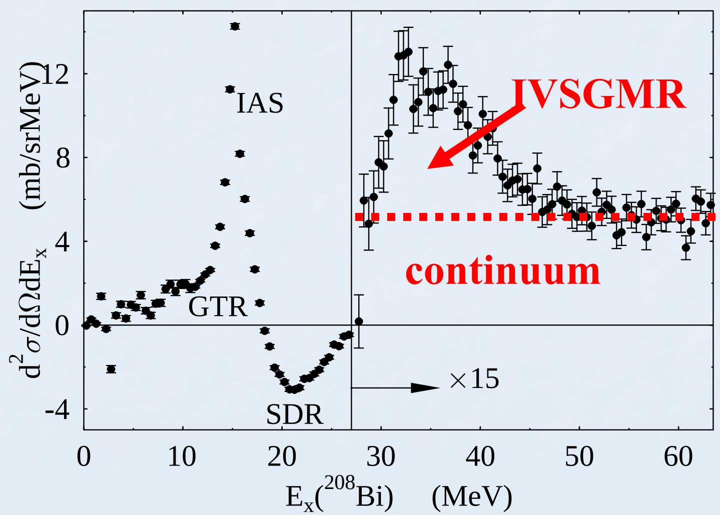

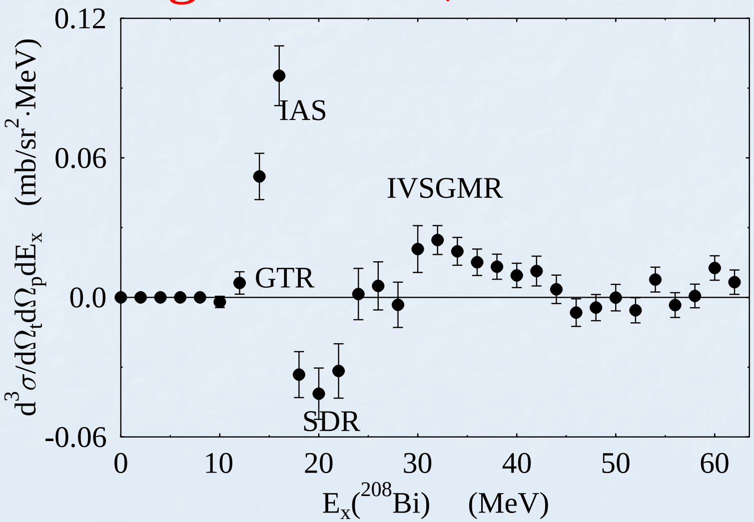

Angular distribution

Use difference-of-angle method between narrow angular bins to extract angular distribution of the resonance

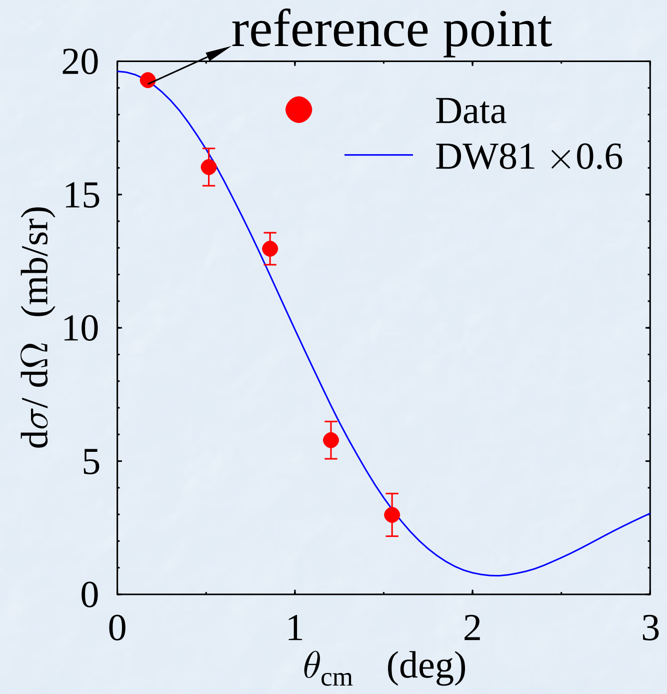

IVSGMR angular distribution confirmed

Strength exhaustion

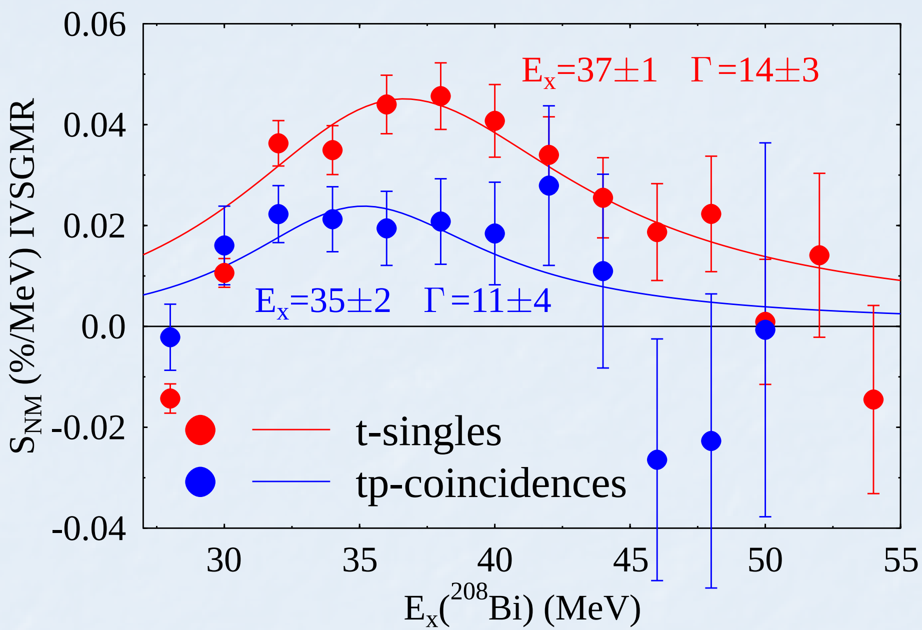

Summed strength: $(46 \pm 4 \pm 10) \cdot 10^3$ fm^4
(contribution from IVGMR subtracted)

method	Exhaustion(%) ($\pm\sigma_{stat} \pm \sigma_{sys}$)
Normal modes	**60±5±14**
Tamm-Dancoff Hamamoto & Sagawa PRC 62, 024319	**68±6±17**
Continuum RPA Rodin & Urin NPA 687, 276c	**103±9±25**
HF-RPA* Auerbach & Klein PRC 30, 1032	**210±16±45**

Systematic errors:
- **extrapolation of continuum: 5%**
- **high-lying GT strength: small**
- **tail of the IVSGDR: 10%**
- **DWBA: 10% of measured value**

*** Different operator, includes GT**

Proton decay from the IVSGMR

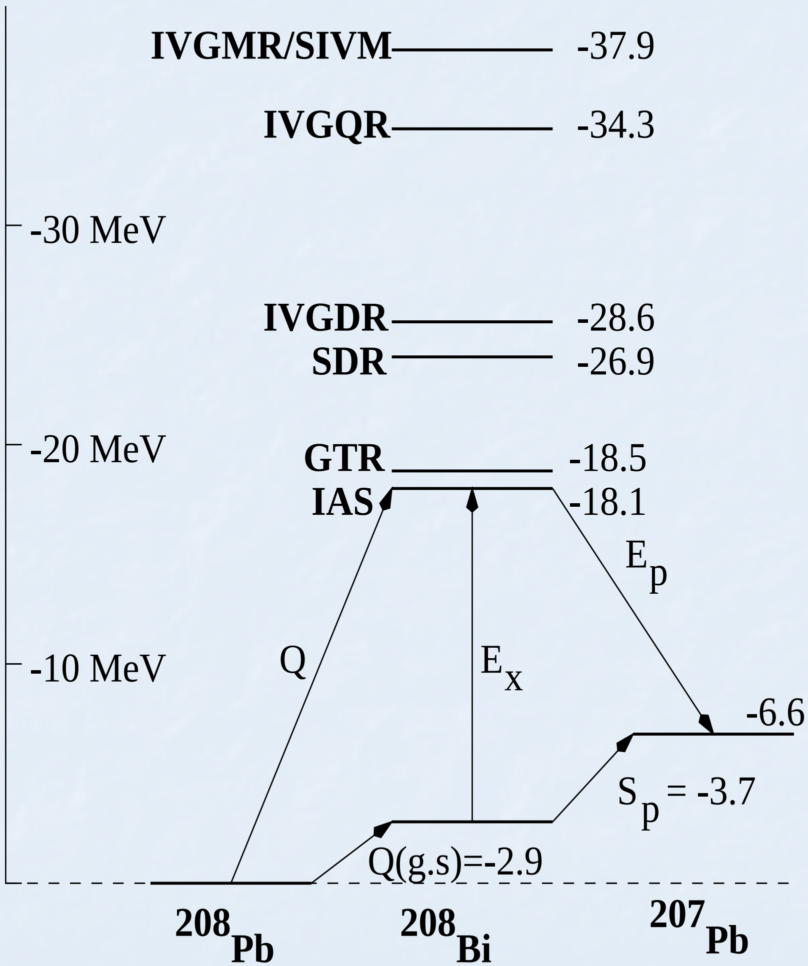

Final state spectra

$E_x(^{208}Bi)$<30 MeV (IAS+GTR+SDR+....)

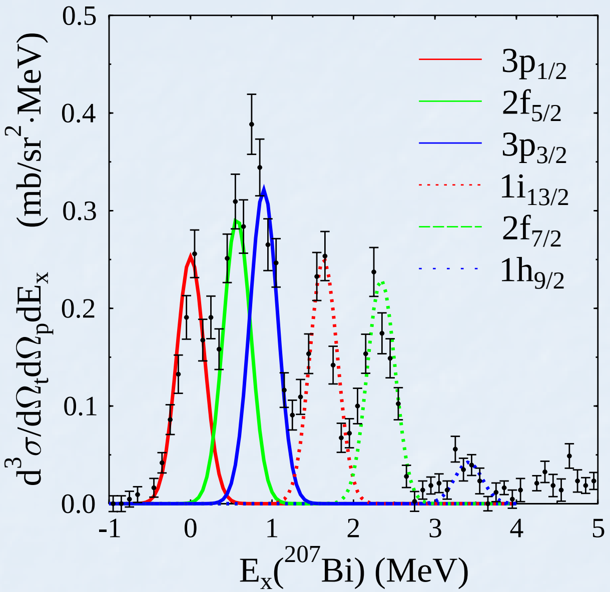

IVSGMR (30<$E_x(^{208}Bi)$<45 MeV difference of angles

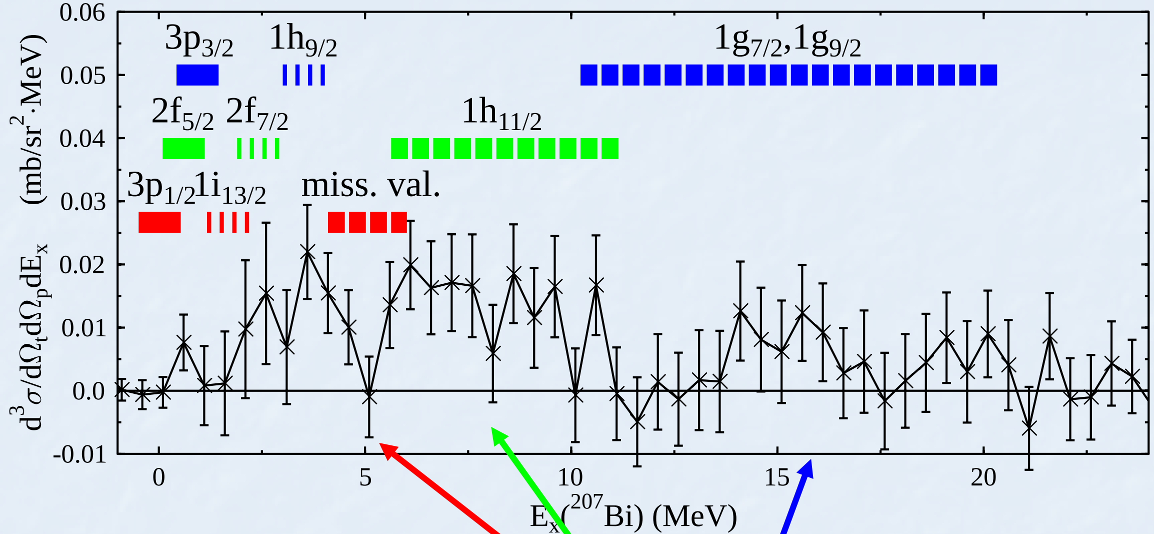

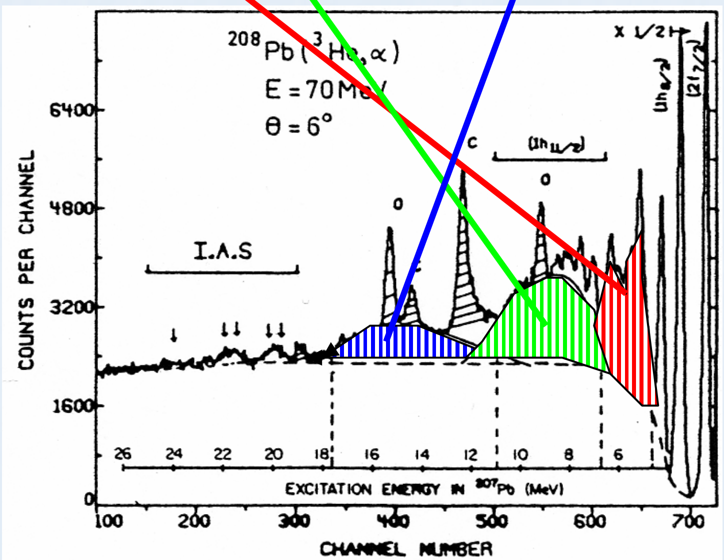

Comparison with
$^{208}Pb(^3He,\alpha)$
Galès *et al.*
Phys. Rep. 166,255

Final state population in ^{207}Pb

Final state	Data(%)	Theory(%)*
$3p_{1/2}$ $2f_{5/2}$ $3p_{3/2}$	< 3	11.3
$1i_{13/2}$		21.4
$2f_{7/2}$ $1h_{9/2}$	13±5	9.5
$1h_{11/2}$	22±8	22.8
$1g_{7/2}$ $1g_{9/2}$	17±8	
All	52±12	66

*Rodin & Urin NPA 687, 276c (continuum RPA)

Large discrepancies for partial **branchings**!!

K V I

The (^{3}He,t) reaction at 0 degree.

- Cross sections at E(^{3}He)=450 MeV, q=0 for (^{3}He,t) reactions

$$\frac{d\sigma}{d\Omega} = \frac{\mu_i \mu_f}{(\pi\hbar^2)^2}\left(\frac{k_f}{k_i}\right)(N_\tau^D \,|\, J_\tau \,|^2\, B(F) + N_{\sigma\tau}^D \,|\, J_{\sigma\tau} \,|^2\, B(GT))$$

T. N. Taddeucci et al., Nucl. Phys. A469, 125 (1987)
I. Bergqvist et al., Nucl. Phys. A469, 648 (1987)

- Neutrino absorption cross sections

$$\sigma = \frac{1}{\pi \hbar^4 c^3}\left[G_V^2 B(F) + G_A^2 B(GT)\right] \times F(Z, E_e) p_e E_e$$

Importance of charge-exchange reactions at intermediate energies

Measuring GT strengths

$$\frac{d\sigma}{d\Omega}(q=0) = KN_D \left| J_{\sigma\tau} \right|^2 B(GT)$$

kinematic factor

distortion factor

nucleon-nucleus interaction

Gamow-Teller strength

Calibration of B(GT) to cross section for known transitions (e.g. from β-decay)

M. Fujiwara et al. PRL 85 (2000) 4442.

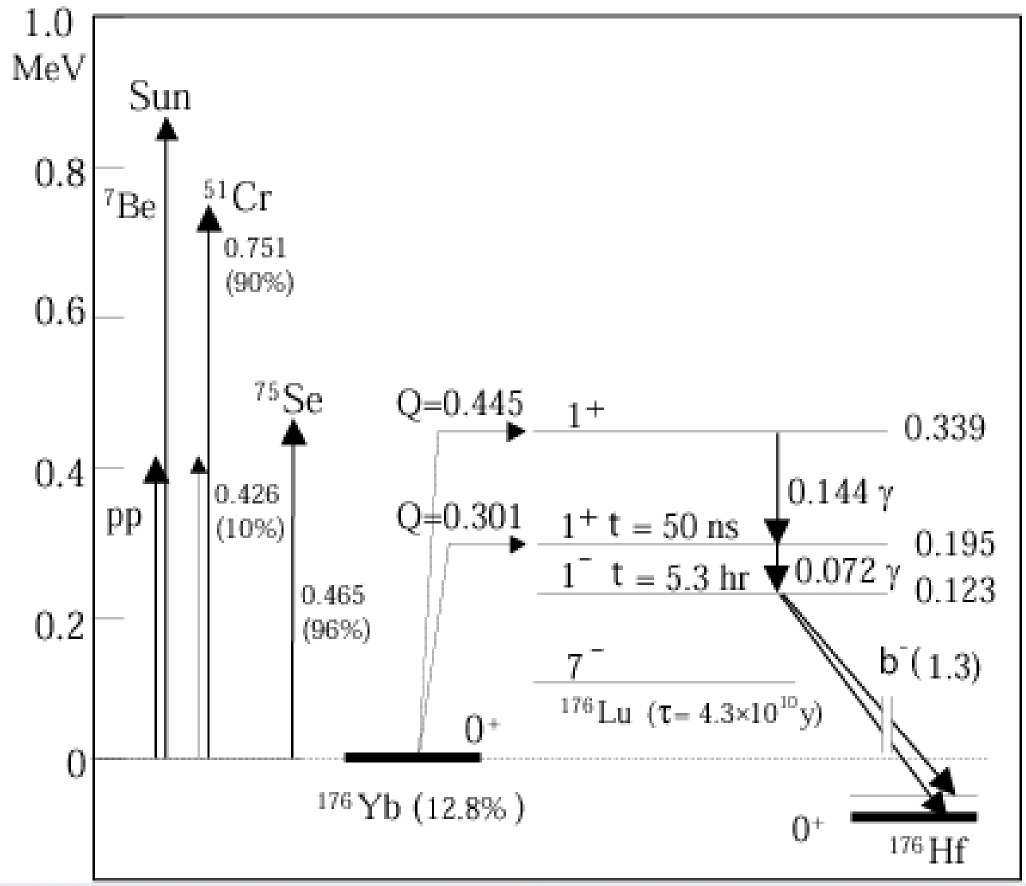

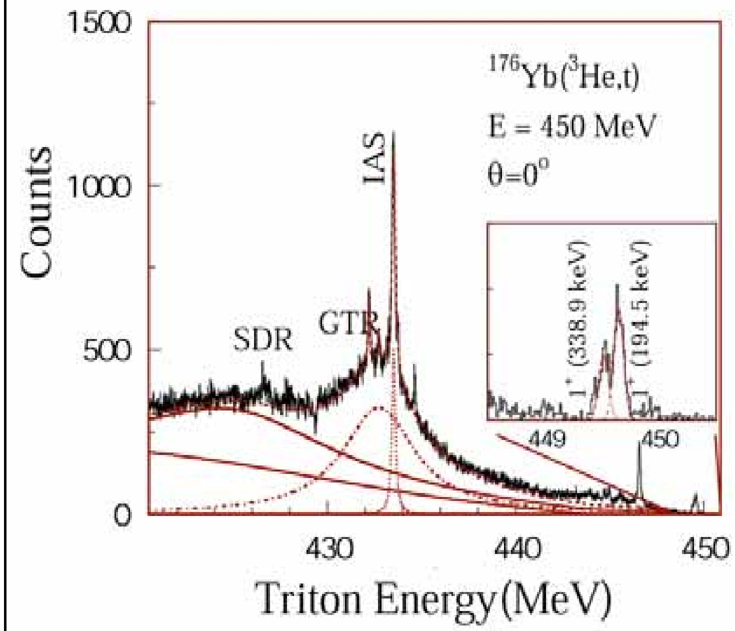

E_x (MeV)	0.195+0.339 (*p,n*)	0.195	0.339 (^{3}He,*t*)
B(GT)	0.32±0.04	0.20±0.04	0.11±0.02

Why are Gamow-Teller transitions in *pf*-shell nuclei important ?

- **Role of pf-shell nuclei in supernova explosions:**
  Core of supernova star is composed of *pf*-shell nuclei.

Neutrino absorption cross sections by *pf*-shell nuclei are essential in understanding of nuclear synthesis by Supernova explosions in cosmos.

→ **Difficulties in shell model calculations for *pf*-shell nuclei.**

→ **Importance of spin-isospin responses of *pf*-shell nuclei**

Beam line WS-course

Grand-Raiden Spectrometer

T. Wakasa et al., NIM A482 ('02) 79.

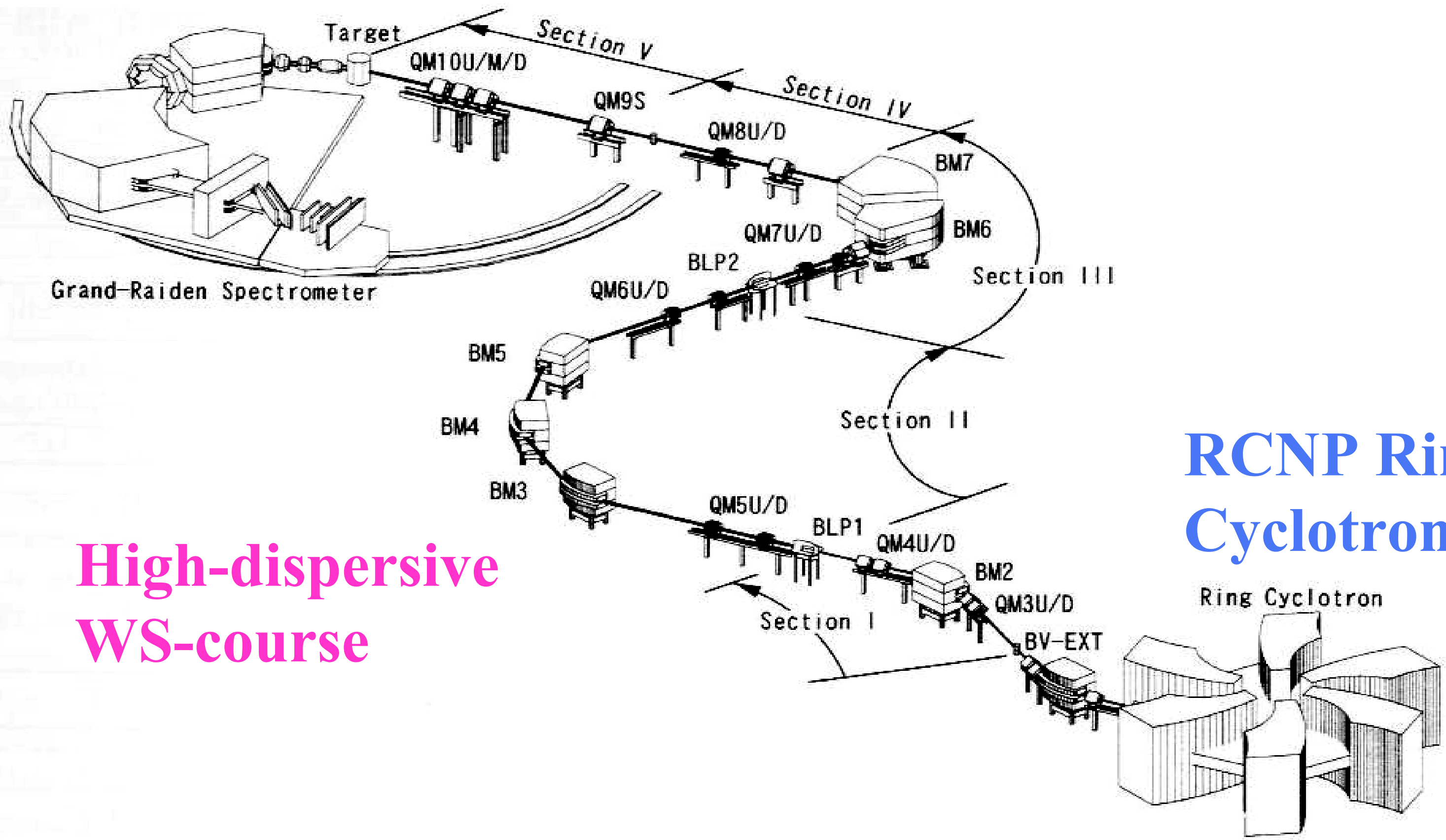

RCNP Ring Cyclotron

High-dispersive WS-course

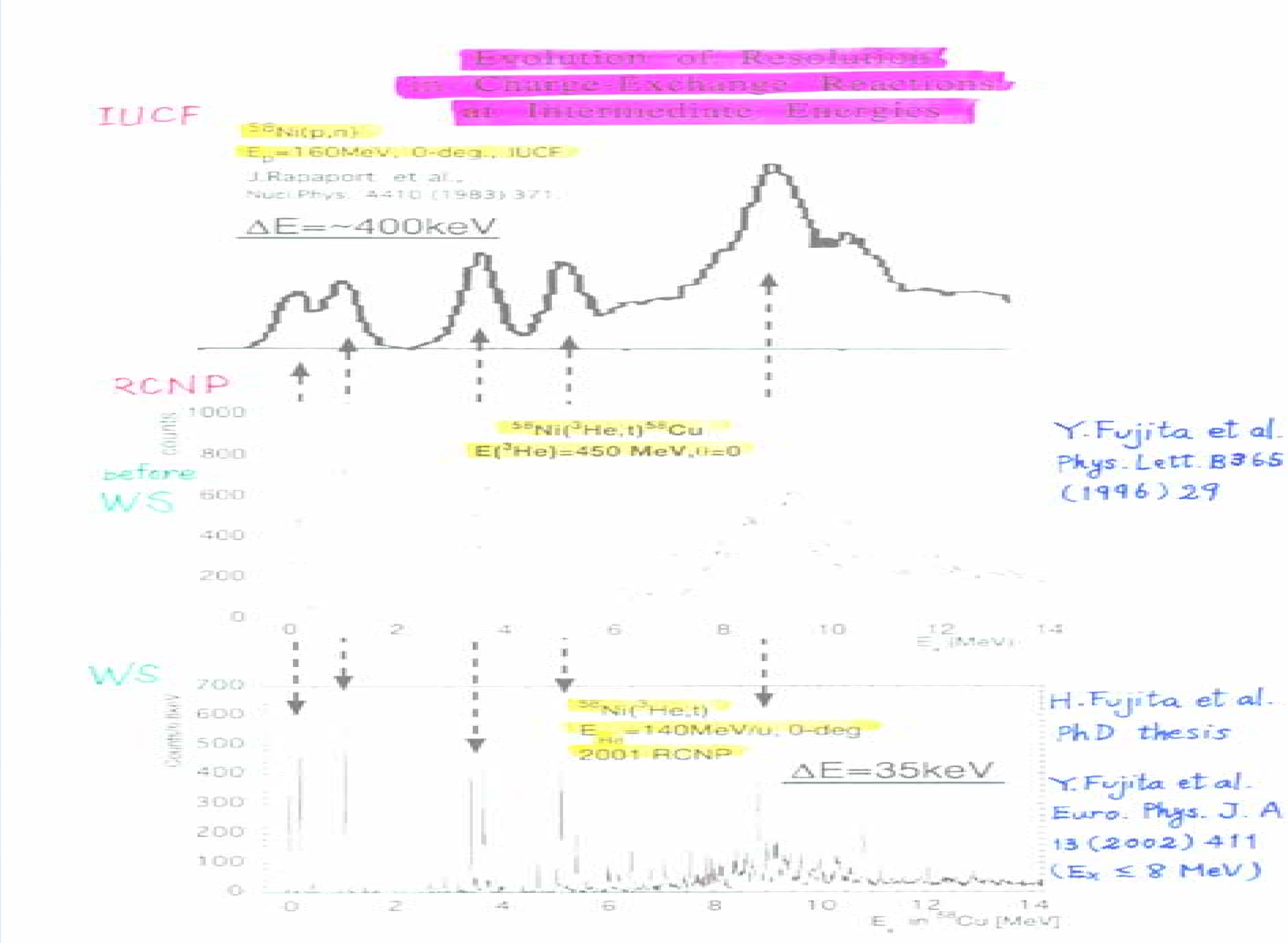
Evolution of Resolution
in Charge-Exchange Reactions
at Intermediate Energies
IUCF
58Ni(p,n)
Ep=160MeV, 0-deg., IUCF
J.Rapaport et al.,
Nucl.Phys. A410 (1983) 371
ΔE=~400keV
RCNP
before
WS
58Ni(3He,t)58Cu
E(3He)=450 MeV,θ=0
counts
1000
800
600
400
200
0
0 2 4 6 8 10 12 14
Ex (MeV)
Y. Fujita et al.
Phys. Lett. B365
(1996) 29
WS
58Ni(3He,t)
EHe=140MeV/u, 0-deg
2001 RCNP
ΔE=35keV
Counts/keV
700
600
500
400
300
200
100
0
0 2 4 6 8 10 12 14
Ex in 58Cu [MeV]
H. Fujita et al.
PhD thesis
Y. Fujita et al.
Euro. Phys. J. A
13 (2002) 411
(Ex ≤ 8 MeV)

Decomposition of the isospin component of the excited state in ^{58}Cu.

- Isospin of ^{58}Ni g.s. : $T_0=1$

- In principle, comparison among (n,p), (p,p), (p,n) spectra

  →separates isospin components

But, very difficult in practice because of high level density for T=1 and T=2 states.

- **CG**

$\sigma_{T=0} : \sigma_{T=1} : \sigma_{T=2} = 2:3:1$ $(T_0=1)$

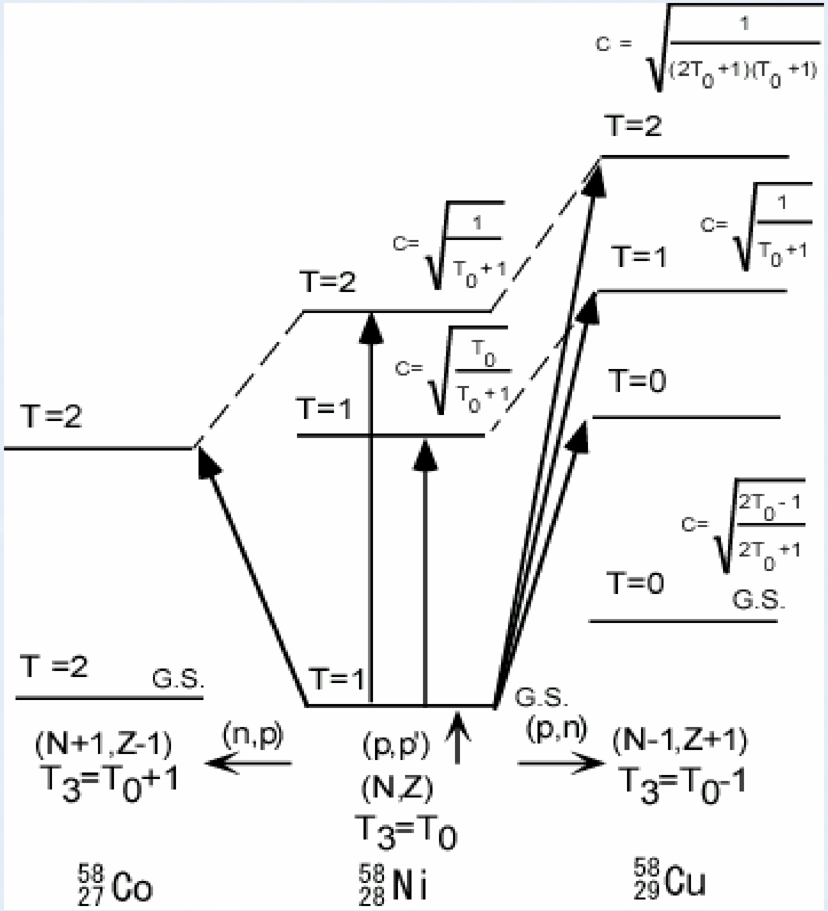

Comparison of (^{3}He,t) and (e,e') spectra

- Comparison of (^{3}He,t) with (e,e') spectra ➔ Try to separate isospin components
- At E_x= 6-10 MeV (T=1 region)
  - Rather good correspondence
- At E_x=10-15 MeV (T=2 region)
  - No good correspondence

Fujita et al., Phys. Lett. B 365, 29 (1996).

Fujita et al., Eur. Phys. J A13, 411 (2002).

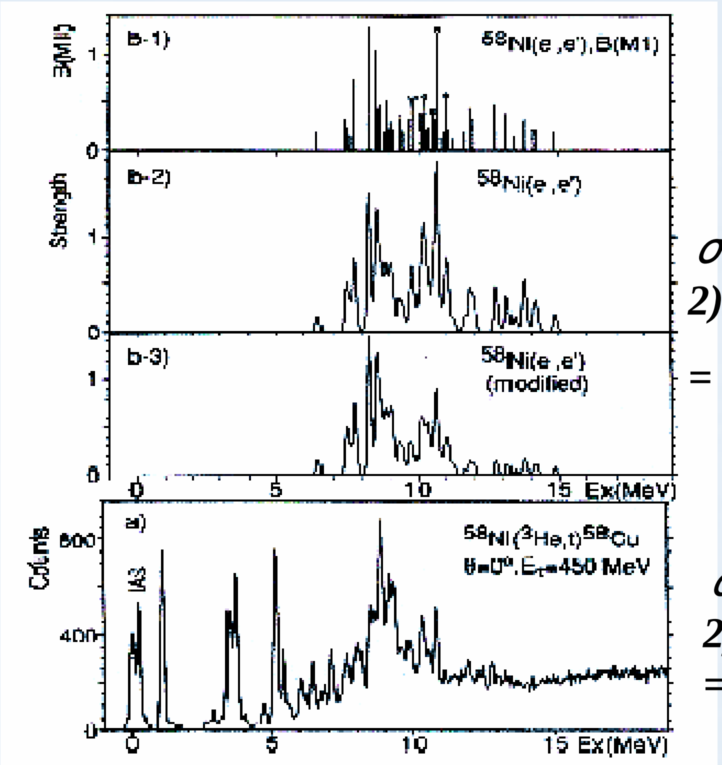

σ(T=1): σ(T=2) = 1 : 1

σ(T=1): σ(T=2) = 3 : 1

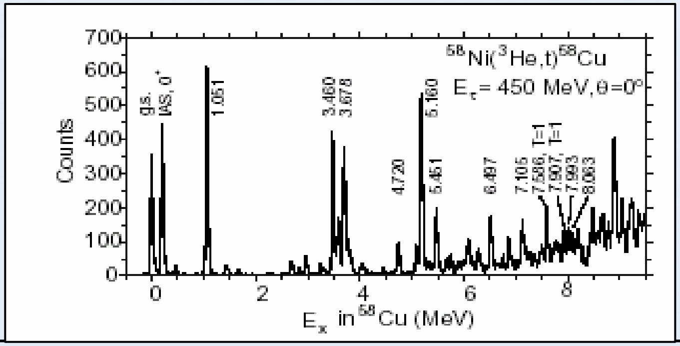

(*p*, *n*) spectra for Fe and Ni Isotopes

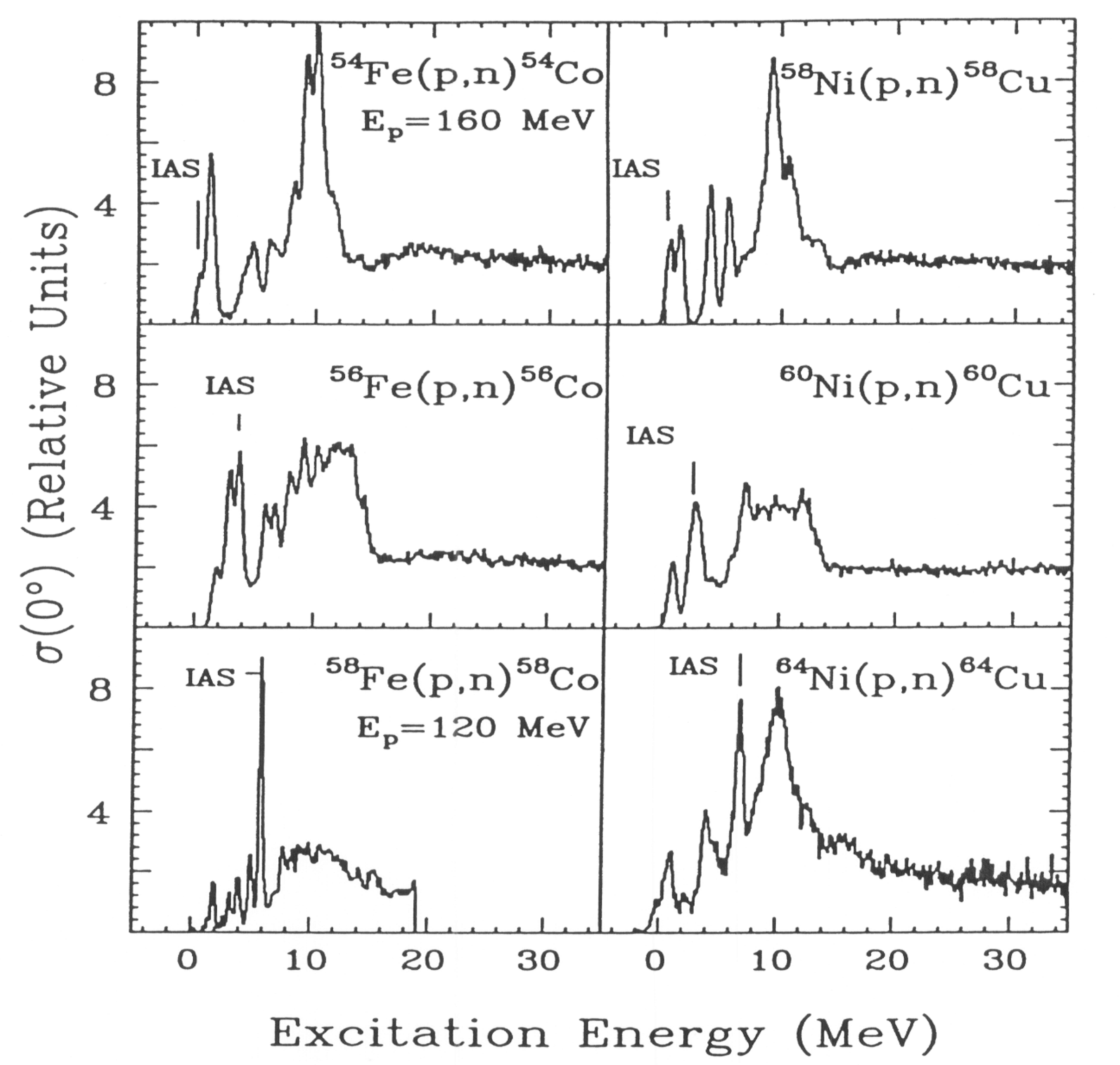

Rapaport
&
Sugarbaker
Rev. Mod. Phys.
('94)

^{26}Mg(p, n)^{26}Al & ^{26}Mg(^{3}He,t)^{26}Al spectra

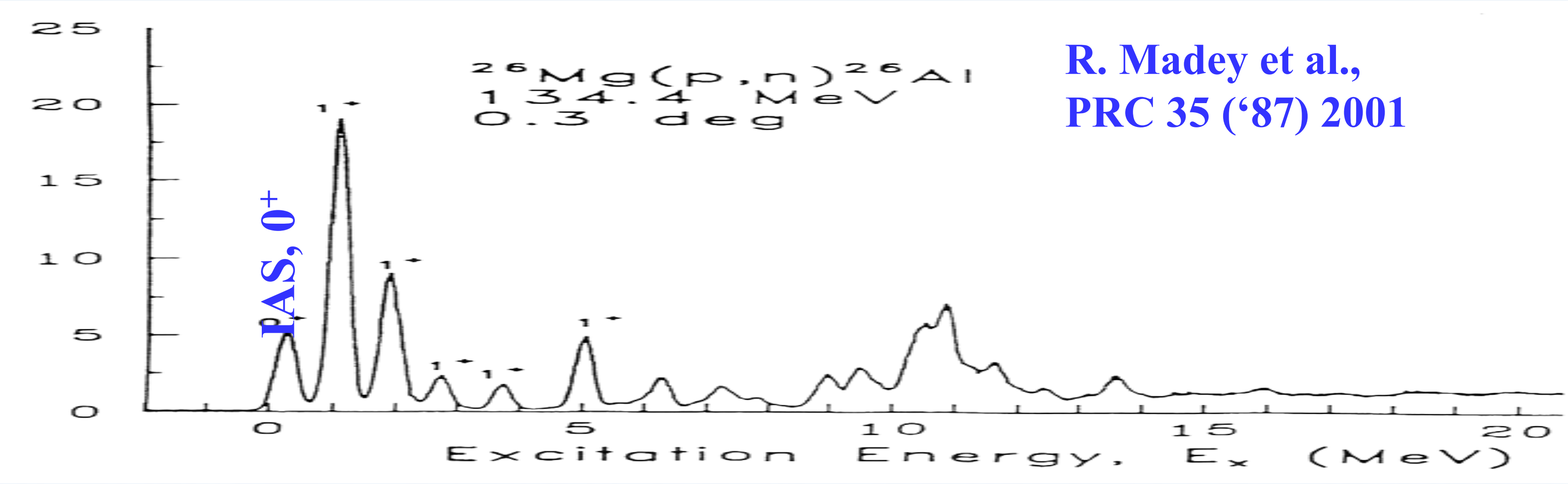

R. Madey et al., PRC 35 ('87) 2001

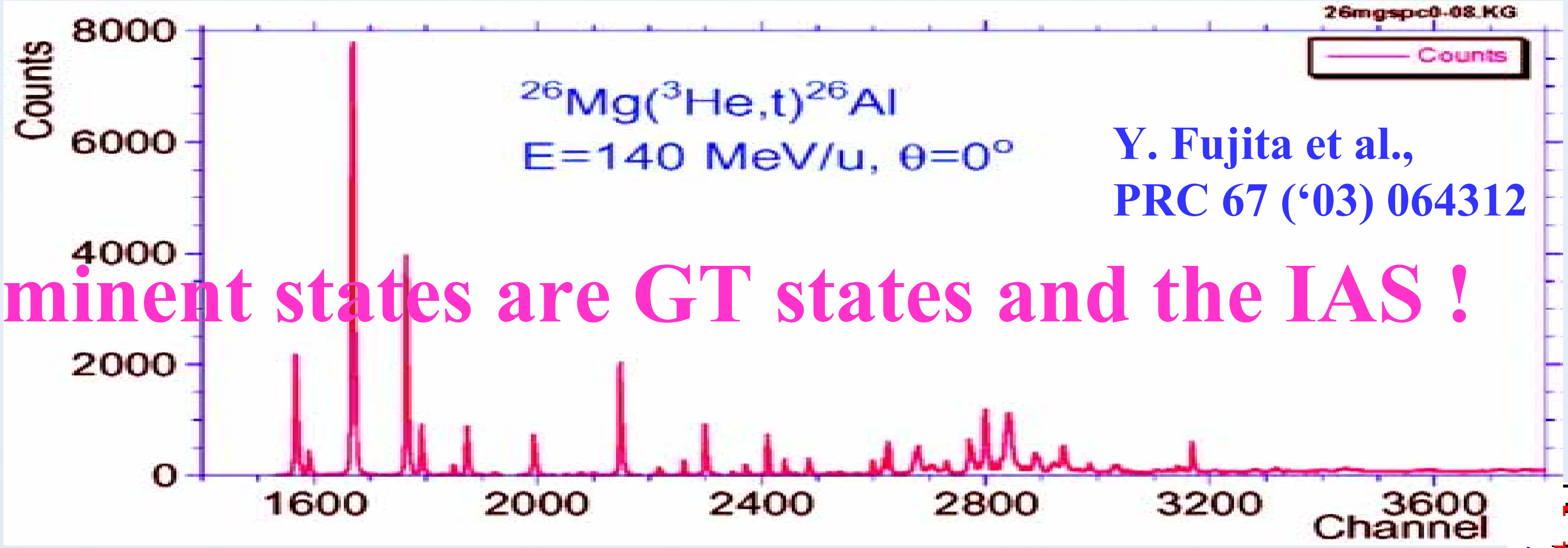

Y. Fujita et al., PRC 67 ('03) 064312

Prominent states are GT states and the IAS !

$^{54}Fe(p,n)$ & $^{54}Fe(^3He,t)$

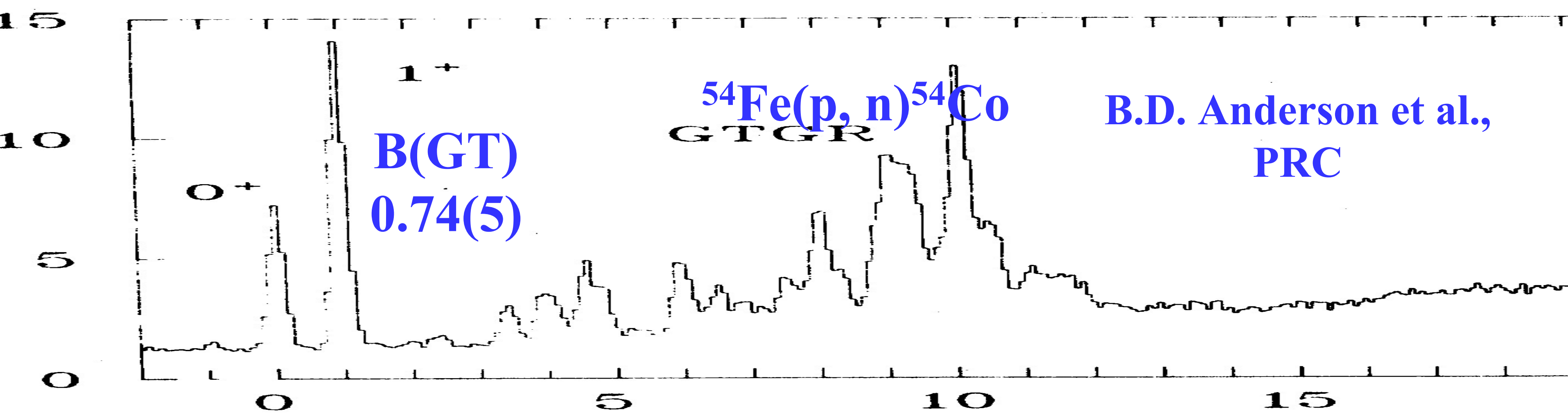

$^{54}Fe(p, n)^{54}Co$

B(GT) 0.74(5)

B.D. Anderson et al., PRC

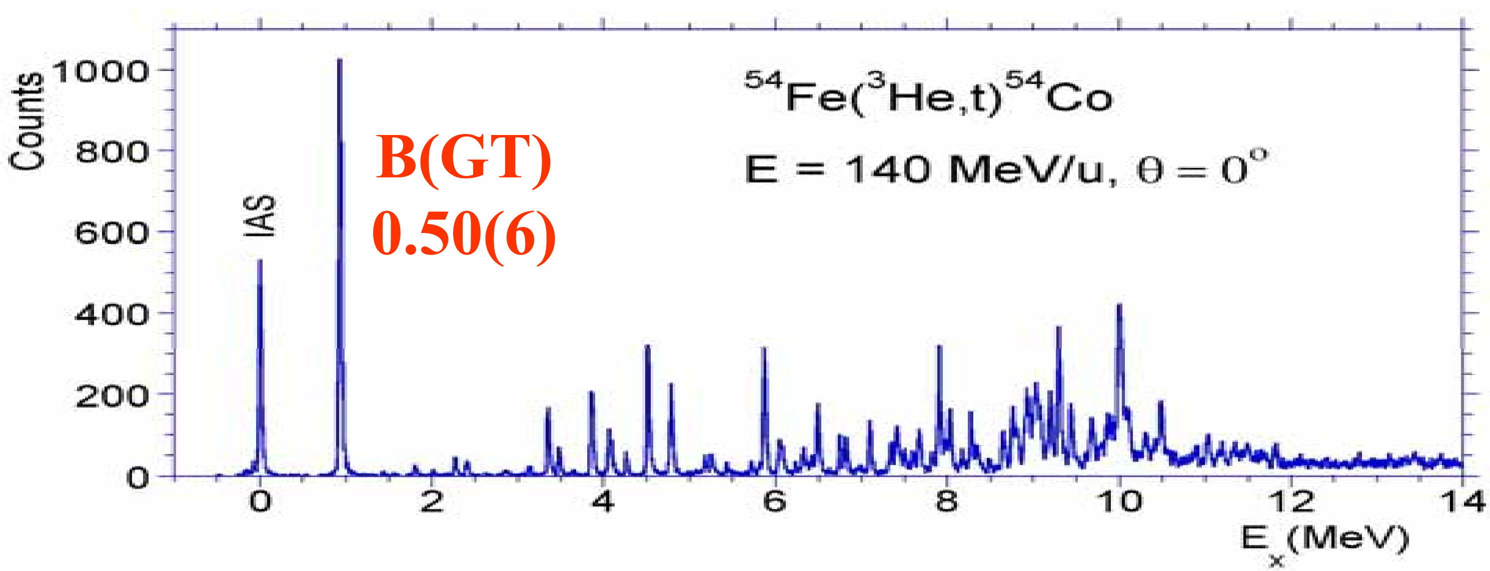

B(GT) 0.50(6)

KVI

Determination of GT$^+$ Strength and its Astrophysical Implications

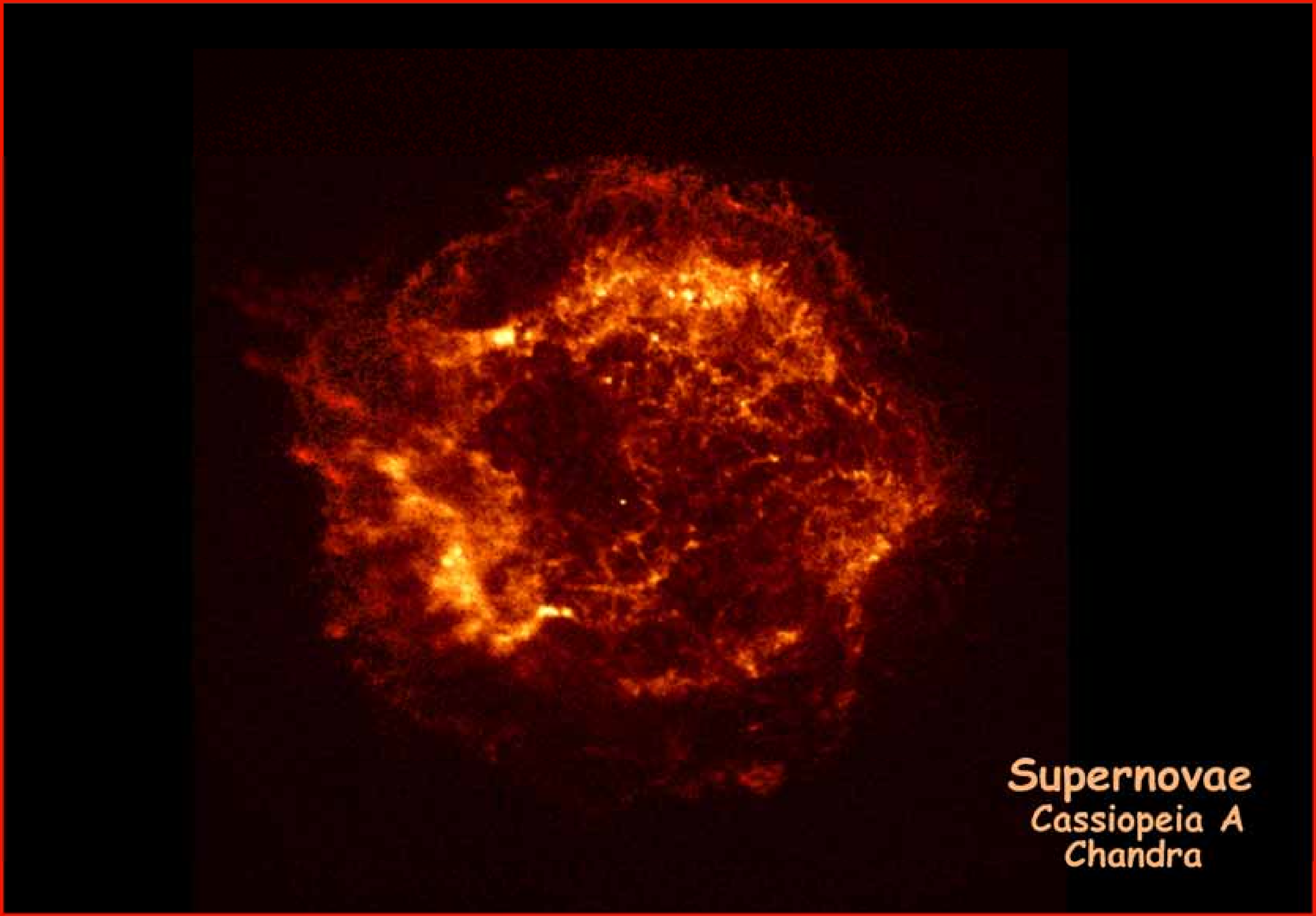
Supernovae
Cassiopeia A
Chandra

Nuclear processes and energy household of supernovae

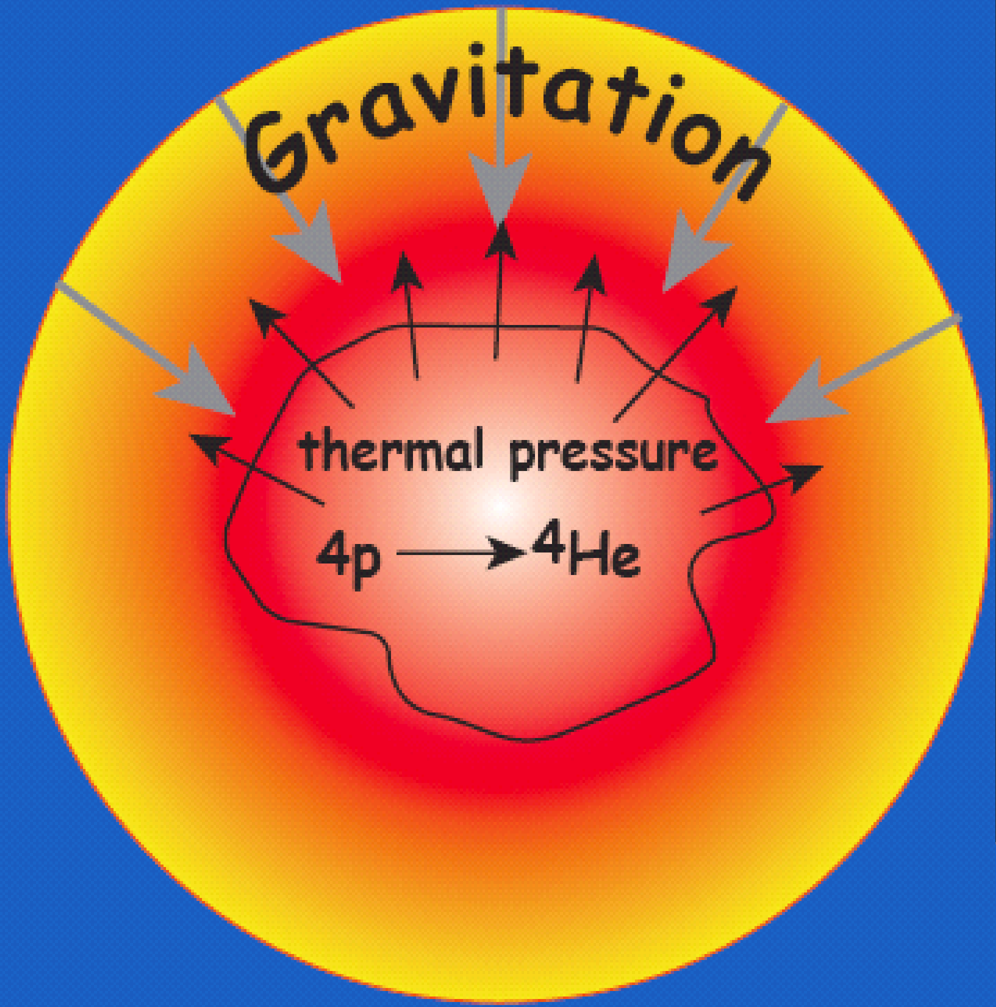

initial condition:
$M > 10\, M_\odot$

energy:
fusion $4p \rightarrow {}^4He$

at: $T \sim 10^7 - 10^8$ K

lifetime: $10^6 - 10^7$ y

after 10^6 - 10^7 y

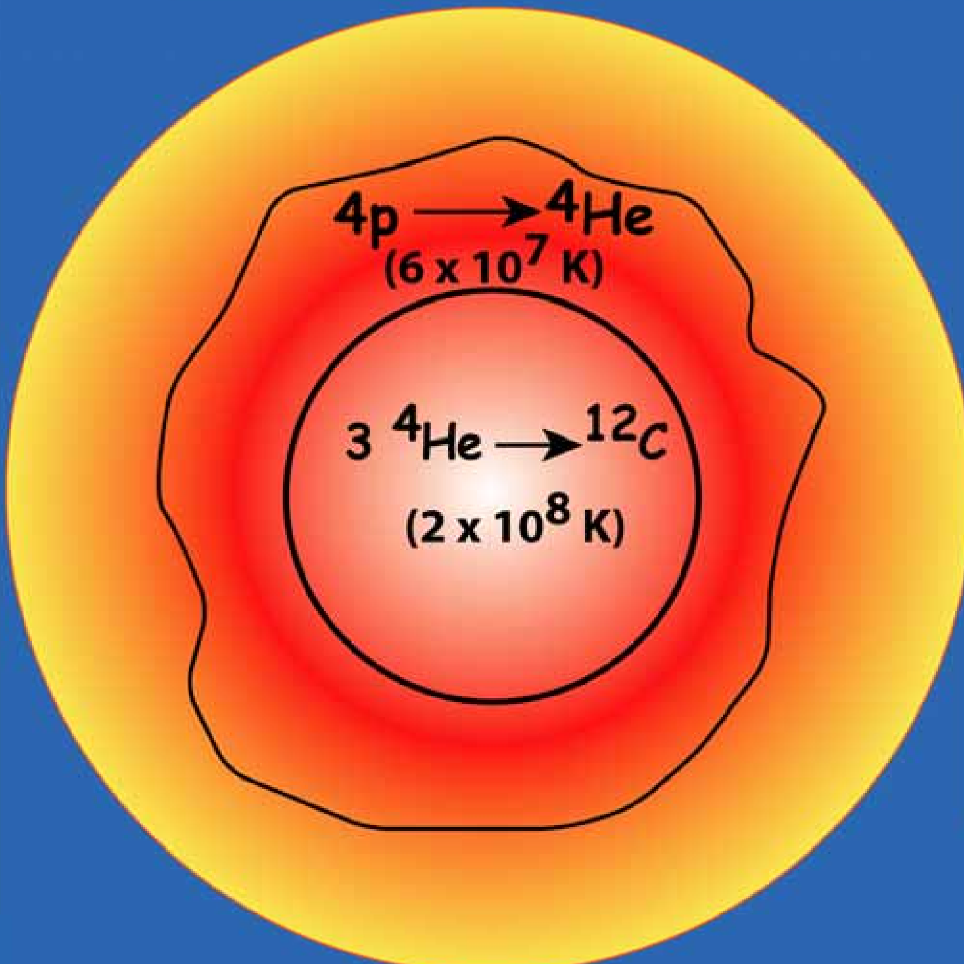

end of H-burning

↓

contraction of star

↓

temperature increase

↓

Red Giant (Super-Giant)

↓

lifetime: 5×10^5 y

end of stellar evolution $M_{star} \sim 15\ M_\odot$

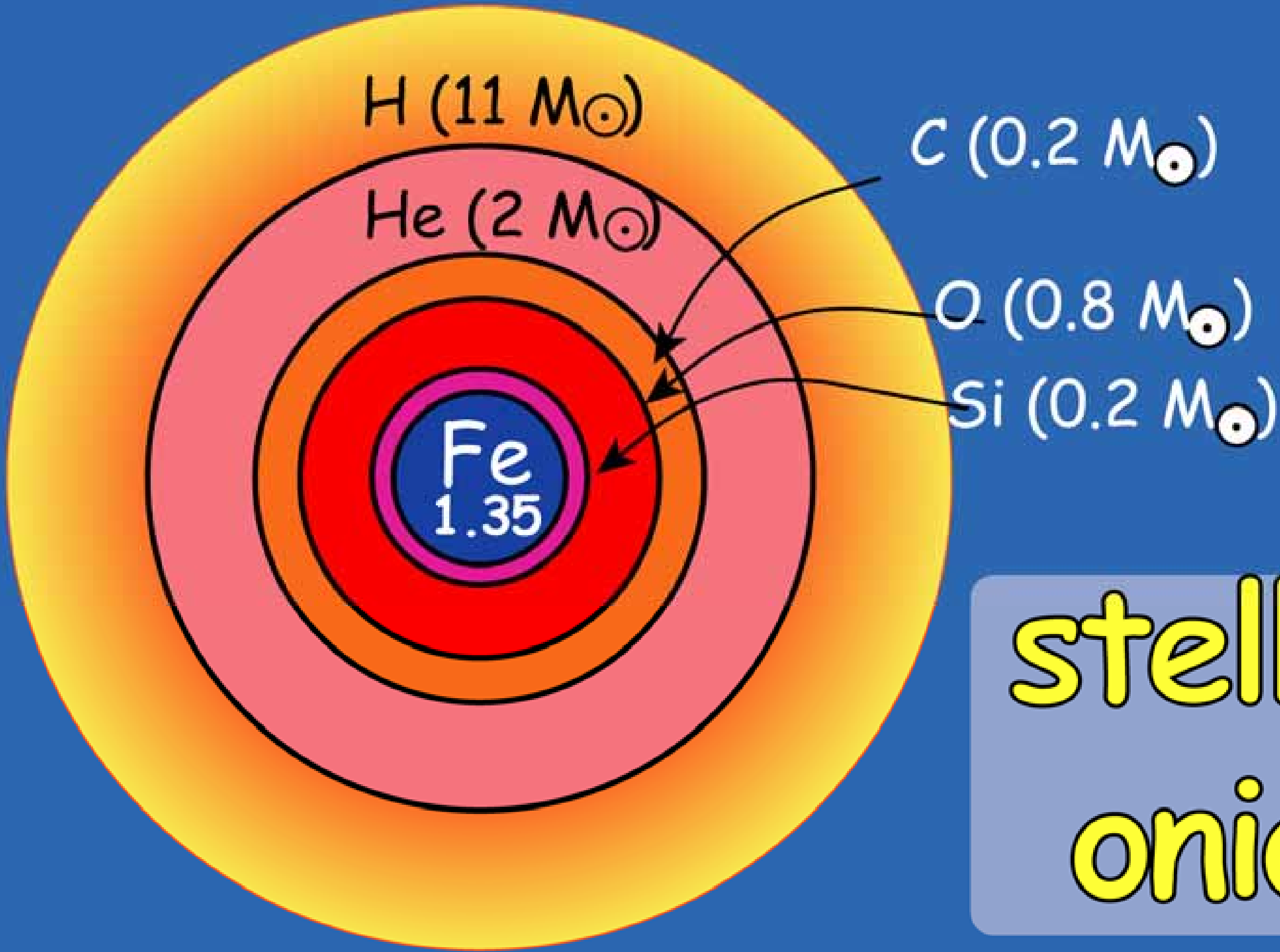

stellar onion

KVI

SN-explosion scenario

- interior of star gets enriched with Fe
- gravitational pressure increases
  balanced by degenerate electron gas up to
  Chandrasekhar limit: $M_{ch} = 1.44\,(2Y_e)^2\,M_\odot$
- start of collapse at
  $T = 10^9$ K and $\rho = 3 \times 10^7$ g/cm^3
  accelerated by neutronization (de-leptonization)

!

$\dfrac{\#\text{ electrons}}{\#\text{ nucleons}}$

$$e^- + p \longrightarrow n + \nu_e$$

$$e^- + (Z,A) \longrightarrow (Z-1,A) + \nu_e$$

escaping

rate determined
by GT-strength
($\Delta S = 1, \Delta T = 1, \Delta L = 0$)

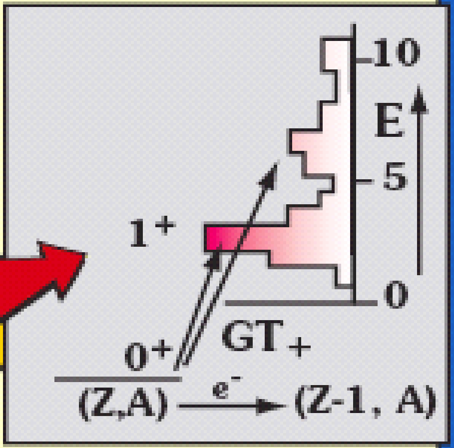

- loss of pressure
- accelerated collapse
- reduction of Y_e
  and loss of energy!!

Y_e at freeze-out determines the explosive energy!!

Electron capture in *fp*-shell

- In supernova explosions, electron capture (EC) on *fp*-shell nuclei plays a dominant role during the last few days of a heavy star [presupernova stage; deleptonization ⇒ core collapse ⇒ subsequent type IIa Supernova (SN) explosion]

  Bethe *et al*. (1979)

- The rate for EC is governed by the GT$^+$ strength distribution at low excitation energy; not accessible to β-decay.

  Fuller, Fowler and Newman (FFN) (1982-1985); estimates of stellar rates in stellar environments using s.p. model.

  Caurier *et al*., Martínez-Pinedo & Langanke (1999), Otsuka *et al*. ⇒ Large shell-model calculations ⇒ marked deviations from FFN EC rate; generally smaller EC rates.

- Experiments and theory relied on (*n,p*) data (TRIUMF) which have a rather poor energy resolution

Stellar EC rates

at a given temperature

important parameters

- location of GT resonance (most important)
- level of quenching
- fragmentation over excitation energy

SM and FFN comparison

from:
Langanke, Martinez-Pinedo
Nucl.Phys. A 673, 481 (2000)

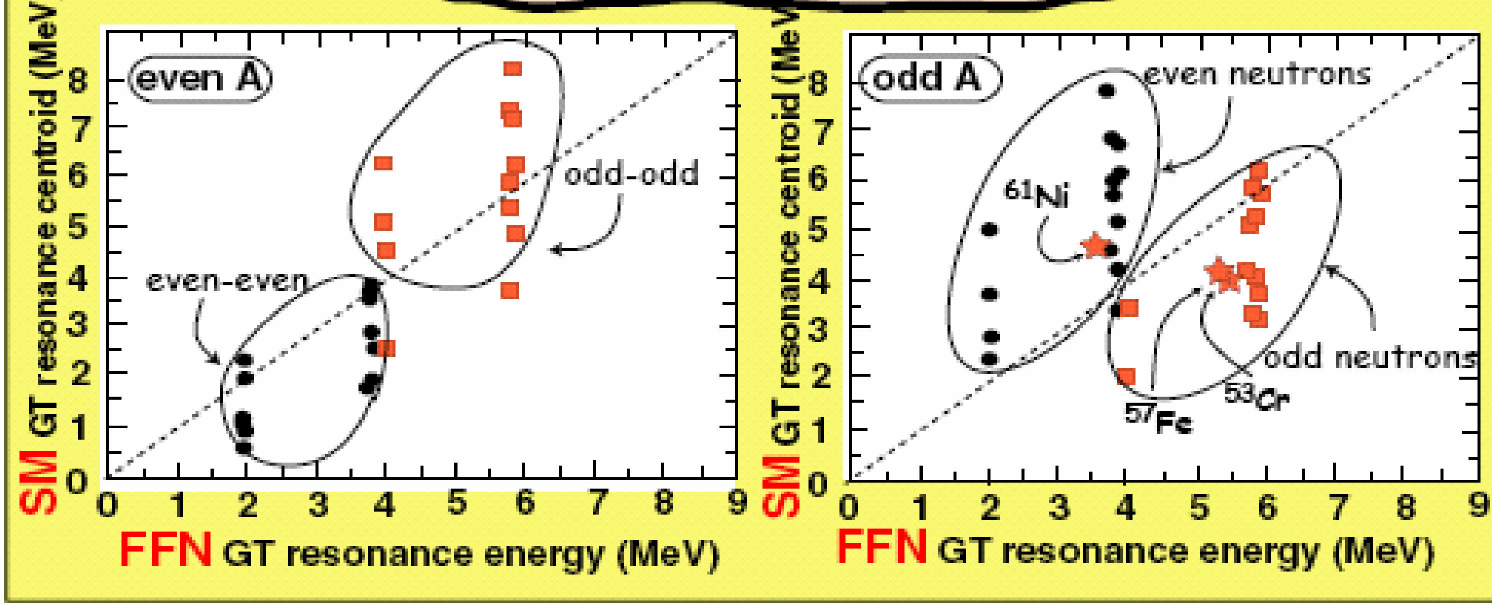

- no exp. data on odd-N nuclei (ususally rare!!)
- no exp. data on odd-odd nuclei (^{50}V is the only stable one)

fp-shell nuclei: large scale shell model calculations

E. Caurier *et al.*
NPA 653 (1999) 439

- Stellar weak reaction rates with improved reliability
- **Large scale shell model (SM) calculations**
- **Tuned to reproduce GT$^+$ strength measured in (*n,p*)**

- **(*n,p*) data from TRIUMF**
- **GT$^+$ strength from SM**
- **Folded with energy resolution**

Case study: ^{58}Ni

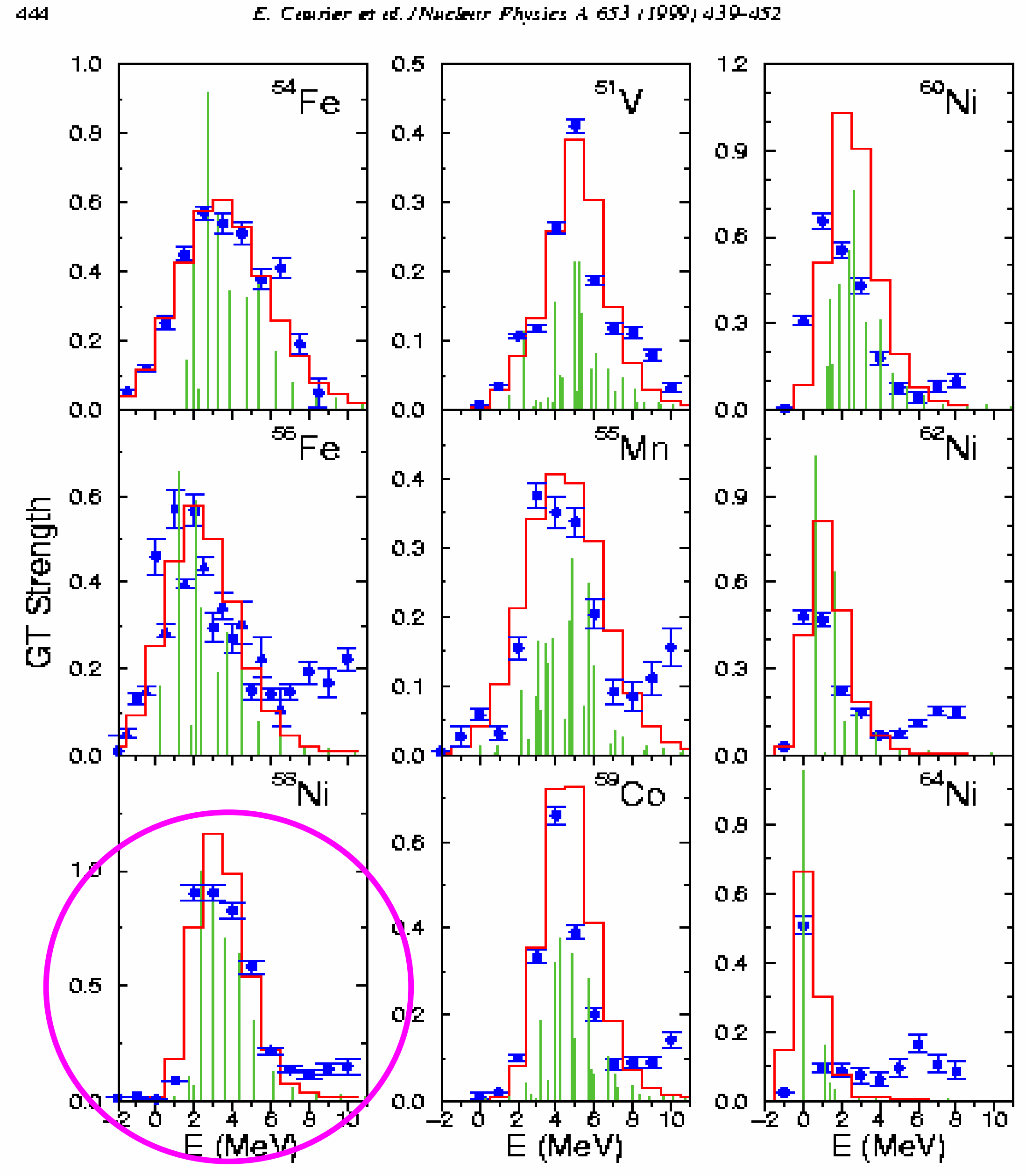

Exclusive excitations $\Delta S = \Delta T = 1$: (d, ^{2}He)

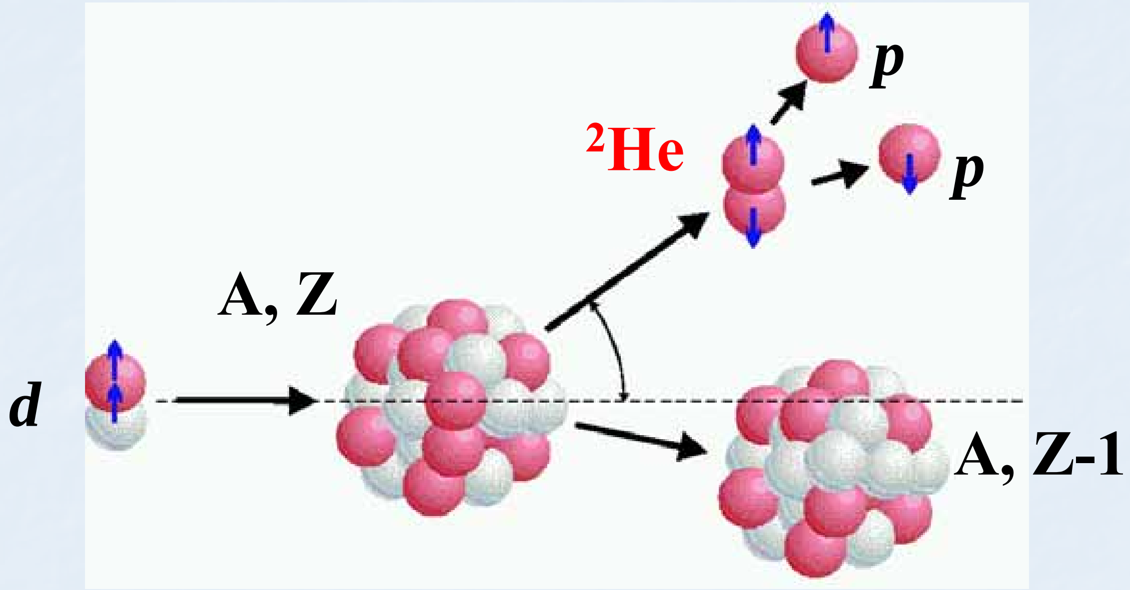

$^3S_1$ deuteron $\Rightarrow$ $^1S_0$ di-proton (^{2}He)

$^1S_0$ dominates if (relative) proton kinetic energy $\varepsilon < 1$ MeV

(n,p)-type probe with exclusive $\Delta S=1$ character (GT^+ transitions)

But near 0°: tremendous background from d-breakup

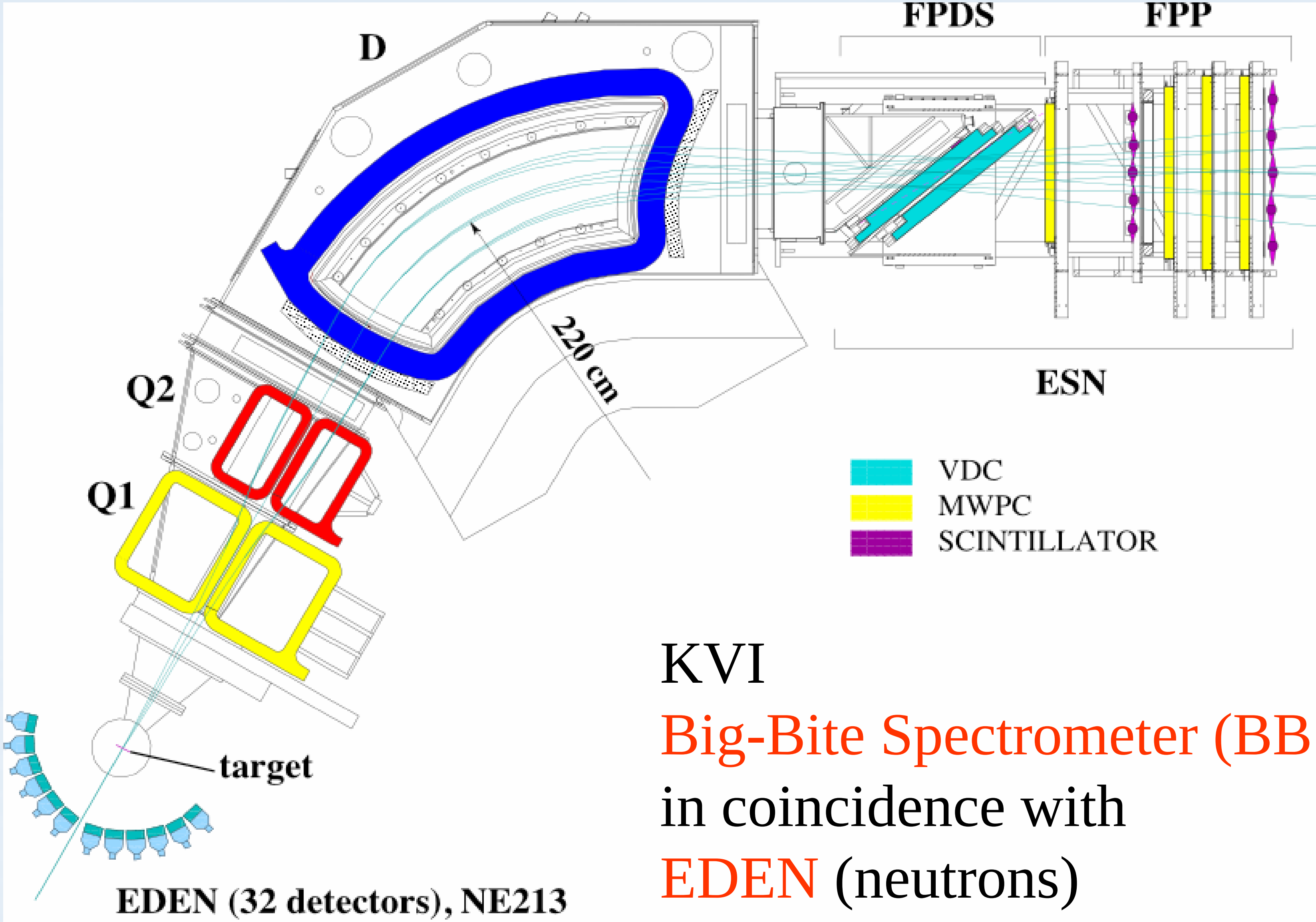

KVI

Big-Bite Spectrometer (BBS)

in coincidence with

EDEN (neutrons)

SiLi ball (protons)

KVI

Setup: ESN detector

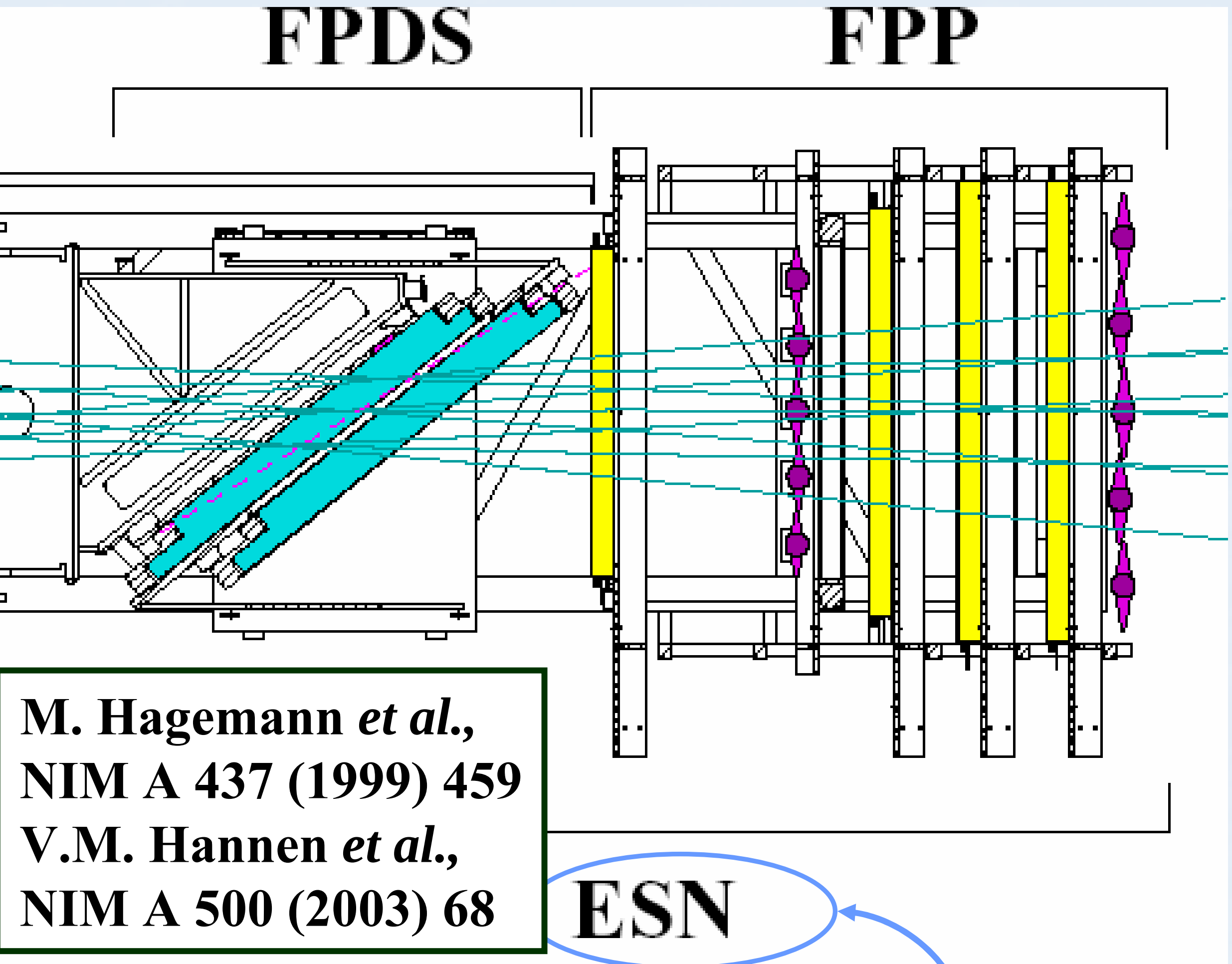

M. Hagemann *et al.*,
NIM A 437 (1999) 459
V.M. Hannen *et al.*,
NIM A 500 (2003) 68

Focal-Plane Detector:
(FPDS): 2 VDCs

Focal-Plane Polarimeter:
(FPP): 4 MWPCs & graphite analyzer

features a.o.:
fast readout
VDC readout pipeline
TDC's
VDC decoding using imaging techniques
DSP based online analysis

Bari, Darmstadt, Gent, Iserlohn, KVI, Milano, Münster, TRIUMF

- **Good double tracking**
- **Use VDC information**
- **Good phase space coverage for small relative proton energies**

S. Rakers *et al.*
NIM A481 (2002) 253

measured

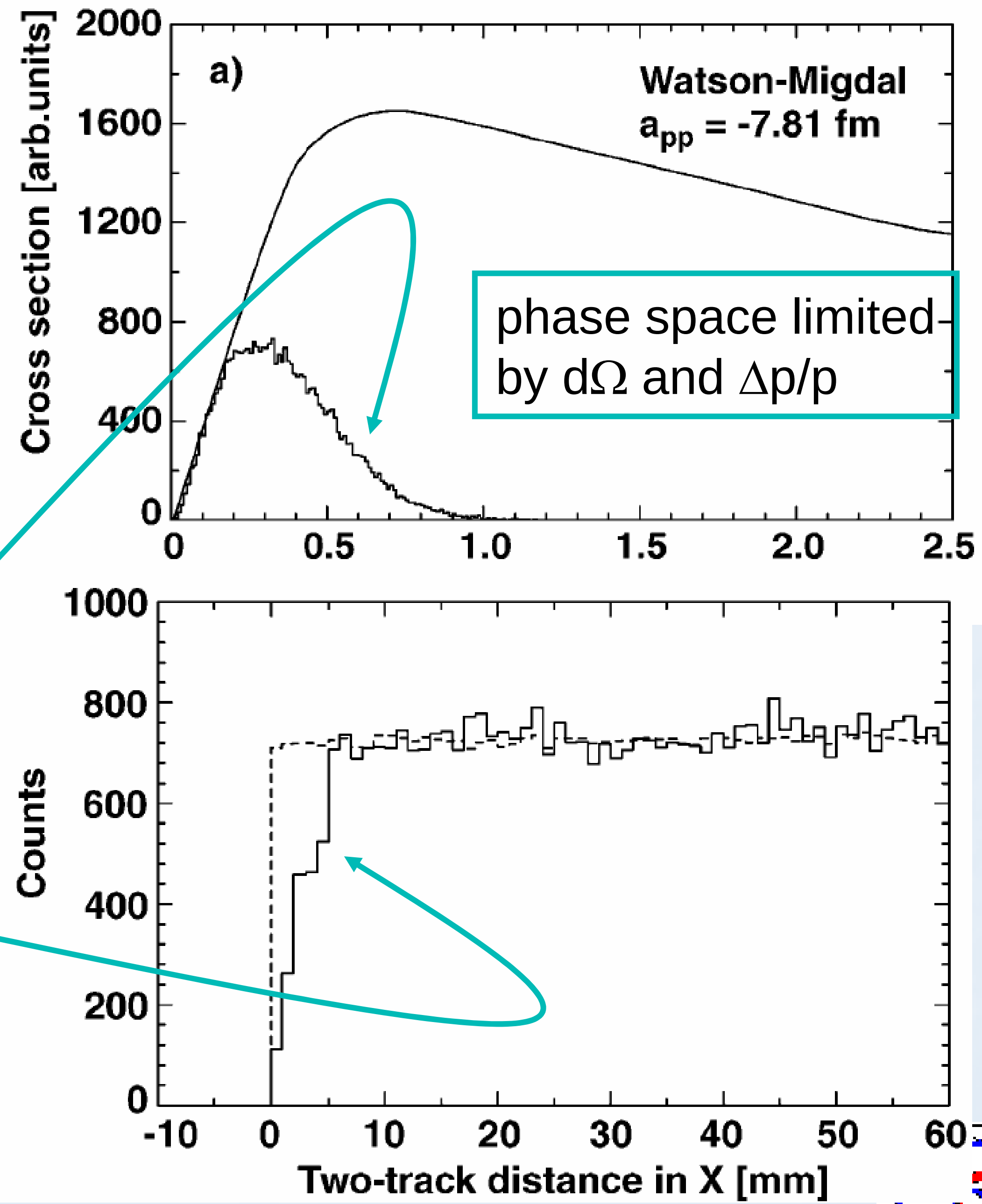

Exclusive measurement of ΔS= ΔT =1 strength: $^{12}C(d, {}^{2}He)^{12}B$

E_0 = 171 MeV, θ = 0°

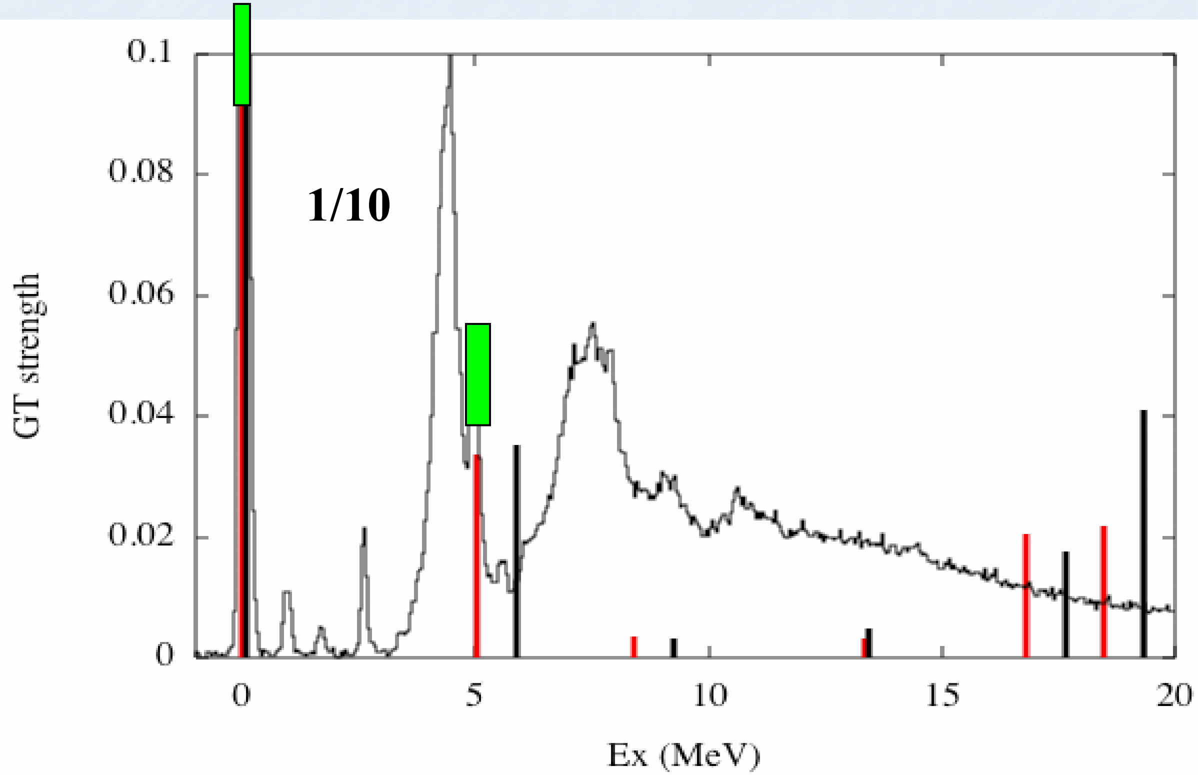

- shell model calculations 4 ħω & 6 ħω (G. Martinez-Pinedo)
- B (GT^{+}) (S. Rakers)

(p,n) vs ($d,^2$He): calibration

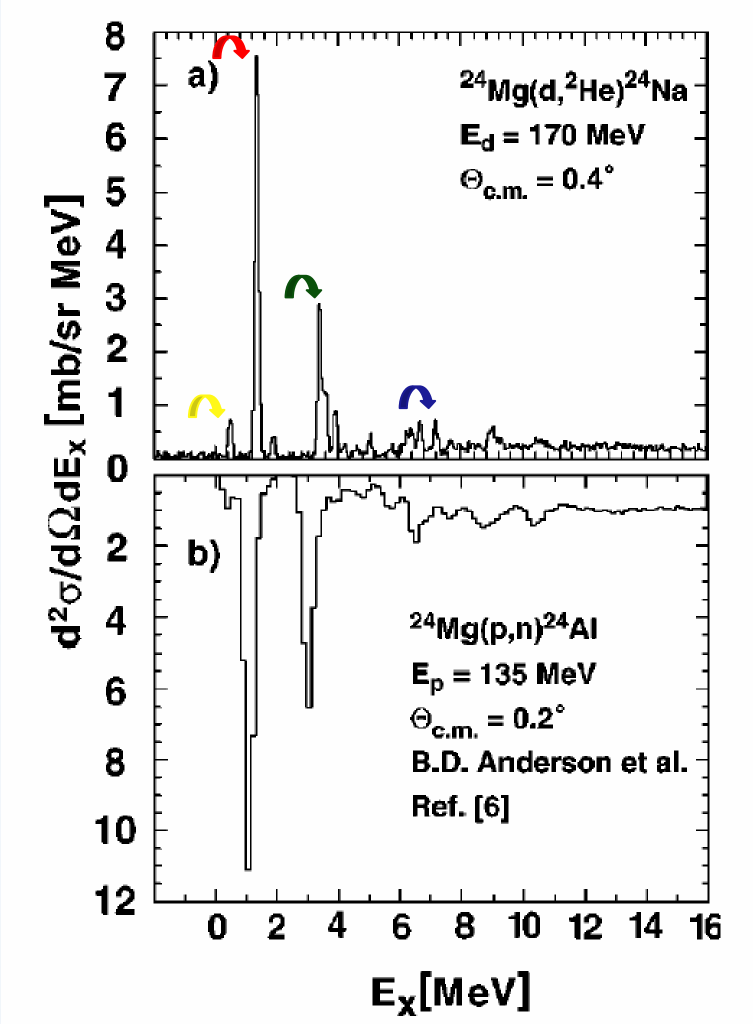

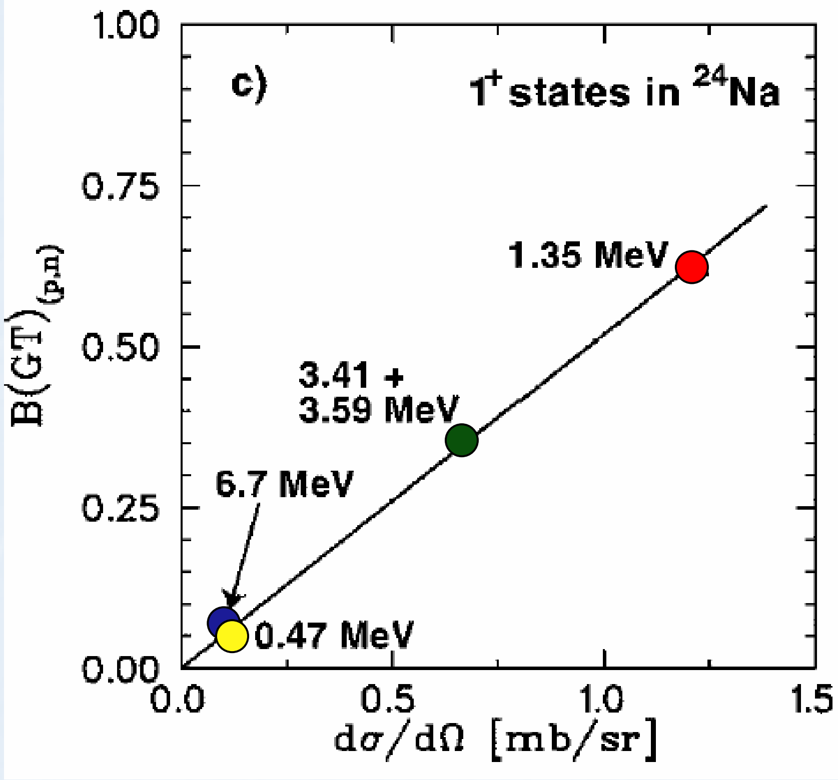

Self-conjugate ^{24}Mg

S. Rakers *et al.*
PRC **65** (2002) 044323

Experimental cross section and GT strength

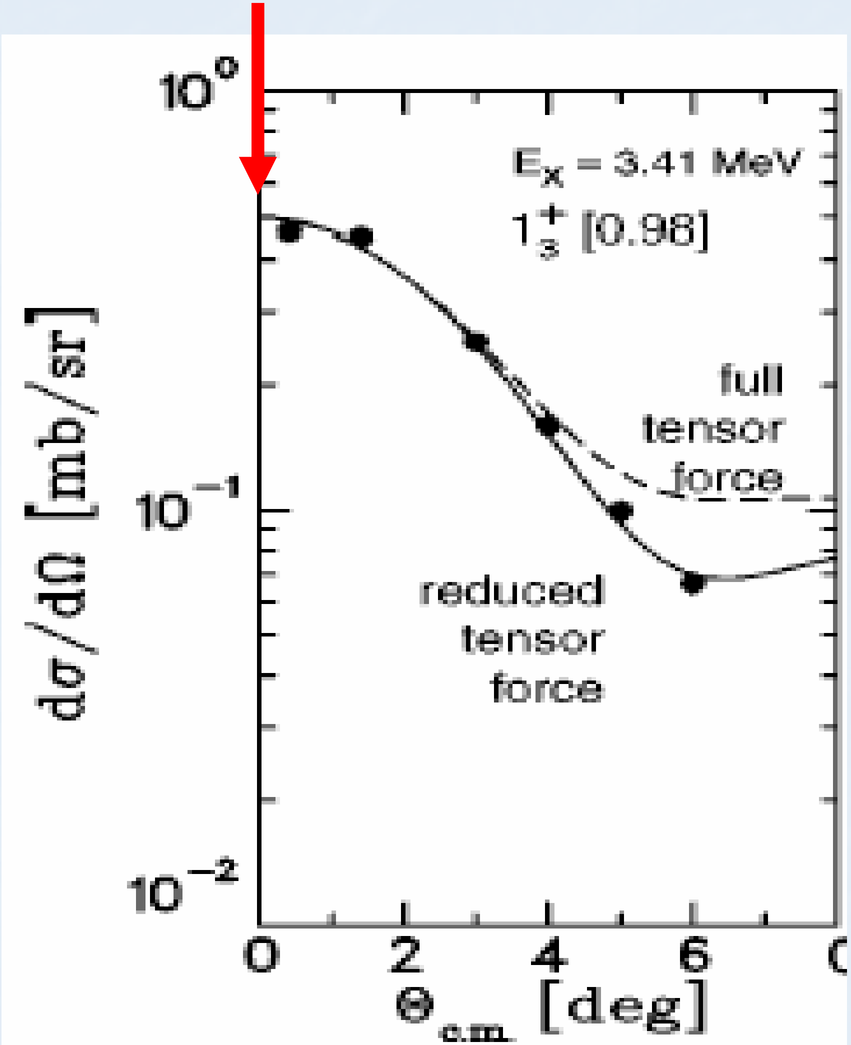

$$\mathbf{B}_{\mathrm{exp}}(\mathrm{GT+}) = \frac{\mathrm{d}\sigma(q=0)}{d\Omega} \cdot \left[\frac{d\sigma(GT)}{d\Omega}\right]^{-1}$$

extrapolated (DWBA)

unit cross section

GT Strength in ^{12}B and ^{24}Na from (d,^{2}He) reaction

Target	Reference data		Present data			
	E_x [MeV]	$B(GT_-)$	E_x [MeV]	$d\sigma/d\Omega(q=0)$ [mb/sr]	$\sigma(L=0)/\sigma(\tau o \tau)$ (q=0)	$B(GT_+)$ (C=0.267)
^{12}B	0.00	0.998	0.00	2.580±0.138	0.988	0.930±0.050
			5.00	0.138±0.010	0.976	0.050±0.004
^{24}Na	0.44	0.050	0.47	0.138±0.012	0.821	0.049±0.004
	1.07	0.613	1.35	1.563±0.085	0.948	0.654±0.035
	1.58	0.020	1.89	0.087±0.026	0.649	0.025±0.008
	2.98	0.362	3.41	0.667±0.039	0.980	0.290±0.016
			3.59	0.266±0.018	0.806	0.095±0.006
	3.33	0.059	3.92	0.193±0.058	0.809	0.070±0.022
	4.69	0.015	5.06	0.093±0.027	0.561	0.024±0.007
			6.24	0.086±0.026	0.818	0.031±0.010
	6.46	0.068	6.70	0.161±0.012	0.972	0.071±0.005
	6.87	0.029	7.20	0.173±0.013	0.642	0.050±0.004

(d,^{2}He) as GT$^+$ probe in *fp* shell nuclei

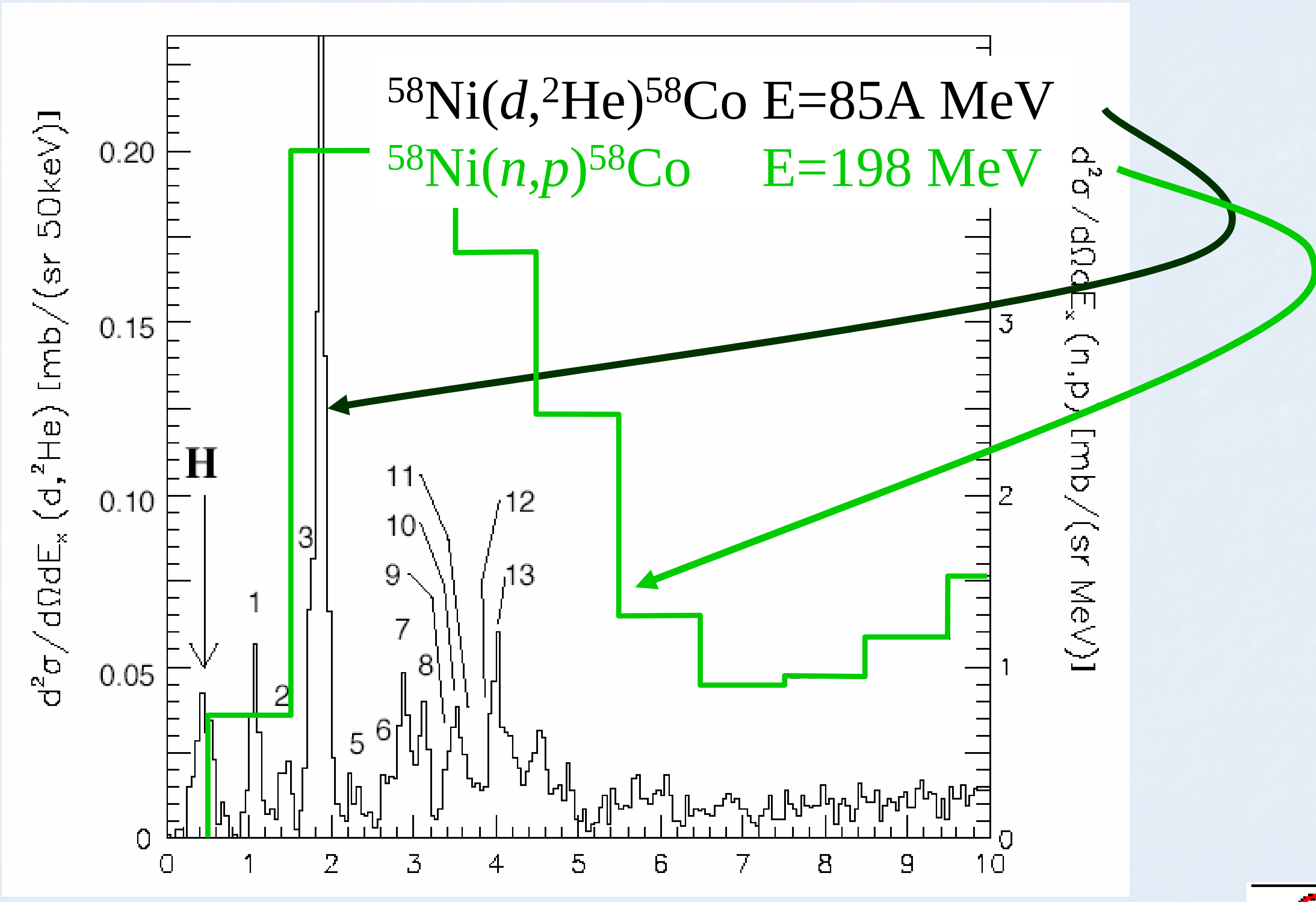

KVI

GT Strength in ^{58}Co from (d,^{2}He) reaction

E_x [MeV]	dσ/dσ(0.5°) [mb/sr]	σ(L=0)/σ(τoτ)	B(GT+)
1.050	0.159±0.009	0.88	0.15±0.01
1.435	0.078±0.006	1.00	0.09±0.01
1.729	0.148±0.014	1.00	0.16±0.02
1.868	0.648±0.020	1.00	0.72±0.05
2.249	0.047±0.004	1.00	0.05±0.01
2.660	0.057±0.005	0.96	0.06±0.01
2.860	0.145±0.009	0.99	0.17±0.01
3.100	0.126±0.008	0.99	0.15±0.01
3.410	0.065±0.007	0.96	0.07±0.01
3.520	0.080±0.009	0.95	0.09±0.01
3.625	0.067±0.007	0.87	0.07±0.01
3.900	0.062±0.006	0.97	0.07±0.01
4.030	0.155±0.010	1.00	0.19±0.01
4.05-5.00	0.381±0.061		0.49±0.09

GT$^+$ strength: comparison (*n,p*), (*d*,^{2}He) & theory

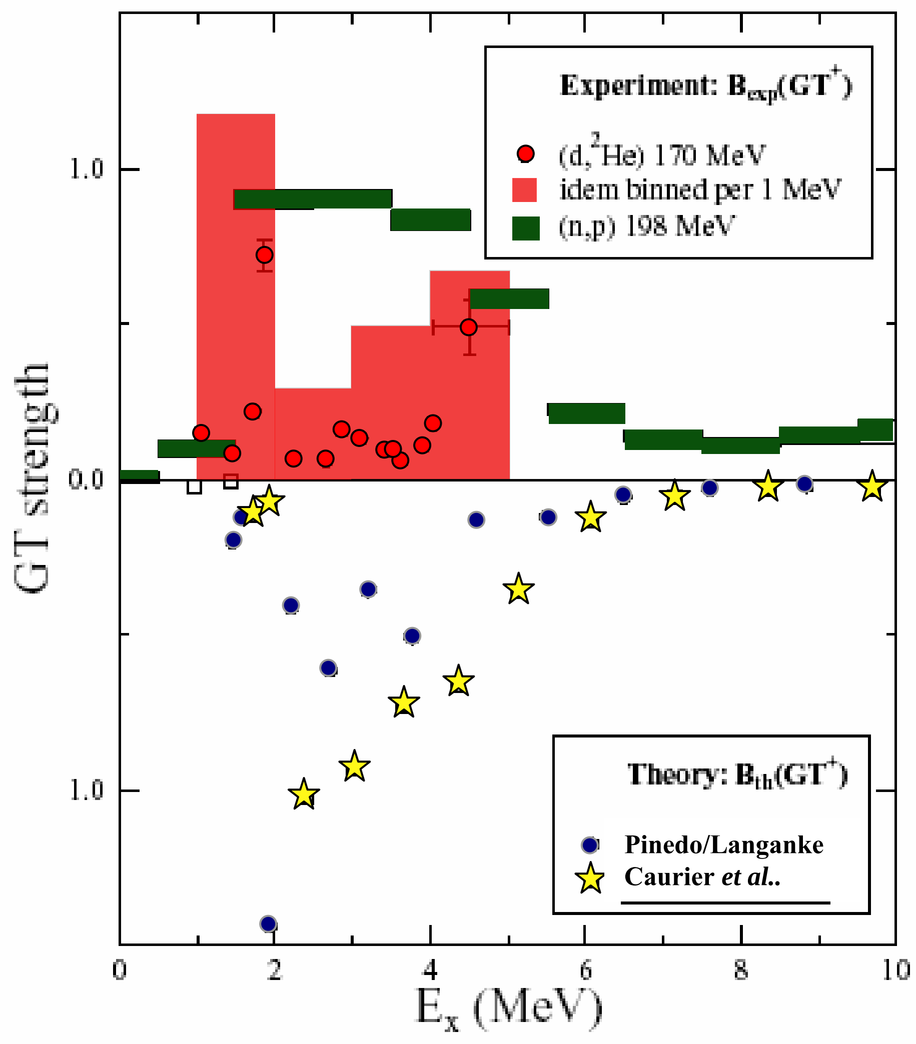

Up to 4 MeV excitation:

13 GT transitions measured (*d*,^{2}He)

Strength rebinned in 1 MeV bins

Significant differences

Updated shell model calculations by Pinedo/Langanke

Electron capture rate

$$\lambda_{ec} \approx \sum_i B_i(GT) \int_{\omega_l}^{\infty} \omega p \left(Q_i + \omega\right)^2 F(Z,\omega) S_e(\omega,T) d\omega$$

With

- ***$B_i(GT)$*** **Gamow-Teller strength distribution**
- ***ω*** **and** ***p*** **energy and momentum electrons**
- ***$S_e(\omega,T)$*** **Fermi-Dirac distribution electron gas at temperature** ***T***

e^--capture rates using experimental strengths
(Pinedo, Langanke)

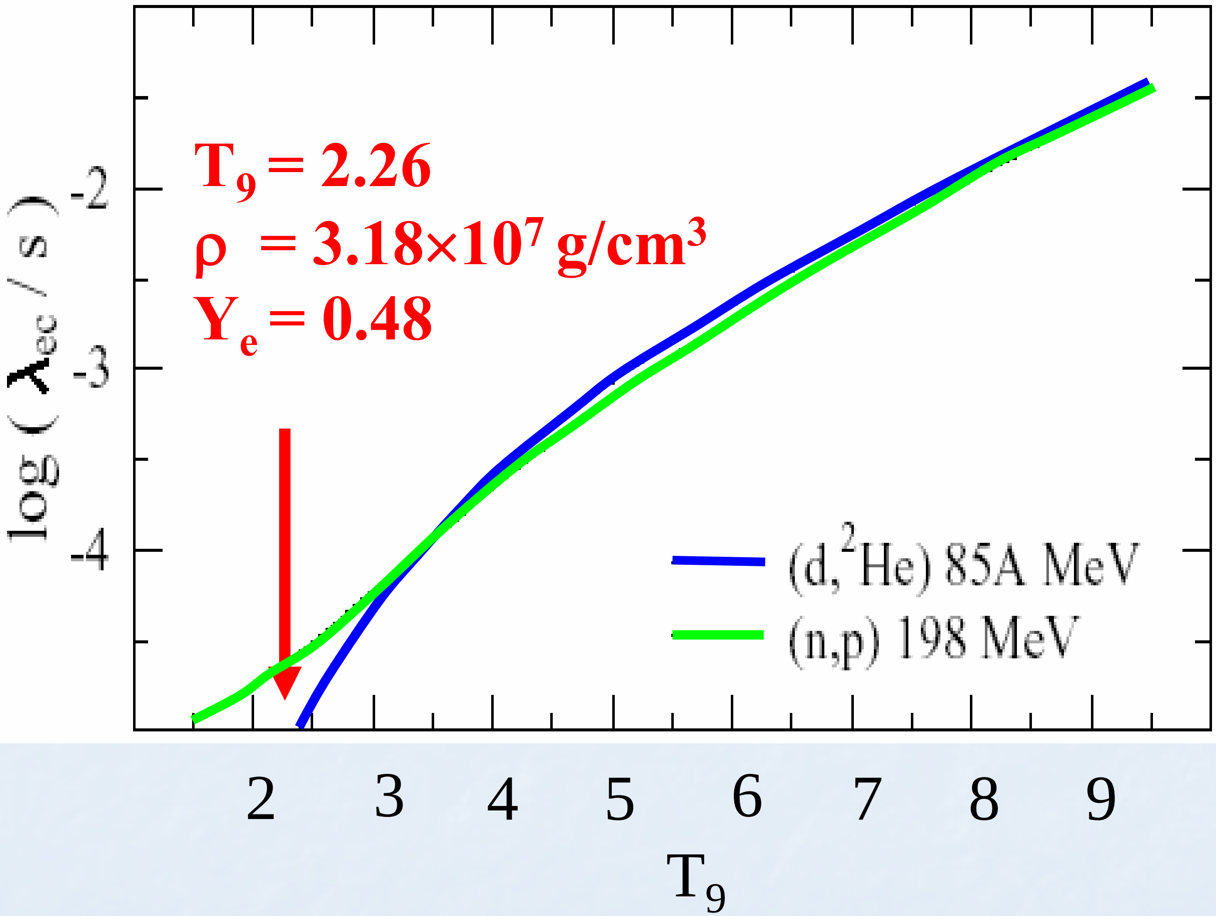

Evolution of core of 25 $M_\odot$ star. Conditions following silicon depletion. [Heger *et al.*, Astrophys. J. 560 (2001) 307]

$T_9 = 4.05$
$\rho = 3.18\times10^7$ g/cm^3
$Y_e = 0.48$

Calculate EC rates for g.s. as a function of T_9

Strength deviations at low excitation: rates deviation at low T

^{58}Ni: comparison of e-capture rates theory/experiment

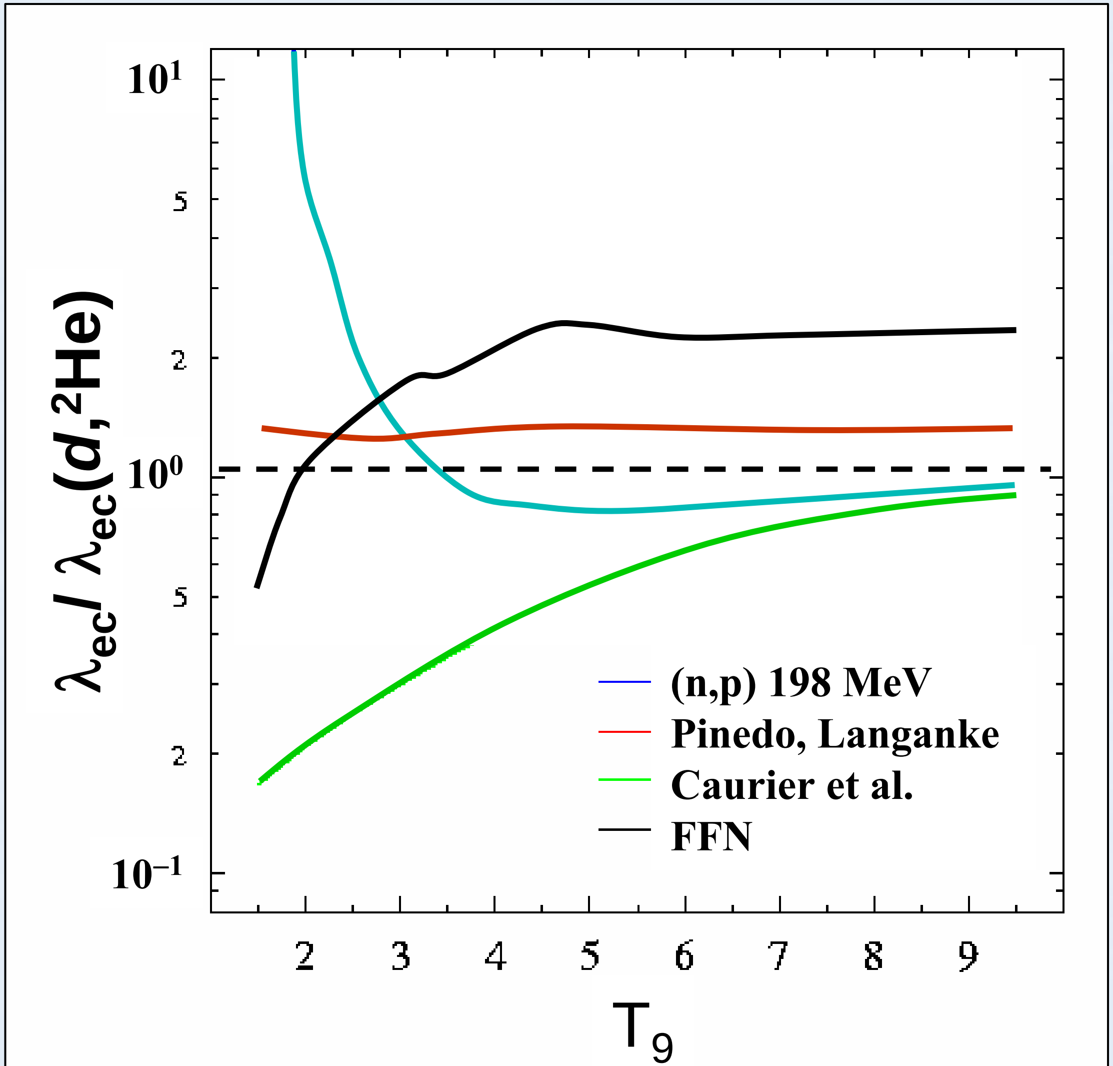

- Influence of GT strength distribution on calculated capture rate is dramatic, especially at low temperatures
- rates vary up to a factor 5-6
- FFN not too far off
- large scale shell-model calculations fail at low T
- calculations with improved residual interaction in reasonable agreement

$^{51}V(d,^2He)^{51}Ti$: B(GT$^+$) for proton-odd fp-shell nucleus

^{51}V g.s. ($J^\pi=7/2^-$, T=5/2) $\Rightarrow$ ^{51}Ti ($J^\pi=5/2^-, 7/2^-, 9/2^-$, T=7/2)

Independent single-particle model (FFN): E_x(GTR)=3.83 MeV

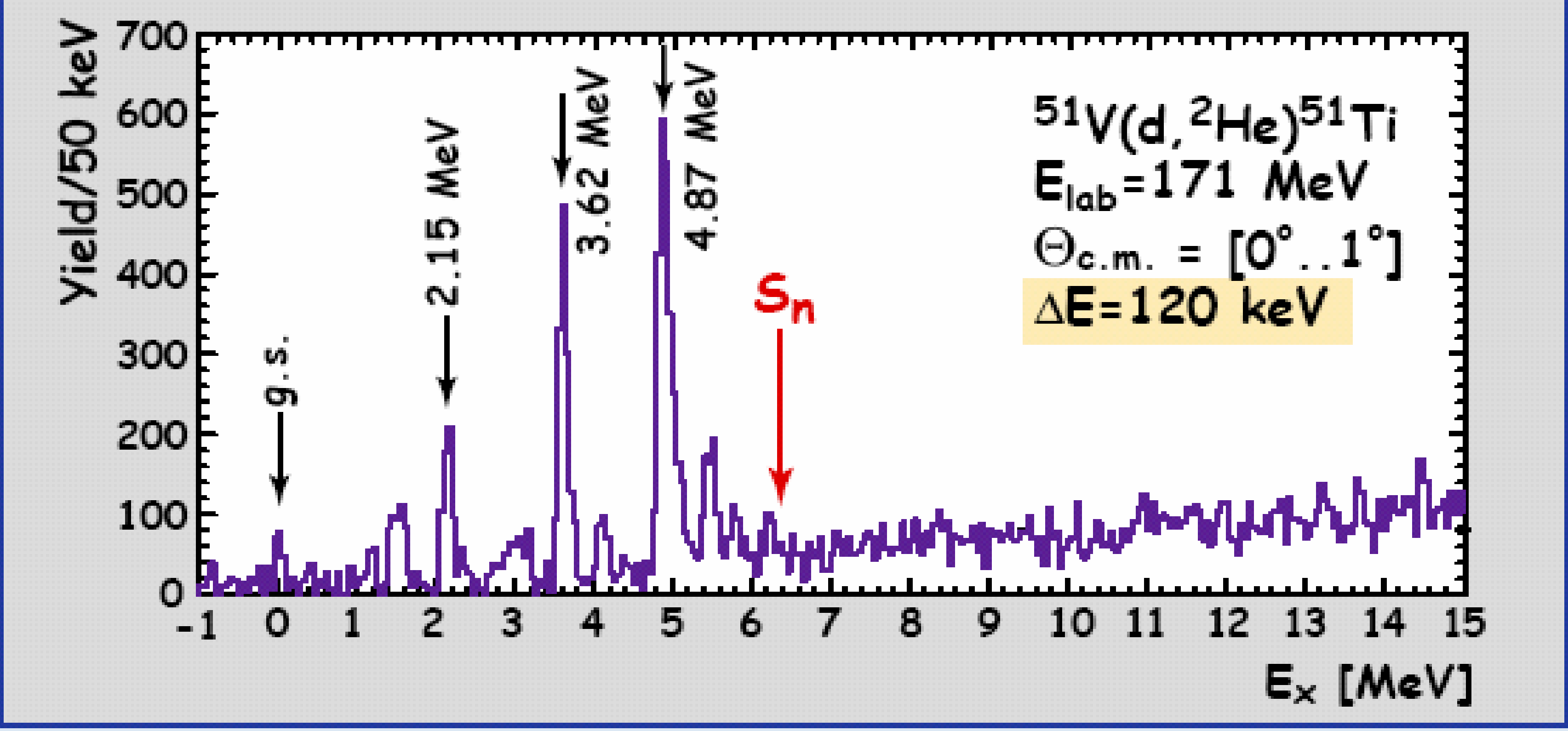

C. Bäumer *et al.*, PRC **68**, 031303(R) (2003)

C. Bäumer *et al.*,
PRC **68**, 031303(R)
(2003)

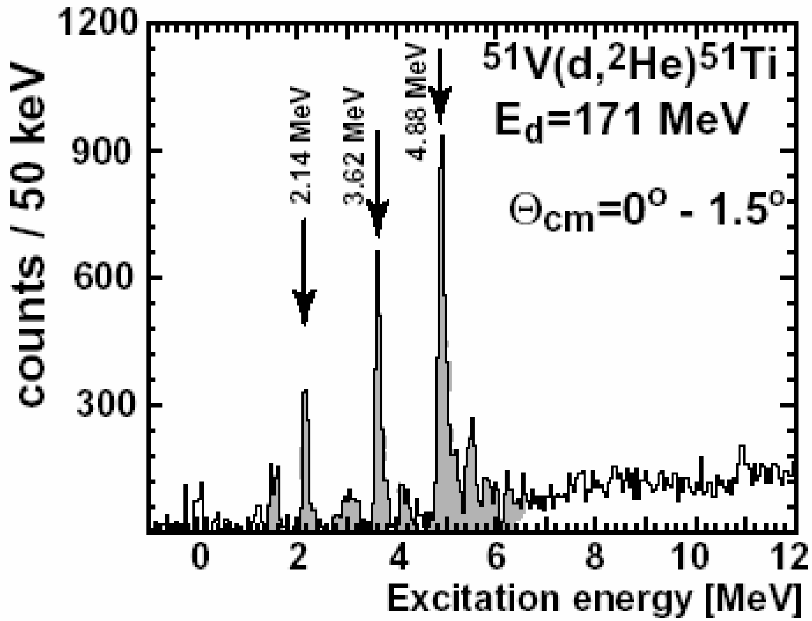

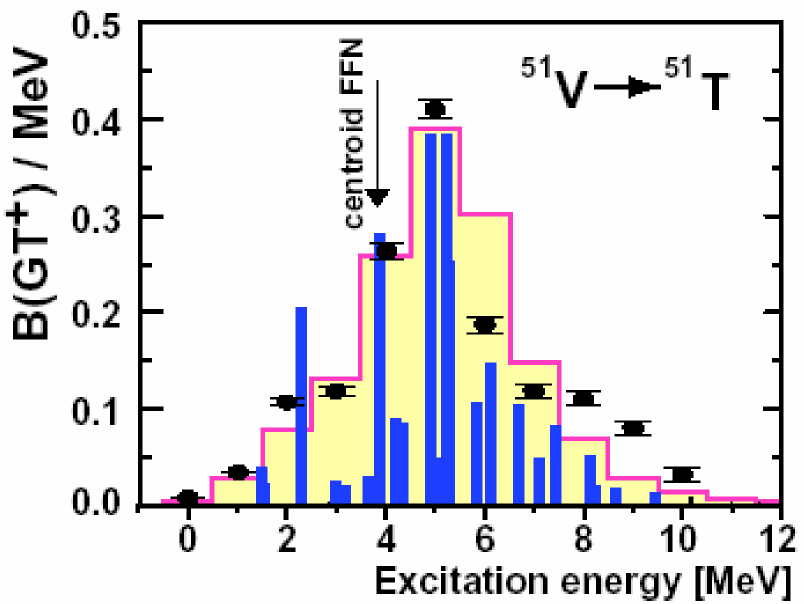

$^{51}V(d,^{2}He)$: Angular distributions of $d\sigma/d\Omega$

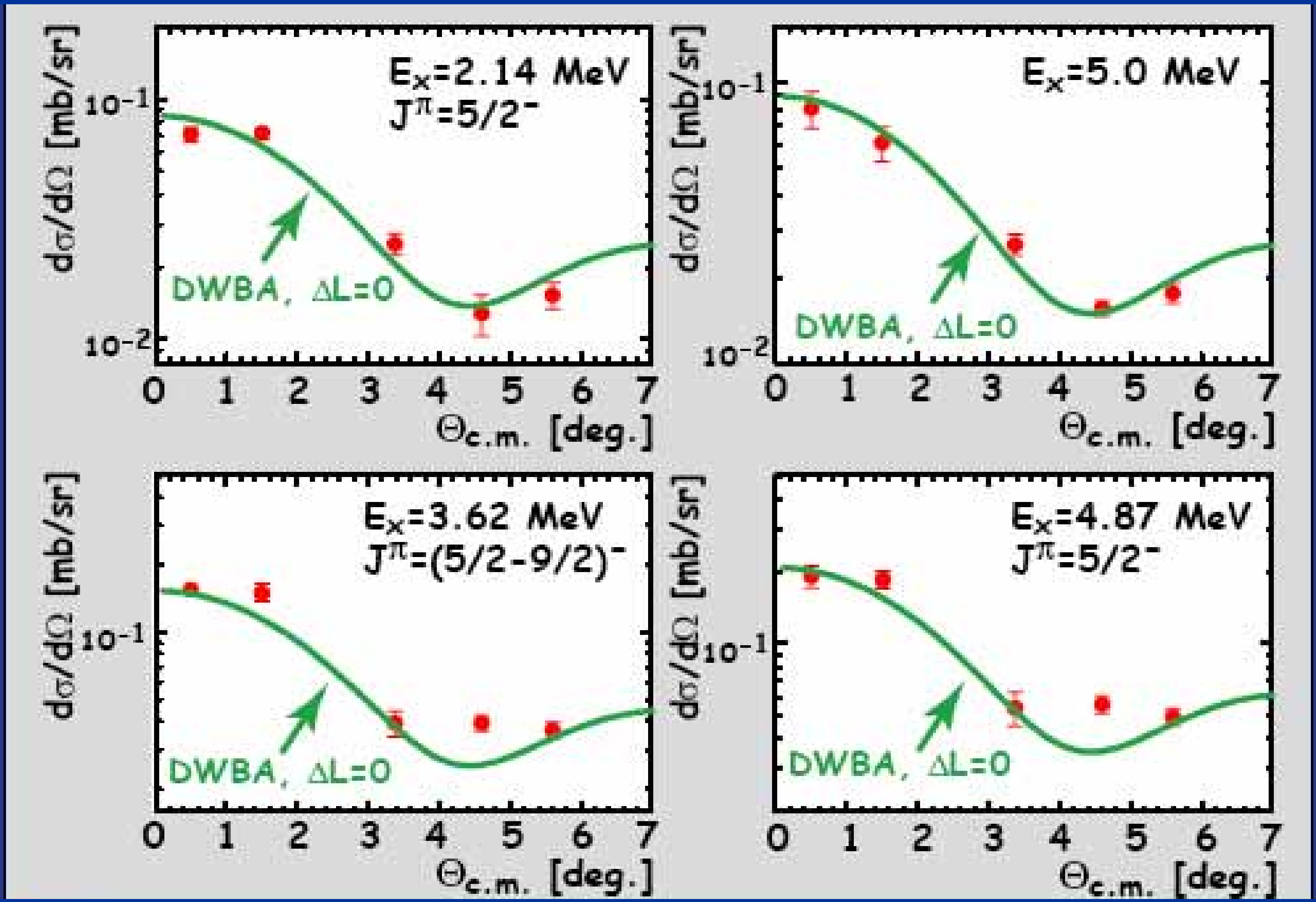

$^{51}V(d,^2He)$: Comparison with shell-model calculations

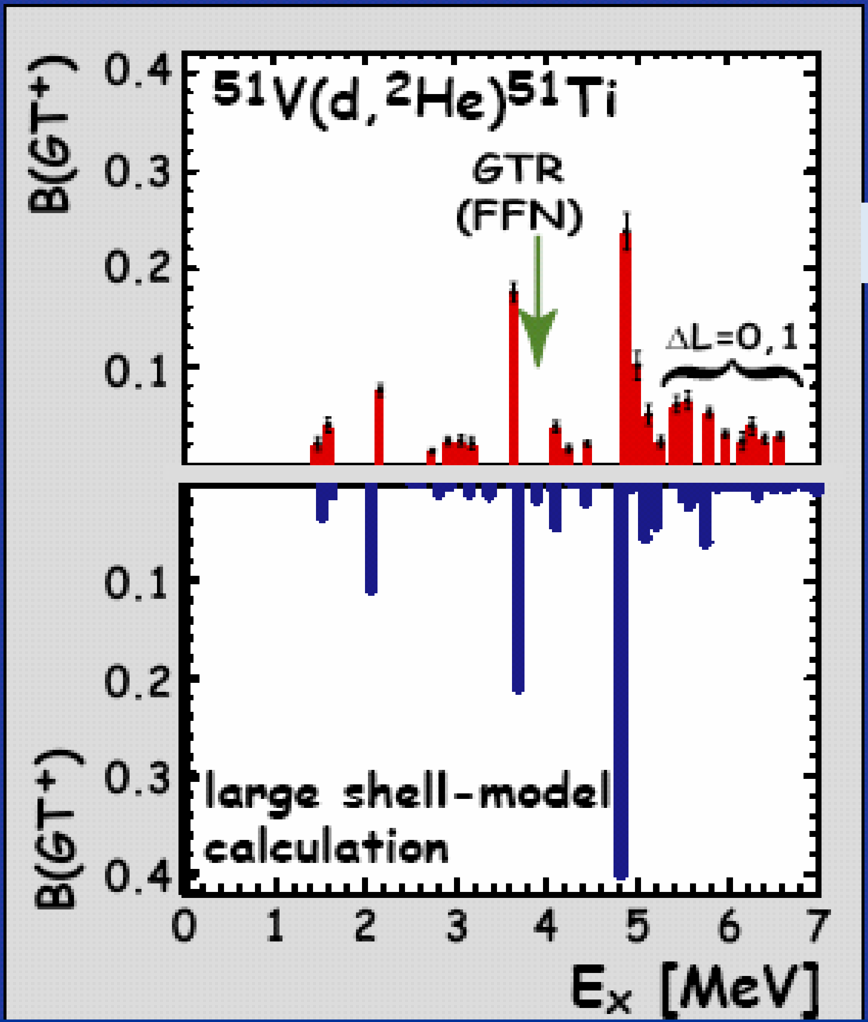

← Experimental result

← Calculations
G. Martínez-Pinedo,
K. Langanke

$^{50}V(d,^2He)$: GT^+ transitions from odd-odd nucleus

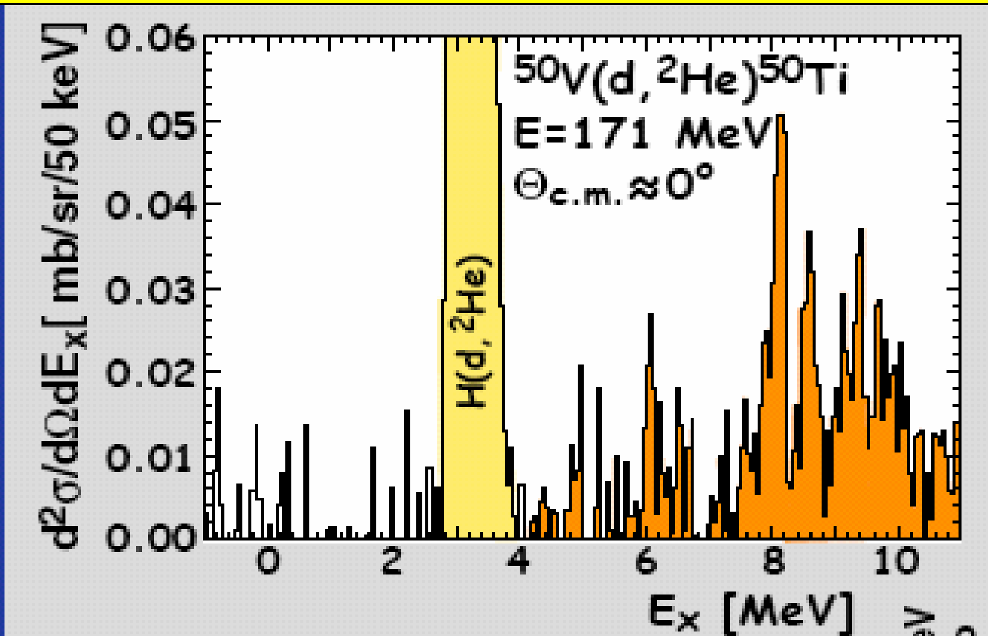

^{50}V	GT^+	^{50}Ti
$J^\pi=6^+$	$\rightarrow$	$J^\pi=5^+, 6^+, 7^+$
T=2		T=3

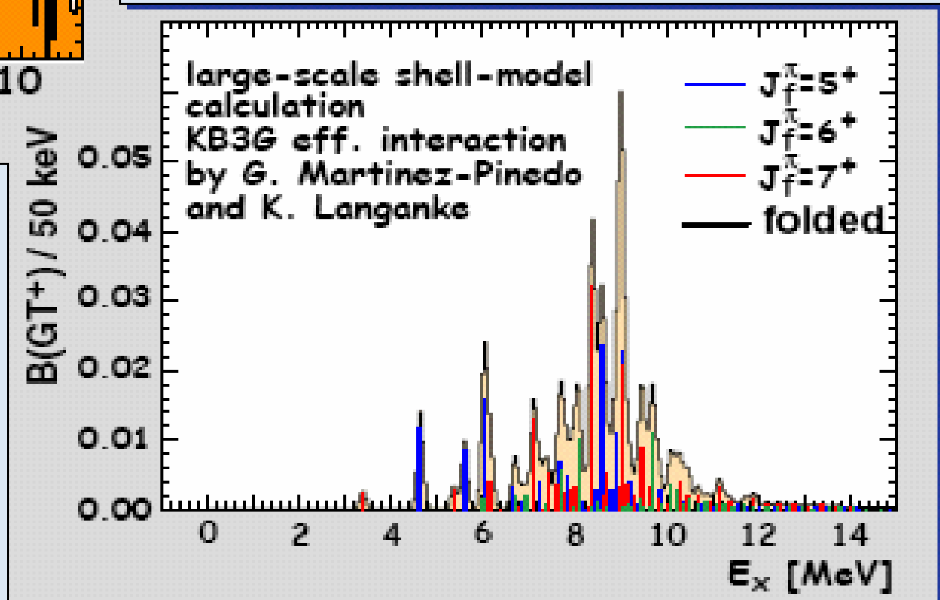

GT-centroid located at ~ 9 MeV

Spectrum of the $^{56}Fe(d,^{2}He)^{56}Mn$-Reaction

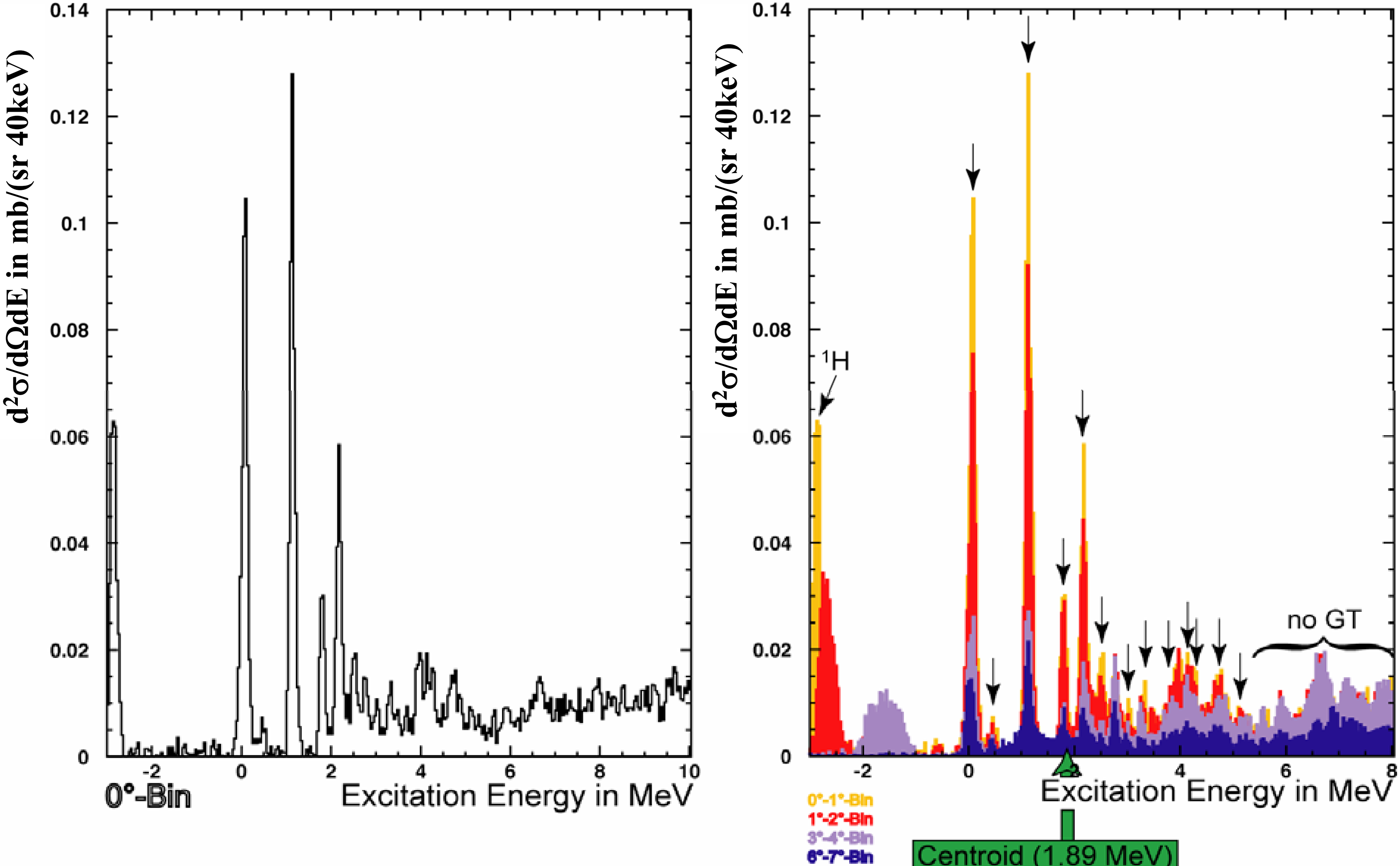

^{56}Fe(d,^{2}He): Comparison with shell-model calculations

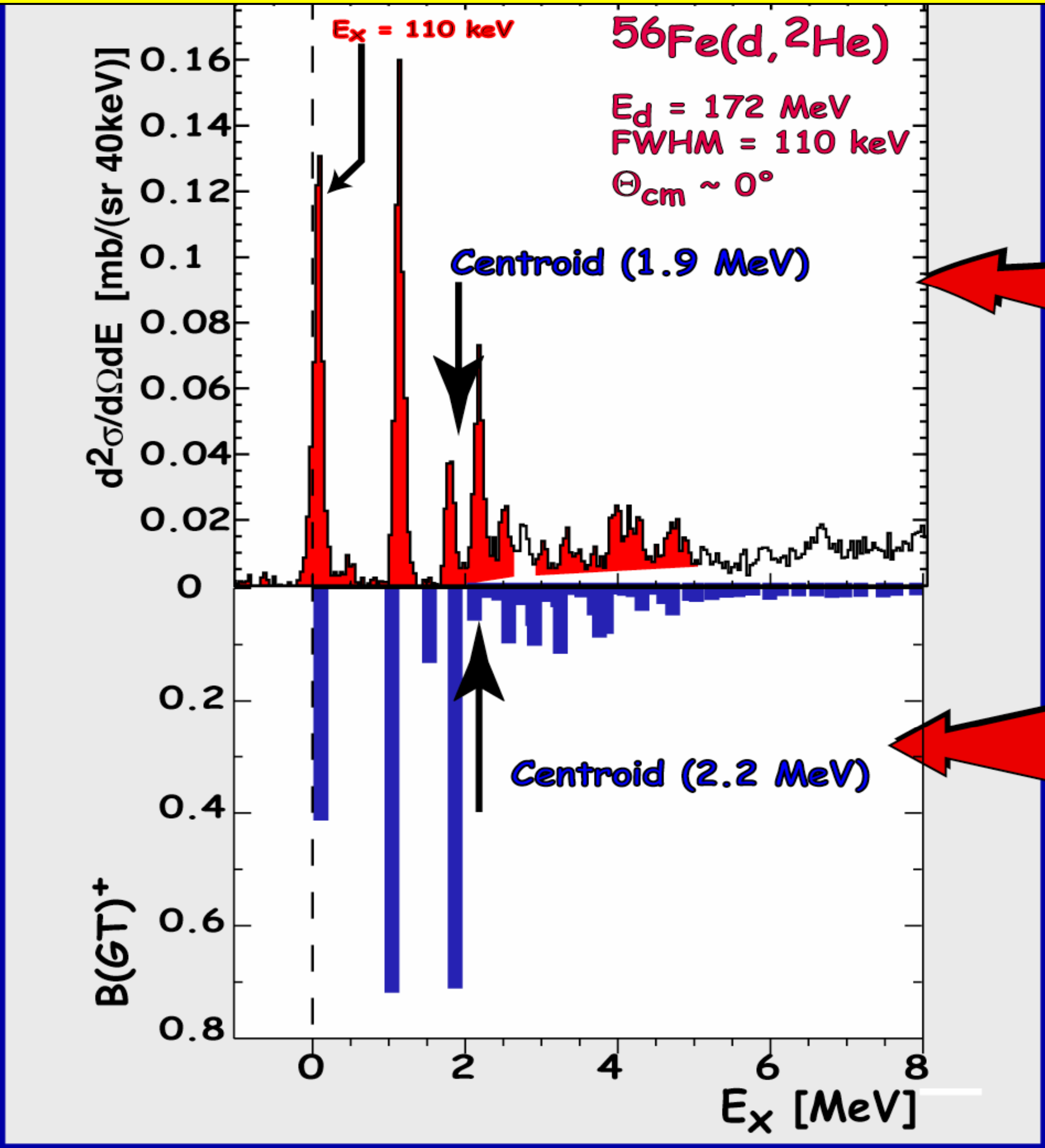

Experiment

Full *fp*-shell model calculations (KG3G) (G. Martínez-Pinedo)

Spectrum of the $^{57}Fe(d,^{2}He)^{57}Mn$-Reaction

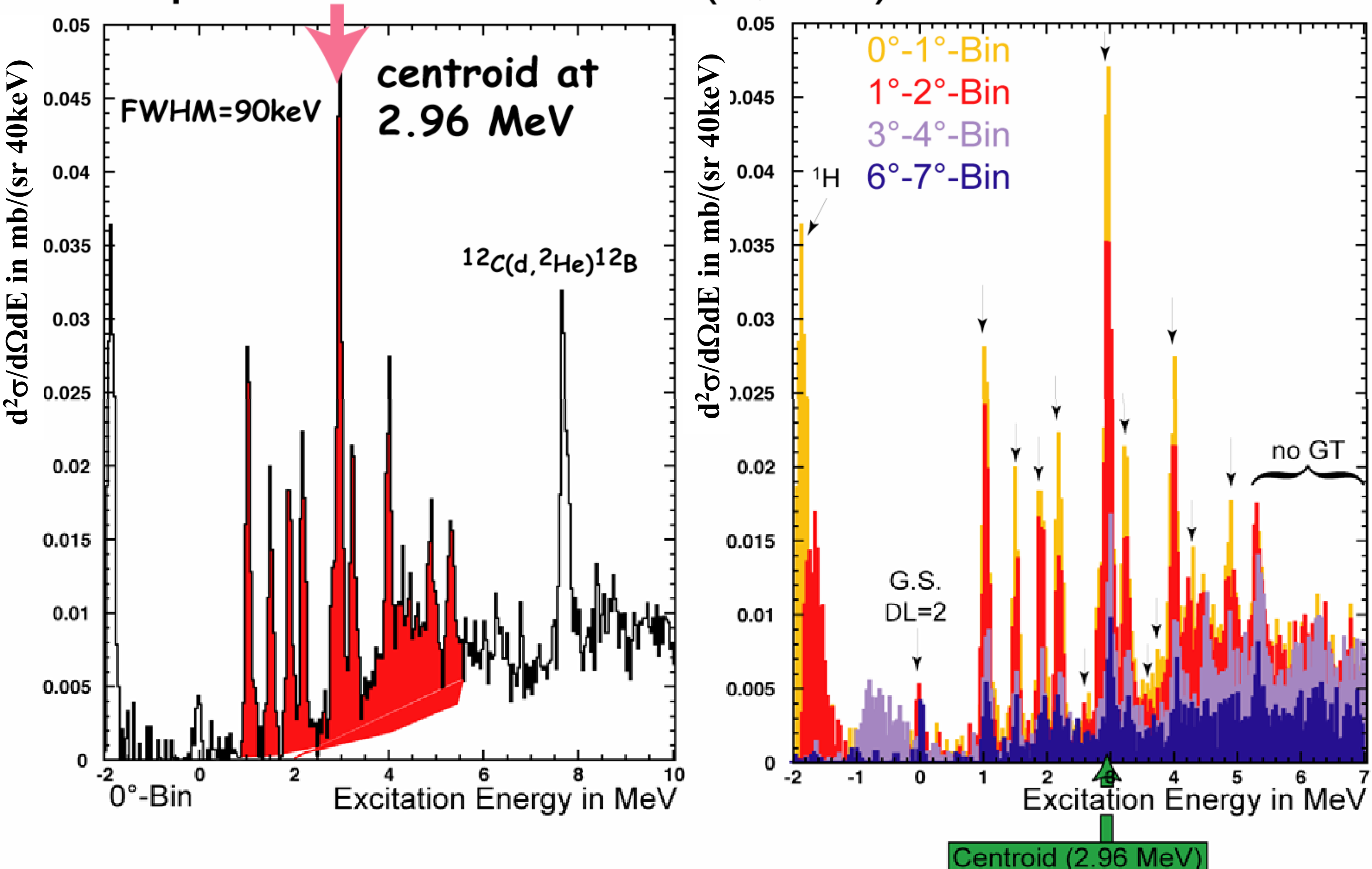

^{61}Ni(d,^{2}He)^{61}Co: GT$^+$ distribution

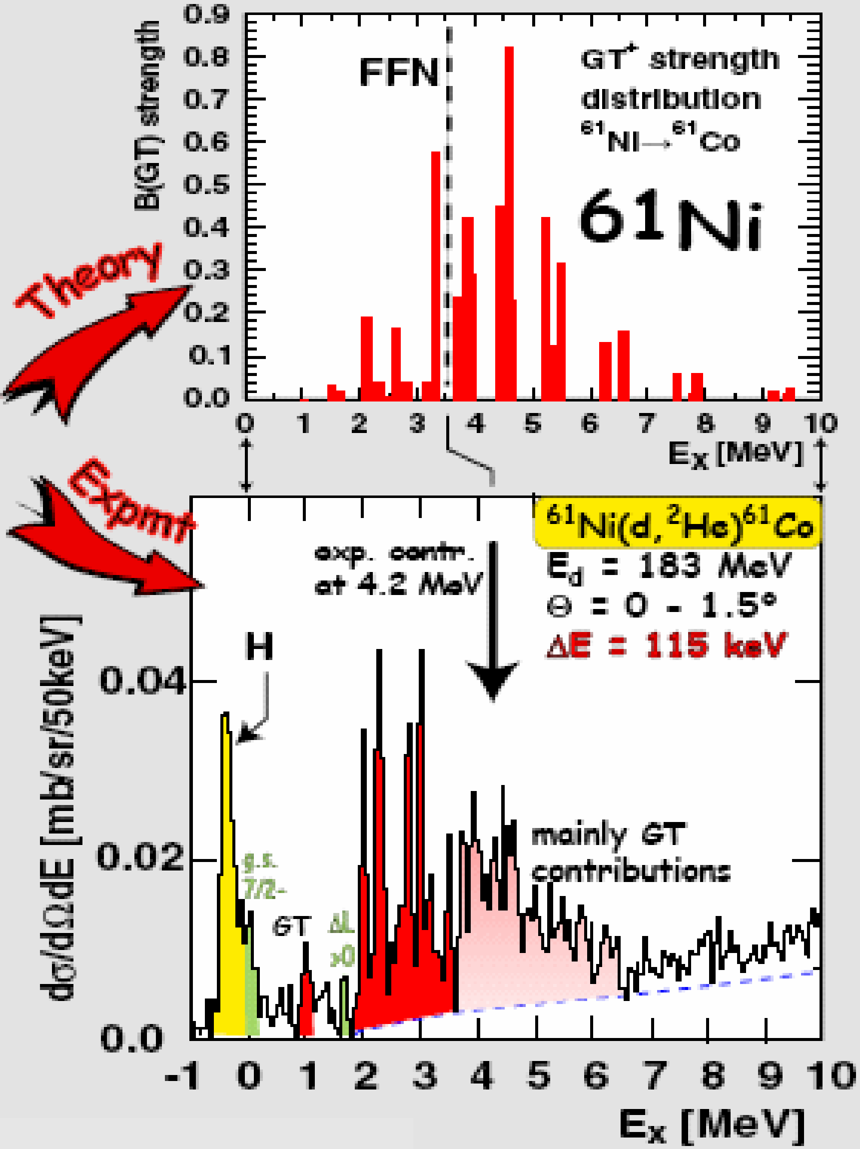

^{57}Fe(d,^{2}He)^{57}Mn: GT$^+$ distribution

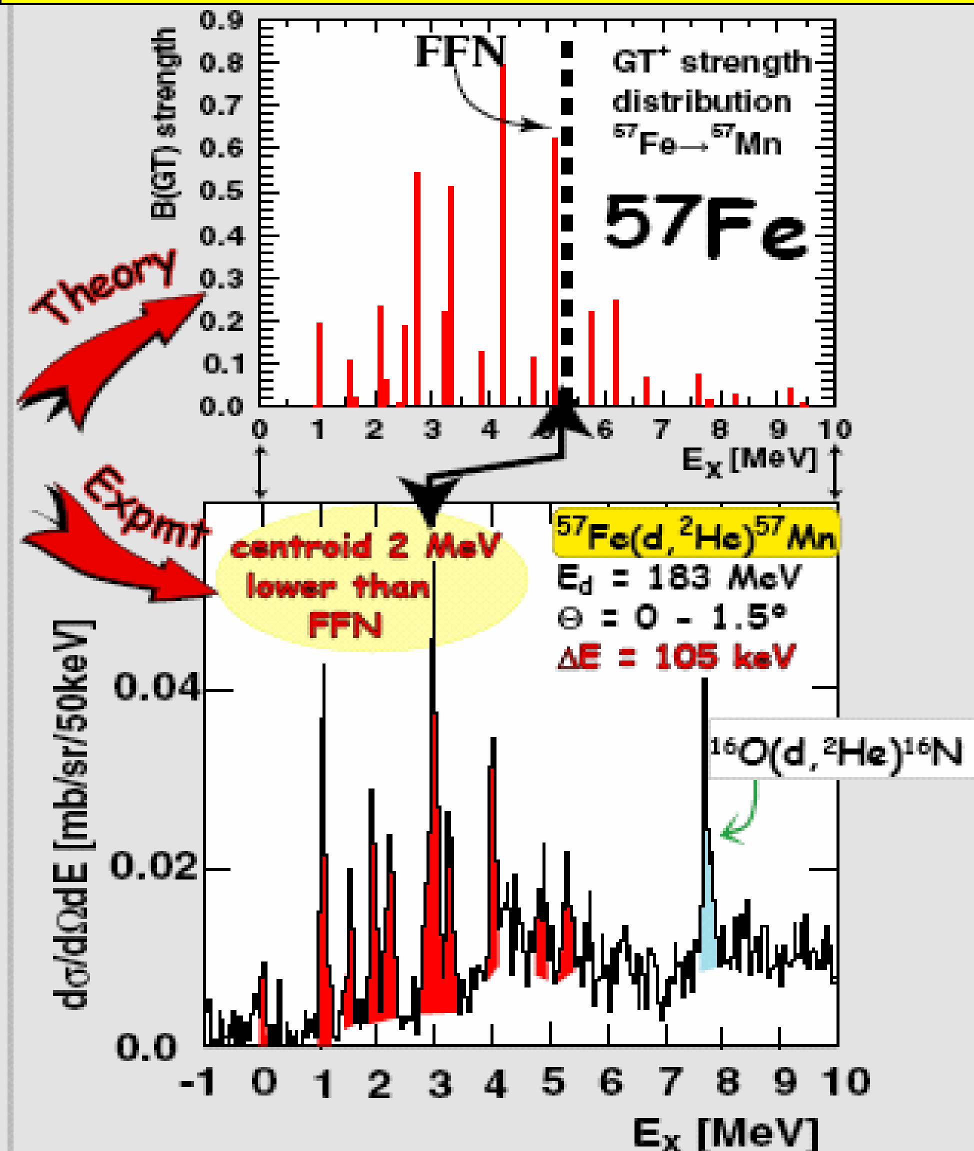

$^{67}Zn(d,^{2}He)^{67}Cu$: GT^{+} distribution

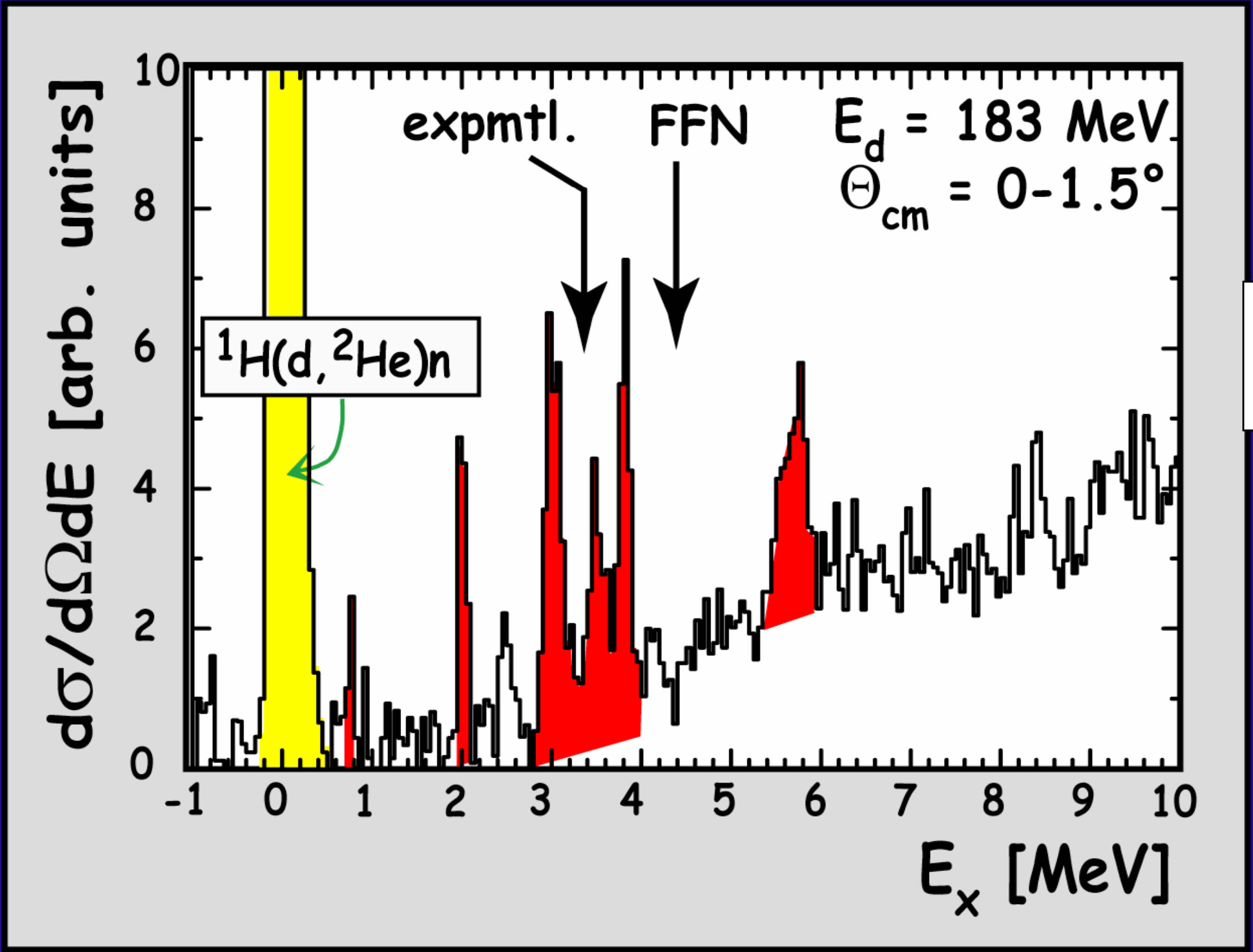

No shell-model calculations yet

GT$^+$ centroid comparison

		FFN	SM	Exp.
even-even	Fe-56	3.8	2.2	1.9
	Ni-58	3.8	3.6	3.4
odd-A odd-p	V-51	3.8	4.7	**4.1**
odd-A odd-n	Fe-57	5.3	4.1	2.9
	Ni-61	3.5	4.6	4.2
	Zn-67	4.4	--	3.4
odd-odd	V-50	9.7	8.5	8.8

Conclusions

- **Presupernova models depend sensitively on EC rates.**
- **GT^+ transitions in *fp*-shell nuclei play a decisive role in determining EC rates and thus provide input into modeling of explosion dynamics of massive stars.**
- **Large shell-model calculations are needed especially as function of T. (Caurier *et al*.; Martínez-Pinedo & Langanke [KB3G]; Otsuka *et al*. [GXPF]) ⇒ smaller EC rates for A=45-60 than FFN ⇒ Larger Y_e (electron to baryon ratio) and smaller iron core mass (Heger *et al*.)**
- New high resolution (d,^{2}He) experiments provide essential tests for shell model calculations at 0 T.

Outlook

Radioactive ion beams will be available at energies where it will be possible to study GRs (RIKEN, SPIRAL2, NSCL, FAIR, RIA, EURISOL)

- **Multipole strength functions in unstable n-rich nuclei**

  soft modes, pygmy resonances, low-lying non-collective strength, modification of effective NN interaction

  but also various Giant mulitpole resonances
- **ISGMR in a long chain of isotopes determine K_{sym}**
- **Determine GT strength in unstable *sd* & *fp* shell nuclei**
- **Use GRs as tools to determine n-skin [IV(S)GDR]**
- **Exotic excitations such as Double GT**

SHARAQ

Spectroscopy of HAdron systems with RadioActive Quantum beams

RI Beam (E = 150-400 MeV/A) as a new PROBE to nuclear systems

- **Large Isospin iso-tensor excitations**
- **Large internal energy (q,ω) inaccessible by stable beams**

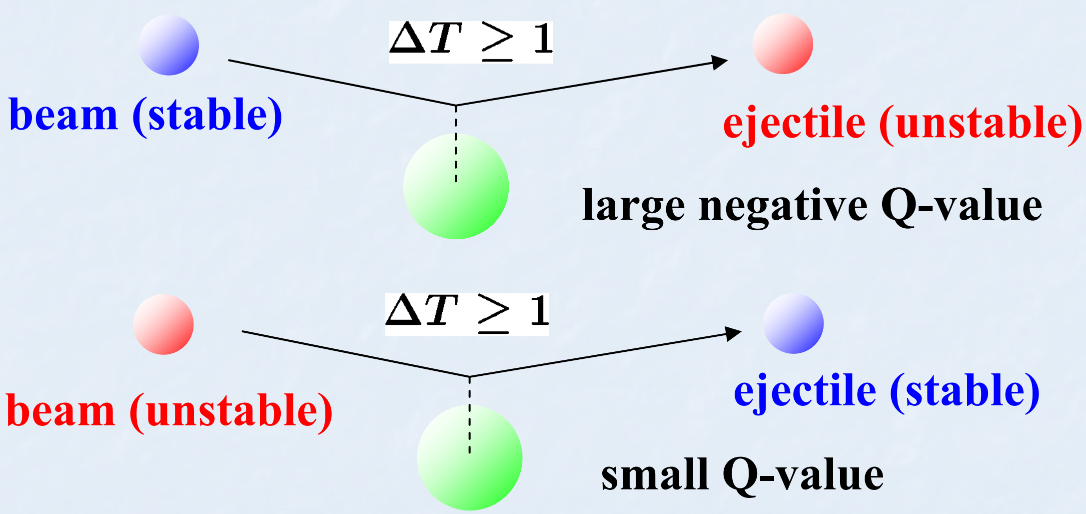

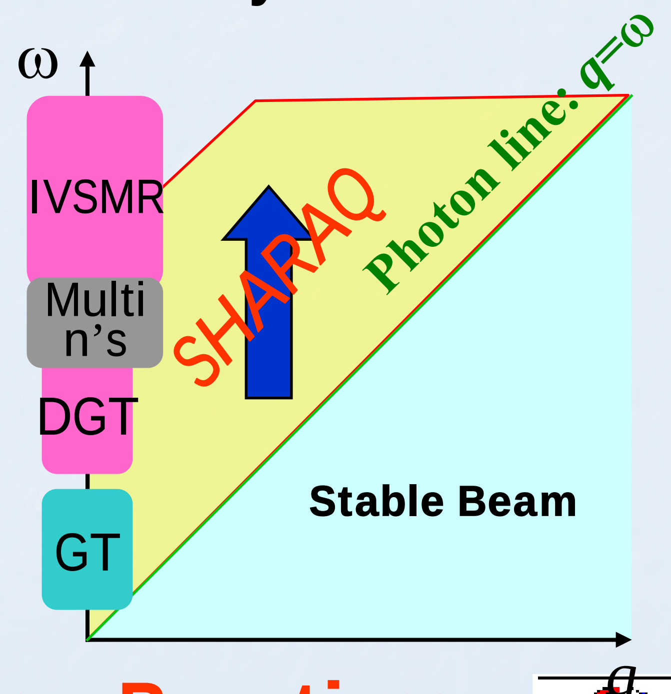

Exothermal Charge Exchange Reactions

END